Wind Erosion in the Sahelian Zone of Niger:

Processes, Models, and Control Techniques

CENTRALE LANDBOUWCATALOGUS
0000 0795 0443
ISN 937266

Promotoren: dr. ir. L. Stroosnijder
hoogleraar in de erosie en bodem- en waterconservering

dr. ir. P.A.C. Raats
hoogleraar in de continuümmechanica

NN08201, 2242

Wind Erosion in the Sahelian Zone of Niger:

Processes, Models, and Control Techniques

Geert Sterk

Proefschrift

ter verkrijging van de graad van doctor
op gezag van de rector magnificus,
dr. C.M. Karssen,
in het openbaar te verdedigen
op dinsdag 1 april 1997
des namiddags te vier uur in de Aula
van de Landbouwuniversiteit te Wageningen.

ISN: 937266

Thesis Wageningen Agricultural University
ISBN 90-5485-672-6

BIBLIOTHEEK
LANDBOUWUNIVERSITEIT
WAGENINGEN

This study was financially supported by the Netherlands Foundation for the Advancement of Tropical Research (WOTRO), which is part of the Netherlands Organization for Scientific Research (NWO). Project number W 76-151.

Cover design: Ernst van Cleef.

2242

Stellingen

1. In de Sahel-zone van Niger veroorzaakt winderosie een veel ernstiger bodemdegradatie dan watererosie.
   - dit proefschrift.
   - Taylor-Powell, E. 1991. Integrated management of agricultural watersheds: Land tenure and indigenous knowledge of soil and crop management. TropSoils Bulletin 91-04. Texas A&M Univ., College Station, TX.

2. De veronderstelling van Scott-Wendt et al. en Manu et al. dat winderosie en -depositie de belangrijkste oorzaken zijn van variabiliteit in gewasgroei op zandgronden in Niger is waar.
   - dit proefschrift.
   - Scott-Wendt, J., R.G. Chase, and L.R. Hossner. 1988. Soil chemical variability in sandy Ustalfs in semi-arid Niger, West Africa. Soil Sci. 145: 414-419.
   - Manu, A., A. Pfordresher, S.C. Geiger, L.P. Wilding, and L.R. Hossner. 1996. Soil parameters related to crop growth variability in western Niger, West Africa. Soil Sci. Soc. Am. J. 60: 283-288.

3. Het gebruik van geringe hoeveelheden (≤ 1000 kg ha^{-1}) gierststengels als bescherming tegen winderosie in Niger kan averechts werken. Tijdens zware stormen met windsnelheden boven ca. 10 m s^{-1} zal de ruwheid van de stengels juist meer erosie veroorzaken door een toename van de turbulentie-intensiteit.
   - dit proefschrift.

4. Nigerijnse boeren hebben een goede, kwalitatieve kennis van winderosie en onderkennen het gevaar van bodemdegradatie door wind. Het niet voldoende beschermen van de bodem is dus geen gevolg van onwetendheid, maar moet worden verklaard uit economische en culturele factoren.
   - dit proefschrift.

5. Het aanleggen van bomenrijen voor bodem- en gewasbescherming in de Sahel is een slechte maatregel. Regeneratie van natuurlijke vegetatie met verspreid staande bomen en struiken is beter.
   - dit proefschrift.
   - McNaugthon, K.G. 1988. Effects of windbreaks on turbulent transport and microclimate. Agric. Ecosyst. Environ. 22/23: 17-39.

6. Het concept van precisielandbouw is het reaktiveren van boerenkennis die verloren is gegaan door mechanisering en schaalvergroting in de westerse landbouw.
   - De precisieboer voegt zich naar zijn land. de Volkskrant, 25 januari 1997.

7. De armste landen van de wereld zijn weinig tot niet gebaat bij ontwikkelingshulp in de vorm van landbouwkundige projecten. Het is beter om de financiële middelen aan te wenden voor verbetering van onderwijs en infrastructuur.

8. De meteorologische term 'windrichting' is wiskundig gezien onjuist.

9. Door het gericht fokken van dieren wordt inteelt bevorderd.

10. In de huidige wetenschapsbeoefening wordt teveel nadruk gelegd op de kwantiteit en te weinig op de kwaliteit van artikelen in vaktijdschriften.

11. *I don't have a drinking problem, except when I can't get a drink.*
    - Uit: Bad liver and a broken heart, Tom Waits, Small Change, 1976.
    - Wijsheid opgedaan tijdens veldwerk in Niger.

Stellingen behorende bij het proefschrift:
'Wind Erosion in the Sahelian Zone of Niger: Processes, Models, and Control Techniques'.
Geert Sterk, Wageningen, 1 april 1997.

"The wind carries away fertile sand and leaves a fertility which is less fertile"

Hassane Adamou

Farmer in Liboré Bangou Banda, Niger

Acknowledgments

The research described in this thesis was carried out at the Department of Irrigation and Soil & Water Conservation, Wageningen Agricultural University (WAU), The Netherlands, and the International Crops Research Institute for the Semi-Arid Tropics (ICRISAT) Sahelian Center at Sadoré, Niger. The scientific and logistic support from these two institutions is gratefully acknowledged.

Many people have contributed in some way to the completion of the thesis, and I am grateful to all of them for their cooperation and support. A special word of thanks goes to the following persons: my supervisors Leo Stroosnijder and Pieter Raats, for their never ending support; the fellow graduate students at ISC, Holger Brück, Steve Gaze, Jörg Haigis, Ludger Herrmann, Martina Mayus, Mark Smith, and Alex Wezel, for their cooperation, friendship and the many lifts to and from ISC; Habibou Halidou, Boubacar Soumana, and many day-labourers for their great help with the field work at times with temperatures well above 40°C; Syne van der Beek, for the many stimulating e-mails and discussions at the Vlaamsche Reus.

Last but not least, I want to thank Anita, who typed a lot of text, made some very good figures for the thesis, helped me with software problems, but at the same time, she made me realize that obtaining a Ph.D. is nice, but not the most important thing in life.

Contents

Chapter 1	Introduction	1
Chapter 2	The effect of turbulent flow structures on saltation sand transport in the atmospheric boundary layer	11
Chapter 3	Comparison of models describing the vertical distribution of wind-eroded sediment	33
Chapter 4	Mapping wind-blown mass transport by modeling variability in space and time	51
Chapter 5	Wind-blown nutrient transport and soil productivity changes in southwest Niger	71
Chapter 6	Wind erosion control with crop residues in the Sahel	91
Chapter 7	Farmers' knowledge of wind erosion processes and control methods in Niger	111
Chapter 8	Towards a regional mass budget of eolian transported material in a Sahelian environment	125
Chapter 9	Summary and conclusions	137
	Samenvatting en conclusies	143
	Résumé et conclusions	147
	Curriculum vitae	152

Chapter 1

Introduction

Introduction

The Sahelian zone of Africa drew world attention during the 17 years of drought that started in 1968. Some 25 million people faced famine as well as social and economic disruption. The long period of drought was even more tragic as the Sahel, already one of the world's poorest regions, is also the most subjected to desertification (Valentin, 1995). The tragedy painfully highlighted the urgent social need to investigate causes and consequences of drought and desertification in the Sahel.

The term "Sahel" is derived from the Arabic word *Sahil* which means a coast or border (Hillel, 1991). The region can be seen as the transition zone between the arid Sahara in the north and the more humid Sudan zone in the south. In this thesis, the Sahel is defined as the zone approximately 200 - 400 km wide, centered on latitude 15°N, just south of the Sahara. It covers significant portions of Senegal, Mauritania, Mali, Burkina Faso, Niger, Chad, Sudan, and Eritrea. The limits correspond roughly with a mean annual rainfall of 200 mm in the north and 600 mm in the south (Le Houerou and Popov, 1981).

About 90% of the Sahelian population lives in villages and is largely dependent on subsistence agriculture (Sivakumar, 1989). The agricultural environment is characterized by chemically and physically impoverished soils that generally have sandy to sandy loam textures, low organic matter contents, and low native fertility, with phosphorus being the nutrient most limiting crop growth (Manu et al., 1991). These sandy soils are structurally unstable, prone to crusting and hardsetting (Valentin, 1995), and have low water-holding capacities (Payne et al., 1990). In addition, climatic conditions are harsh, with highly variable rainfall during a short rainy season, high temperatures, and potential evapotranspiration exceeding precipitation for most of the year (Fig. 1). This combination of poor soils and harsh climatic conditions makes crop production difficult.

The sedentary farming systems of the Sahel combine free-roaming livestock with rainfed crop production. Most farmers keep sheep, goats, and sometimes cattle, for milk and meat. The major crop is pearl millet (*Pennisetum glaucum*), which is often intercropped with a legume, usually cowpea (*Vigna unguiculata*). Millet is sown with the first rains in the rainy season. In intercropping systems the second crop is not sown until 2 to 3 weeks after the millet (Spencer and Sivakumar, 1987). More favorable micro-environments with better moisture and nutrient conditions are used for

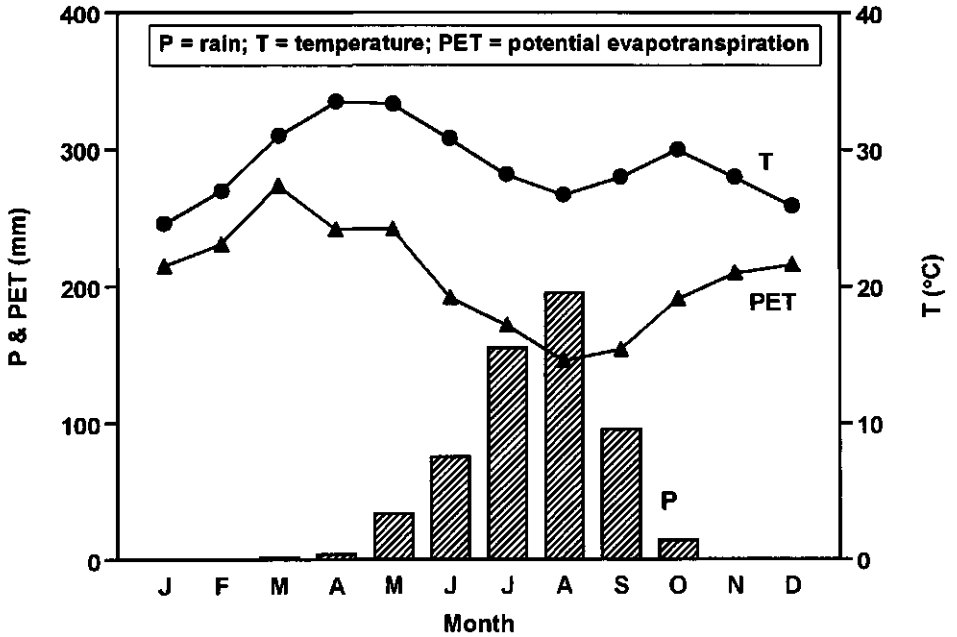

Figure 1. Agroclimatic conditions for Niamey, Niger. Adapted from FAO (1984).

sorghum (*Sorghum bicolor*), maize (*Zea mays*), sorrel (*Hibiscus sabdarifa*), okra (*Hibiscus esculentus*), and peanuts (*Arachis hypogaea*). Manioc (*Manihot esculenta*) is often grown in gardens near villages, and women usually cultivate small vegetable plots (Taylor-Powell, 1991).

Continuous cropping causes soil organic matter and plant-available nutrients to decline. To restore soil fertility, farmers traditionally kept land under bush fallow for periods of 10 to 20 years. However, rapid population growth, at annual rates of ≈3% during recent decades, has increased demand for food. Instead of intensifying farming systems, for instance by using mineral fertilizers, farmers have tried to enhance production by expanding the cropped area. The previously sustainable fallow system has broken down, yields have declined, and more marginal land, which used to be communal grazing land, is now cropped (Broekhuyse and Allen, 1988). Consequently, over-exploitation has resulted in land degradation, or desertification, on a large scale (Hillel, 1991). Land degradation implies a reduction of resource potential by a single process or a combination of processes acting on the land. These processes include erosion by water and wind, crusting and hardsetting of soils, salinization and alkalinization, and long-term reduction in the amount or diversity of natural vegetation (Dregne et al., 1991; Valentin, 1995).

WIND EROSION

Wind erosion can become a problem whenever the soil is loose, dry, bare or nearly bare, and the wind velocity exceeds the threshold velocity for initiation of soil particle movement (Fryrear and Skidmore, 1985). In the Sahel, the farming systems and soil conditions are very favorable for wind erosion. Except for a few months in the growing season, the ground is mostly bare and no adequate measures are taken to sufficiently control wind erosion. Moreover, the sandy textures and dry climatic conditions make soils very susceptible to erosion for most of the year.

Erosive winds that exceed the threshold wind speed may occur during two distinct seasons. During the dry season (October - April), the area is invaded by dry and rather strong northeastern winds, locally known as *Harmattan*, that may result in moderate wind erosion (Michels et al., 1995a). The Harmattan winds originate over the Saharan desert, and from January to March they usually carry much dust from remote sources. Part of the transported dust is deposited in the Sahel, enriching soils with nutrients (Drees et al., 1993). Dust deposits are particularly rich in sodium, potassium, magnesium, and calcium, but poor in phosphorus (Herrmann et al., 1996).

The second and most important wind erosion period is the early rainy season (May - July), when rainfall comes with heavy thunderstorms that move westward through the Sahel. Within a fully developed thunderstorm strong vertical downdrafts occur, causing a forward outflow of cold air that creates the typical dust storms of the Sahel. These events are usually short-lived, approximately 10 to 30 minutes, but the storms may result in intense soil movement (Michels et al., 1995a). Generally, three different modes of particle transport are distinguished (Bagnold, 1973). Saltating sand grains jump and bounce over the soil surface, thereby inducing creep, the rolling and sliding of large particles over the surface, and suspension, the raising of fine soil particles (Fig. 2). The latter transport mode results in the spectacular dust clouds, which are often seen to be pushed forward by a thunderstorm. Part of the dust may be redeposited by the rain that immediately follows the dust storm (Herrmann et al., 1996).

Crop seedlings suffer from abrasion and burial in sand during these early rainy season storms. Abrasion, or sand blasting, damages plants by the scouring effect of saltating sand particles. Young plants buried during storms suffer from the weight of the sand, reduced sunlight interception, and high soil temperatures during daytime. The damage ranges from reduced growth and development to total destruction of crops (Michels et al., 1995b).

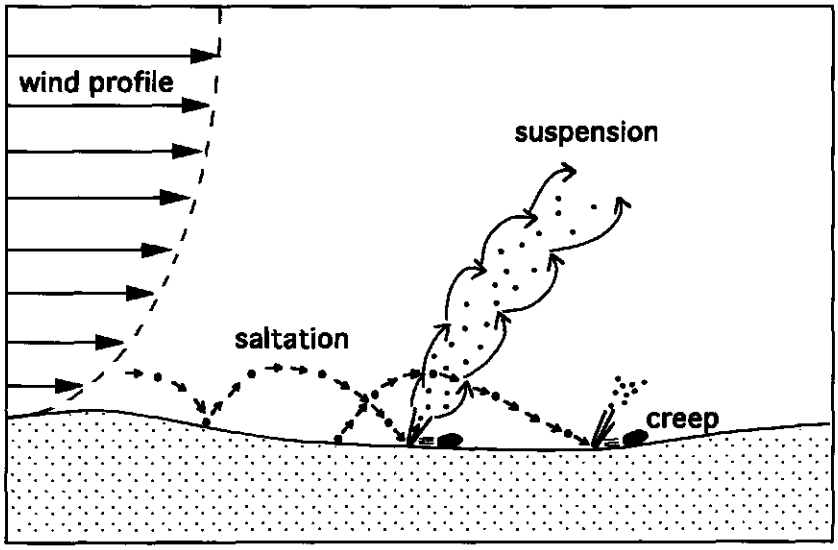

Figure 2. Three modes of wind-blown particle transport.

Apart from direct damage to seedlings, wind erosion contributes to soil degradation by the loss of topsoil. This is because most plant-available nutrients are located in the top few centimeters of the soil and wind erosion preferentially removes the organic matter and clay, which hold these nutrients (Lal, 1988). However, it is unknown how much damage is actually done to soils (Dregne, 1990). In the literature, there are no reports of studies that have quantified soil and nutrient losses by wind erosion in the Sahel. According to Fryrear and Lyles (1977), part of the problem is the lack of satisfactory sampling equipment for studying wind erosion in the field and the complex nature of the processes involved. Although sampling techniques have improved greatly during the past 20 years (Fryrear et al., 1991), no entirely adequate techniques for quantifying losses of soil particles and nutrients have been developed.

The growing problem posed to crop production by wind erosion is emphasized by Taylor-Powell (1991). In a survey in the Hamdallaye watershed in Niger, she found that farmers seldom mentioned water erosion as a problem. However, wind erosion emerged as a major concern because farmers fear its potential damaging effects. Ways of coping with these problems mentioned by the farmers included a change in their crop residue management in the previous 10 years. Crop residues are now left on the field after harvest to protect the soil against erosive winds.

Millet residue is by far the most commonly used mulch material for soil conservation, but its availability is limited because of its multiple uses for fuel, fodder and construction material (Lamers and Feil, 1993). According to Michels et al. (1995a), at least 2000 kg ha^{-1} of millet residue is needed for adequate soil protection in the Sahelian zone. Under the current biomass production levels of 2200 kg ha^{-1} (Manu et al., 1991) and the high demand for other purposes, it is unrealistic to expect that farmers will be able to adequately protect most of their fields. Hence, there is a need for improved crop residue management, and possibly for additional measures for wind erosion control.

Although the technical methods are well documented (e.g., Fryrear and Skidmore, 1985; Tibke, 1988), much less is known about the adoption of those methods by Sahelian farmers. For instance, although protection against wind erosion by erecting wind breaks is a promising measure, farmers are reluctant to implement it because of uncertainty about its benefits (Michels, 1994).

An important requirement for designing wind erosion control measures is that they fit into the local, Sahelian situation. This is illustrated by Ben Salem (1991): "Building upon, not abandoning, traditional land management is the real challenge for sustainable development of renewable natural resources in arid regions. The problem of wind erosion needs to be addressed within this broader context." Indigenous knowledge of wind erosion and traditional methods for soil and crop protection should form the basis for improving or designing wind erosion control measures in the Sahel. On-farm surveys like the study by Taylor-Powell (1991) are important for ascertaining the feasibility of wind erosion control methods in the land management systems of the Sahel.

AIM

The aim of the study described in this thesis is to improve understanding of wind erosion processes in the Sahel during early rainy season storms. In particular, an attempt is made to quantify the effect of erosive storms on changes in soil productivity in pearl millet cropping systems, and to explore the feasibility of wind erosion control measures that fit into the current farming systems.

STUDY OUTLINE

The field work for this study was done during three measurement campaigns in southwest Niger, in a pearl millet field of 170 by 90 m. Each campaign lasted 3 months, from mid-May until mid-August in the years 1993, 1994, and 1995. During the field work, wind-blown sediment moving between the soil surface and a height of 1 m was studied. This height range comprised all three transport

modes of creep, saltation, and suspension (Fig. 2). Fine, suspended dust moving above 1 m height was not studied, since the apparatus required for this was not available.

In order to study wind erosion processes in the field, adequate measurement techniques are needed. During the first field campaign in 1993, emphasis was on the development of measurement techniques and related models to quantify the mass of soil particles and nutrients transported during storms. In chapter 3, a simple sediment catcher for measuring horizontal mass fluxes of wind-blown particles is described, and a method to calculate the total mass transport rate at the point of observation is developed. Using 21 sediment catchers in a plot of 40 by 60 m made it possible to study spatial variation in mass transport. In chapter 4, geostatistical theory is applied to model spatial dependence between observations, and to produce storm based maps of mass transport. These maps are used to calculate soil losses from the experimental plot. Moreover, the losses of four nutrients (K, C, N, and P) during two severe storms are calculated from chemical analysis of the trapped sediments (chapter 5).

The second and third field seasons in 1994 and 1995 dealt with (i) the effect of turbulent flow structures on transport of sand by saltation, (ii) wind erosion protection created by small quantities of millet residues, and (iii) farmers' perceptions of wind erosion processes and soil conservation techniques.

Turbulence is a natural characteristic of wind. It causes fluctuations in wind velocity that create additional shear stress superimposed on the shear stress resulting from the average flow condition. Fluctuations in shear stress at the soil surface are considered to be important for wind erosion processes. Measurements of instantaneous wind speed and saltation flux enabled the role of velocity and shear stress fluctuations on soil particle movement by saltation to be described (chapter 2).

Given the limited availability of mulch material for soil protection, it is essential to manage crop residues efficiently. Therefore, the effect of two low applications of millet residue on storm based sediment transport was quantified. In chapter 6, the optimum quantity of millet residues for wind erosion control in the Sahel is determined.

To complement the experiments, an on-farm survey was conducted in seven villages in southern Niger. In total, 138 farmers were interviewed to ascertain their knowledge of wind erosion and deposition processes, the damage caused by blowing sand, and their traditional techniques for wind erosion control (chapter 7).

The soil and nutrient losses calculated in this thesis are from one field only. To quantify the impact of wind erosion on farming systems at a regional scale, different measurement and computation techniques need to be integrated in the same area. In chapter 8, a method is proposed to calculate a regional mass budget of wind-blown material. The method combines a wind erosion model with a geographical information system. Input data for the model are obtained from remote sensing and ground based experiments in key areas selected for their typical surface characteristics. Chapter 9, finally, summarizes the main conclusions of this thesis.

REFERENCES

Bagnold, R.A. 1973. The physics of blown sand and desert dunes. 5th ed., Chapman and Hall, London.

Ben Salem, B. 1991. Prevention and control of wind erosion in arid regions. Unasylva 164: 33-39.

Broekhuyse, J.T., and A.M. Allen. 1988. Farming systems research. Human Organiz. 47: 330-342.

Drees, L.R., A. Manu, and L.P. Wilding. 1993. Characteristics of aeolian dusts in Niger, West Africa. Geoderma 59: 213-233.

Dregne, H.E. 1990. Erosion and soil productivity in Africa. J. Soil Water Conserv. 45: 431-436.

Dregne, H.E., M. Kassas, and B. Rosanov. 1991. A new assessment of the world status of desertification. Desertification Control Bull. 20: 6-18.

FAO. 1984. Agroclimatological data for Africa, Vol. 1. Countries north of the equator. FAO Plant Production and Protection Series, no. 22. FAO, Rome, Italy.

Fryrear, D.W., and L. Lyles. 1977. Wind erosion research accomplishments and needs. Trans. ASAE 20: 916-918.

Fryrear, D.W., and E.L. Skidmore. 1985. Methods for controlling wind erosion. p. 443-457. *In* R.F. Follet and B.A. Stewart (ed.) Soil erosion and crop productivity. ASA-CSSA-SSSA, Madison, WI.

Fryrear, D.W., J.E. Stout, L.J. Hagen, and E.D. Vories. 1991. Wind erosion: Field measurement and analysis. Trans. ASAE 34: 155-160.

Herrmann, L., K. Stahr, and M.V.K. Sivakumar. 1996. Dust deposition on soils of southwest Niger. p. 35-47. *In* B. Buerkert et al. (ed.) Wind erosion in West Africa: The problem and its control. Proc. Int. Symp., Stuttgart, Germany. 5-7 Dec. 1994. Margraf Verlag, Weikersheim, Germany.

Hillel, D.J. 1991. Out of the earth: Civilization and the life of the soil. The Free Press, New York.

Lal, R. 1988. Soil degradation and the future of agriculture in sub-Saharan Africa. J. Soil Water Conserv. 43: 444-451.

Lamers, J.P.A., and P.R. Feil. 1993. The many uses of millet residues. ILEIA Newsletter 9: 15.

Le Houerou, H.N., and G.F. Popov. 1981. An eco-climatic classification of intertropical Africa. FAO Plant Production and Protection Paper, no. 31. FAO, Rome, Italy.

Manu, A., A. Bationo, and S.C. Geiger. 1991. Fertility status of selected millet producing soils of West Africa. Soil Sci. 152: 315-320.

Michels, K. 1994. Wind erosion in the southern Sahelian zone: Extent, control, and effects on millet production. Verlag Ulrich E. Grauer, Stuttgart, Germany.

Michels, K., M.V.K. Sivakumar, and B.E. Allison. 1995a. Wind erosion control using crop residue I. Effects on soil flux and soil properties. Field Crops Res. 40: 101-110.

Michels, K., M.V.K. Sivakumar, and B.E. Allison. 1995b. Wind erosion control using crop residue II. Effects on millet establishment and yields. Field Crops Res. 40: 111-118.

Payne, W.A., C.W. Wendt, and R.J. Lascano. 1990. Root zone water balances of three low-input millet fields in Niger, West Africa. Agron. J. 82: 813-819.

Sivakumar, M.V.K. 1989. Agroclimatic aspects of rainfed agriculture in the Sudano-Sahelian zone. p. 17-38. *In* Soil, crop, and water management in the Sudano-Sahelian zone. Proc. Int. Worksh., Niamey, Niger. 11-16 Jan. 1987. ICRISAT, Patancheru, India.

Spencer, D.S.C., and M.V.K. Sivakumar. 1987. Pearl millet in African agriculture. p. 19-31. *In* Proceedings of the international pearl millet workshop. Patancheru, India. 7-11 April 1986. ICRISAT, Patancheru, India.

Taylor-Powell, E. 1991. Integrated management of agricultural watersheds: Land tenure and indigenous knowledge of soil and crop management. TropSoils Bulletin 91-04. Texas A&M Univ., College Station, TX.

Tibke, G. 1988. Basic principles of wind erosion control. Agric. Ecosyst. Environ. 22/23: 103-122.

Valentin, C. 1995. Sealing, crusting and hardsetting soils in Sahelian agriculture. p. 53-76. *In* H.B. So et al. (ed.) Sealing, crusting and hardsetting soils: Productivity and conservation. Aust. Soc. of Soil Sci., Brisbane, Australia.

Chapter 2

The Effect of Turbulent Flow Structures on Saltation Sand Transport in the Atmospheric Boundary Layer

G. Sterk, A.F.G. Jacobs and J.H. van Boxel

Submitted to: Earth Surface Processes and Landforms.

The Effect of Turbulent Flow Structures on Saltation Sand Transport in the Atmospheric Boundary Layer

ABSTRACT

The effect of turbulent flow structures on saltation sand transport was studied during two convective storms in Niger, West Africa. Continuous, synchronous measurements of saltation fluxes and turbulent velocity fluctuations were made with a sampling frequency of 1 Hz. The shear stress production was determined from the vertical and streamwise velocity fluctuations. The greatest stress bearing events were classified as turbulent structures, with sweep, ejection, inward interaction, and outward interaction described according to the quadrant technique. The classified turbulent structures accounted for 63.5% of the average shear stress during the first storm, and 56.0% during the second storm. The percentage of active time was only 20.6% and 15.8%, respectively. High saltation fluxes were associated with sweeps and outward interactions. These two structures contribute positively (sweeps) and negatively (outward interactions) to the shear stress, but have in common that the streamwise velocity component is higher than average. Therefore, the horizontal drag force is primarily responsible for saltation sand transport, and not the shear stress. This was also reflected by the low correlation coefficients (r) between shear stress and saltation flux (0.12 and 0.14, respectively), while the correlation coefficients between the streamwise velocity component and saltation flux were much higher (0.65 and 0.57, respectively).

A turbulent fluid flow over a solid surface imparts instantaneous and localized levels of shear stress to the fluid-solid interface which are well above the average flow shear stress (Nearing and Parker, 1994). For example, Lapointe (1992) found that 80% of the total shear stress exerted by water in the Fraser River (British Colombia, Canada) could be attributed to isolated events of 3 to 8 s duration, which occupied only 12% of the time. The short events were identified as ejection and inrush structures of the turbulent bursting mechanism.

These turbulent structures can be defined by using horizontal and vertical turbulent velocity fluctuations. The instantaneous streamwise velocity u can be partitioned into a time average $\bar{u}$ and a turbulent fluctuating part u', superposed on the average. The same can be done for the vertical velocity component v. An ejection is an upward movement of low-velocity fluid from near the solid surface ($u' < 0$, $v' > 0$), while a downward movement of high-velocity fluid towards the solid surface ($u' > 0$, $v' < 0$) is called inrush or sweep (Dyer, 1986). Both events result in a downward momentum transport and, hence, a positive contribution to the turbulent shear stress or Reynolds stress. In

addition, two weaker motions, inward and outward interactions, exist. An outward interaction is an upward movement of high-velocity fluid ($u' > 0$, $v' > 0$), and an inward interaction is a downward movement of low-velocity fluid ($u' < 0$, $v' < 0$). Both events result in an upward momentum transport and contribute negatively to the shear stress. For realistic flows, a positive shear stress exists. So, on average the absolute magnitude of the negative contributions have to be lower than the positive contributions given by ejections and sweeps.

Ejection and sweeps have often been associated with detachment and transportation of sediment. Sweeps are usually associated with the initiation and movement of bed-load transport (saltation + creep), whereas ejections are supposed to be more effective in lifting fine suspended material away from the surface (Dyer, 1986). The present knowledge of the links between the turbulent bursting mechanism and sediment transport dynamics was mainly obtained from investigations in water flow, usually under laboratory conditions (e.g., Sutherland, 1967; Müller et al., 1971; Sumer and Oguz, 1978; Sumer and Deigaard, 1981; Grass, 1983), but also in geophysical boundary layers (e.g., Heathershaw and Thorne, 1985; Thorne et al., 1989; Lapointe, 1992). These geophysical studies have confirmed the relation between (i) ejections and suspension transport (Lapointe, 1992), and (ii) sweeps and bed-load transport (Heathershaw and Thorne, 1985; Thorne et al., 1989). In addition, the latter two studies revealed that outward interactions, although weaker and less frequent than sweeps, were capable of supporting bed-load movement as well. Heathershaw and Thorne (1985) hypothesized that shear stress is a necessary but not sufficient condition for bed-load transport, and that form drag on individual particles may have greater dynamical significance than the shear stress.

Although much of relevance to sediment transport in turbulent airflows can be gleaned from the studies in aqueous environments, by comparison the role of turbulence in wind-blown particle transport has received very little attention (Butterfield, 1993). From a few wind tunnel studies, the importance of turbulence for entrainment of particles has been inferred (e.g., Bisal and Nielsen, 1962; Lyles and Krauss, 1971; Braaten et al., 1990), and three wind tunnel studies (Butterfield, 1991 and 1993; Hardisty, 1993) provide data of instantaneous wind speed and sediment transport. Reports of field experiments are even more scarce. Only two studies were found (Lee, 1987; Butterfield, 1991). However, these wind tunnel and field studies did not identify the different turbulent structures to reveal their significance for wind-blown sediment transport.

A better understanding of the wind erosion process, for instance for modeling purposes, requires detailed measurements of particle transport in relation to the turbulent wind flow. According to Butterfield (1993), it is essential that both mass flux and wind velocity histories are characterized to frequencies of at least 1 Hz if realistic and environmentally useful sediment transport relations are to be derived. In this study, data of synchronous measurements of turbulent velocity components and saltation sand transport during convective storms in the West African Sahel were collected. Only saltation transport was measured, because it is generally more easily quantified than creep and suspension transport. Furthermore, saltation is considered to initiate transport by the other two modes (Shao et al., 1993). So, understanding the saltation process gives also insight in creep and suspension transport. The objectives of the study were (i) to determine the magnitude and duration of peak Reynolds stresses, and (ii) to investigate the saltation response to velocity and shear stress fluctuations created by turbulent structures.

MATERIALS AND METHODS

Study Site

A field experiment was conducted at the International Crops Research Institute for the Semi-Arid Tropics (ICRISAT) Sahelian Center in southwest Niger (13°16'N;2°21'E), during the rainy seasons of 1994 and 1995. The climate of the region is typical Sahelian, with one short (4 months) rainy season and high temperatures all year round. In the early rainy season (May - July), large cumulonimbus clouds develop throughout the Sahel and bring the first rains of the new rainy season. Often, cumulonimbus clouds are accompanied by short (10 - 30 min) wind storms that precede rainfall. The storms are the result of strong downdrafts within the cloud that cause a forward outflow of cold air. The violent winds may create a spectacular rolling dust cloud that moves in front of the cumulonimbus cloud. In general, the cumulonimbus clouds move from east to west and the resulting wind direction during storms is usually east.

The field used for the experiment was 90 by 90 m in size. It was bordered by dirt roads at the northern and eastern sides, by a field protected against wind erosion with crop residues in the south, and by a wind break at the western side. The equipment was positioned such that distances from instruments to the field boundaries exceeded 50 m in the northern and eastern directions, and was about 40 m in the southern and western directions. The whole field was planted with pearl millet (*Pennisetum glaucum*) on 17 June 1994 and 21 June 1995. Sowing was done according to the

traditional Sahelian method, with sowing holes, or pockets, at wide spacings of 1 by 1 m. In each hole approximately 50 to 100 seeds were thrown. Three weeks after sowing, the number of plants in each pocket was manually reduced to three.

The soil at the measurement field is a sandy alfisol with 92.2% sand, 3.0% silt, and 4.8% clay in the topsoil. The aggregate size distribution, determined by dry sieving of soil samples, is shown in Table 1. These sandy soils are very prone to crust formation by high-intensity rainfall in the early rainy season. Strong structural crusts are formed that have typically two layers. At some depth (5 - 10 mm), a thin and dense plasmic layer exists, which consists of fine particles (clay, silt, and fine sand) that were washed out from the top layer. The top layer consists of loose, cohesionless sand, which is easily eroded by wind or water. Such a crust existed all the time in the field during the experiments. It was broken by weeding only two times per season, but returned immediately during the next rain.

The soil surface was smooth and without any roughness other than that created by the soil particles themselves, characterized by a roughness length of approximately 0.001 m. Just after weeding the roughness length increased to approximately 0.01 m, but in both seasons, no wind storms occurred during these periods. The roughness created by young millet plants was negligible during the first four weeks after sowing. The limited size of the plants (<0.10 m) and the low planting density assured that saltation transport was not significantly influenced by the crop. In the surroundings of the field, obstacles such as trees and bushes were present. During storms, the upwind distances from the measurement location to the obstacles exceeded in all cases 20 times the height of the obstacle. It was therefore assumed that the wind field at the measurement location was not significantly

Table 1. Aggregate size distribution of topsoil at ICRISAT Sahelian Center.

Size class	Mass
µm	%
< 63	3.1
63 - 125	18.2
125 - 250	35.7
250 - 500	32.8
500 - 1000	10.0
> 1000	0.2

disturbed by those obstacles. Saltating sand entering the field was not observed, but suspended dust from other areas was clearly moving into the field during periods of strong storms.

Measurements

Wind speed was recorded with a Gill UVW propeller anemometer (R.M. Young Co., model 27005), which measures three orthogonal components of the wind vector. It consists of propellers with a diameter of 0.22 m, attached to the anemometer by shaft extensions with a length of 0.45 m. The anemometer was installed at 3 m above the soil surface, which means that the horizontal components U and W were measured at 2.95 and 3.05 m, respectively, and the vertical component V at 3.45 m. Use was made of expanded polystyrene propellers, which have a distance constant of 1.0 m. The propeller responds only to that component of the wind which is parallel to its axis of rotation, and off axis response closely approximates a cosine curve. The propeller does not rotate when wind flow is perpendicular to its axis. The range of wind speeds that can be measured is from 0.3 to 25.0 m s^{-1}. The analog DC voltage signals of the three sensors were sampled with a CR10 datalogger (Campbell Scientific Ltd.). Since the anemometer was new, it was not calibrated prior to field installation. The recorded signals were converted to wind speeds by using the calibration constant given by the manufacturer.

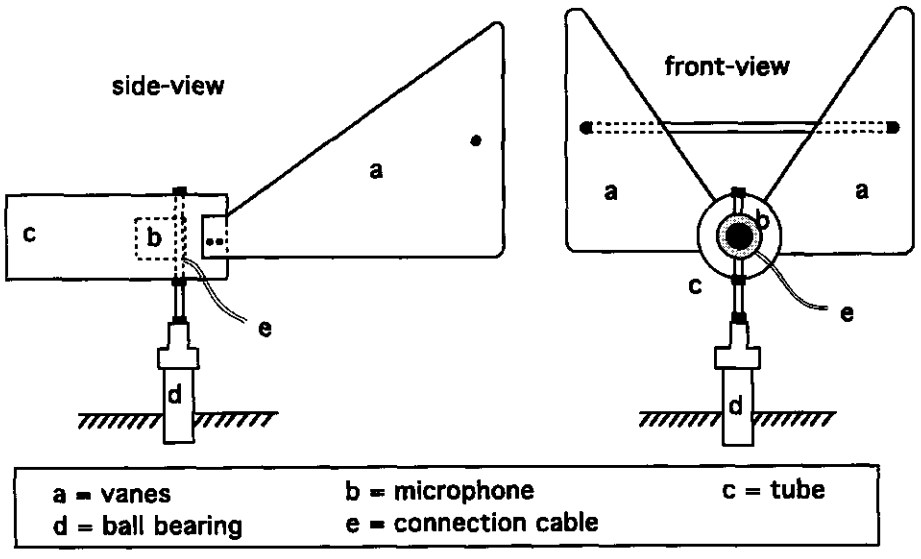

Figure 1. The saltiphone.

Saltation transport was measured with three saltiphones. The saltiphone is a robust saltation sensor that records particle impacts with a microphone. A detailed description of the device was given by Spaan and Van den Abeele (1991). It consists (Fig. 1) of a microphone with a membrane of 201 mm^2, placed inside a stainless steel tube (diameter = 0.05 m, length = 0.13 m). The tube is mounted on a ball bearing and is continuously positioned into the wind by two vanes at the back.

Some of the soil particles moving through the tube hit the membrane of the microphone. The frequency of the created signals depends on the momentum of the impacting particles. High frequency signals are formed by high momentum particles, like saltating sand grains. By amplifying high frequencies and filtering low frequencies, the signals created by saltating sand can be distinguished from other noises, created for instance by wind or suspended dust. The amplified signal of a particle impact produces a pulse that is cut off after 1 ms. Each time a pulse is generated, no other particle impact can be detected. So, theoretically, the maximum number of particle impacts that can be detected is 1000 per second. The actual number of particle impacts can be higher than the number of counted pulses, due to overlap of particle impacts during the same pulse. The output of the saltiphone (S) in counts per unit of time, therefore, is a relative measure of the saltation flux at the height of the microphone. Wind tunnel tests with the saltiphone (Sterk, 1993) showed that the pulse count rate is linearly related to the measured mass flux at the same height (Fig. 2). However, the range of mass fluxes during those experiments was somewhat narrow, and it is uncertain whether the relationship is still valid for higher and lower fluxes.

Three saltiphones were installed in the field. All three sensors were positioned around the UVW anemometer, at 2.0 m from the mast in northern, eastern and southern directions. The height of the center of the microphones above the soil surface was 0.10 m. The saltiphones were connected to a pulse count expansion (SDM-SW8A) on the CR10 datalogger. The maximum input frequency of the SDM-SW8A pulse channels is 100 Hz, which is not sufficient for the saltiphone. In order to reduce the number of incoming pulses, a self-constructed pulse divider was placed between the saltiphone and the datalogger. Of every ten incoming pulses, nine were filtered and only one was sent to the datalogger. In the output, the number of pulses was multiplied again by ten. Furthermore, an automatic rain gauge (tipping-bucket) was installed to determine the exact moment of onset of rainfall. All sensors, UVW anemometer, saltiphones, and rain gauge, were sampled with a frequency of 1 Hz.

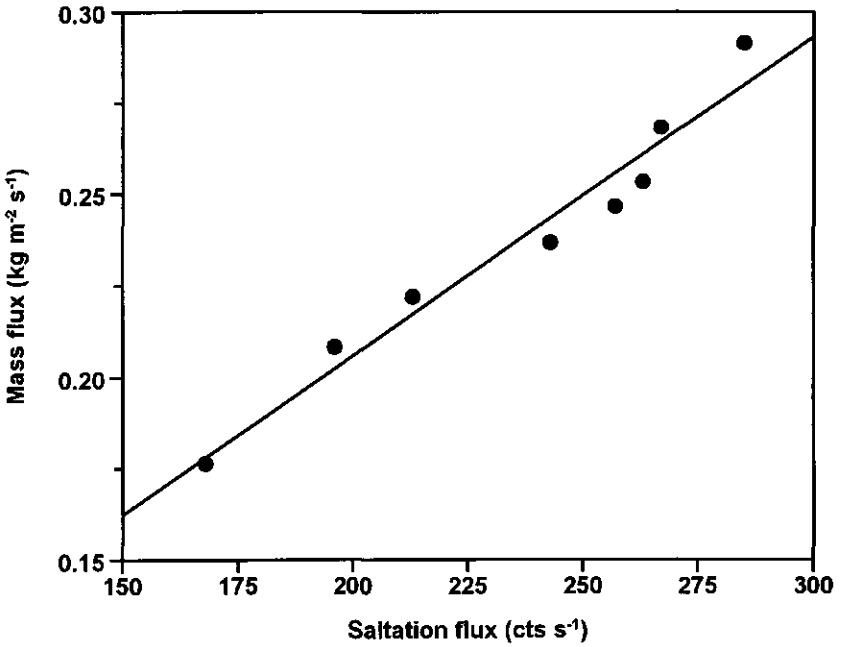

Figure 2. Relationship between saltation flux, measured with a saltiphone, and mass flux, measured with a sediment trap in a wind tunnel.

Analytical Procedure

From the three measured wind components, the instantaneous wind vector F and its direction ω were calculated, with ω being the angle of F relative to the north. The mean wind vector $\overline{F}$ and its direction $\overline{\omega}$ were calculated for the storm duration, or for periods of 10 min, in case of storms with a long duration. A new orthogonal coordinate system was chosen with the positive x-axis parallel to the surface in the direction $\overline{\omega}$ of the mean flow $\overline{F}$, the positive y-axis normal to the surface in upward direction, and the positive z-axis parallel to the surface to the right of the positive x-axis. The instantaneous velocity components U, V, and W were converted to the new components u, v, and w, with u being the instantaneous velocity parallel with x, v the instantaneous velocity parallel with y, and w the instantaneous velocity parallel with z.

The instantaneous velocity components were decomposed into an average and a fluctuating, turbulent part: $u = \overline{u} + u'$; $v = \overline{v} + v'$; $w = \overline{w} + w'$. By definition, $\overline{w}$ is zero, whereas $\overline{v}$ will be close to, but not necessarily equal to zero. Within a convective storm moving ahead of a cumulonimbus cloud, strong updrafts exist that locally result in a positive $\overline{v}$ component. This is equivalent to saying

that the vertical component of the turbulence exerts a net upward fluid force, which appears to explain why dense mineral particles can be transported in suspension by a turbulent wind (Allen, 1994). The time-averaged velocity fluctuations $\overline{u'}$, $\overline{v'}$, and $\overline{w'}$ are zero by definition. The time-averages of the squares and mixed products, however, are non-zero, and create the Reynolds stresses. The average stress component $\overline{\tau}_{xy} = -\rho\,\overline{u'v'}$ (N m^{-2}) gives the streamwise shear stress in a horizontal plane, and is usually considered to be directly related to sediment transport dynamics. Dividing the shear stress by the fluid density (ρ) gives the average kinematic stress $-\overline{u'v'}$ (m^2 s^{-2}), while the corresponding instantaneous values of kinematic stress are represented by $-u'v'$. In the next sections of this paper, emphasis will be on the instantaneous and average values of the streamwise kinematic stress.

For the detection of turbulent flow structures, use was made of the quadrant technique (Wallace et al., 1972). In an Eulerian system, the four discrete categories of momentum exchange, ejection, sweep, inward interaction, and outward interaction, were defined on the basis of the relative signs of u′ and v′ (Fig. 3). In order to avoid the problem of assigning a discrete structure to individual low magnitude stress contributions purely on the basis of the values of u′ and v′, a threshold criterion was defined. Only those events that exceeded the average kinematic stress by at least one standard

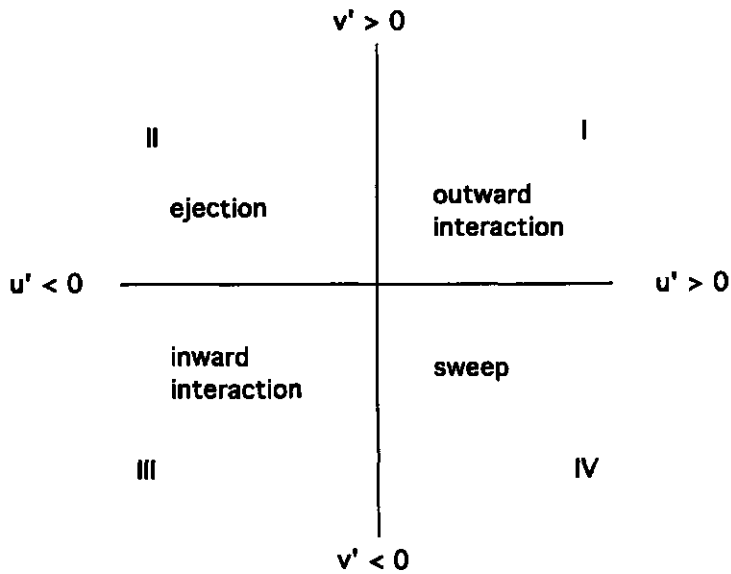

Figure 3. Quadrant plot of four discrete momentum exchange structures, based on the turbulent velocity fluctuations in horizontal (u′) and vertical (v′) directions.

deviation (σ)were identified as structures. Thus, instantaneous contributions to the average kinematic stress in the interval $[-\overline{u'v'} - \sigma, -\overline{u'v'} + \sigma]$ were not assigned by a momentum exchange category from Fig. 3.

RESULTS AND DISCUSSION

A total of 20 storms was recorded during the 1994 and 1995 rainy seasons. Of the collected data, only those periods with more or less continuous saltation transport and without rainfall were used for the analysis. Two typical storms on 27 June 1994 (storm 1) and 25 June 1995 (storm 2), both with a duration of about 10 min and nearly similar average wind speeds (Table 2), were selected. During both storms the wind direction was east, hence, the data from the saltiphone east of the UVW anemometer was used for the analysis.

In Fig. 4, plots of recorded wind speed and saltation response are given for the two storm events. Individual fluctuations in wind speed display a range of periods, or frequencies in the turbulence spectrum. Low frequency oscillations with a periodicity of several minutes are evident as well as short gusts with a duration of 1 to 5 s. The size of the smallest quasi-horizontal structures or eddies that can be detected from the data is determined by the used sampling frequency (1 Hz) and the average wind speed. The wavelength of the smallest detectable structures is equal to the product

Table 2. Descriptive statistics† of wind parameters and saltation transport during two storms at ICRISAT Sahelian Center.

	27 June 1994					25 June 1995				
	F	u′	v′	-u′v′	S	F	u′	v′	-u′v′	S
	m s^{-1}	m s^{-1}	m s^{-1}	m^2 s^{-2}	cts s^{-1}	m s^{-1}	m s^{-1}	m s^{-1}	m^2 s^{-2}	cts s^{-1}
Mean	9.67	0	0	0.41	97.7	9.49	0	0	0.36	42.4
Median	9.45	-0.22	0.02	0.09	40.0	9.41	-0.11	-0.03	0.11	10.0
Stand. dev.	2.31	2.33	0.62	1.49	119.4	2.15	2.15	0.57	1.23	66.5
Skewness	0.44	0.48	0.08	0.94	1.34	0.23	0.22	-0.08	2.17	2.53
Kurtosis	-0.31	-0.28	1.53	5.63	1.11	-0.57	-0.59	2.85	17.49	7.91
Range	12.63	12.65	5.37	15.44	520.0	10.94	10.75	5.59	18.39	480.0
Min	4.59	-4.98	-2.71	-7.83	0	4.06	-5.35	-3.03	-6.82	0
Max	17.22	7.68	2.66	7.62	520.0	15.00	5.39	2.56	11.57	480.0

† F is the wind speed; u′ and v′ are the horizontal and vertical turbulent velocity fluctuations; -u′v′ is the kinematic stress; S is the saltation flux.

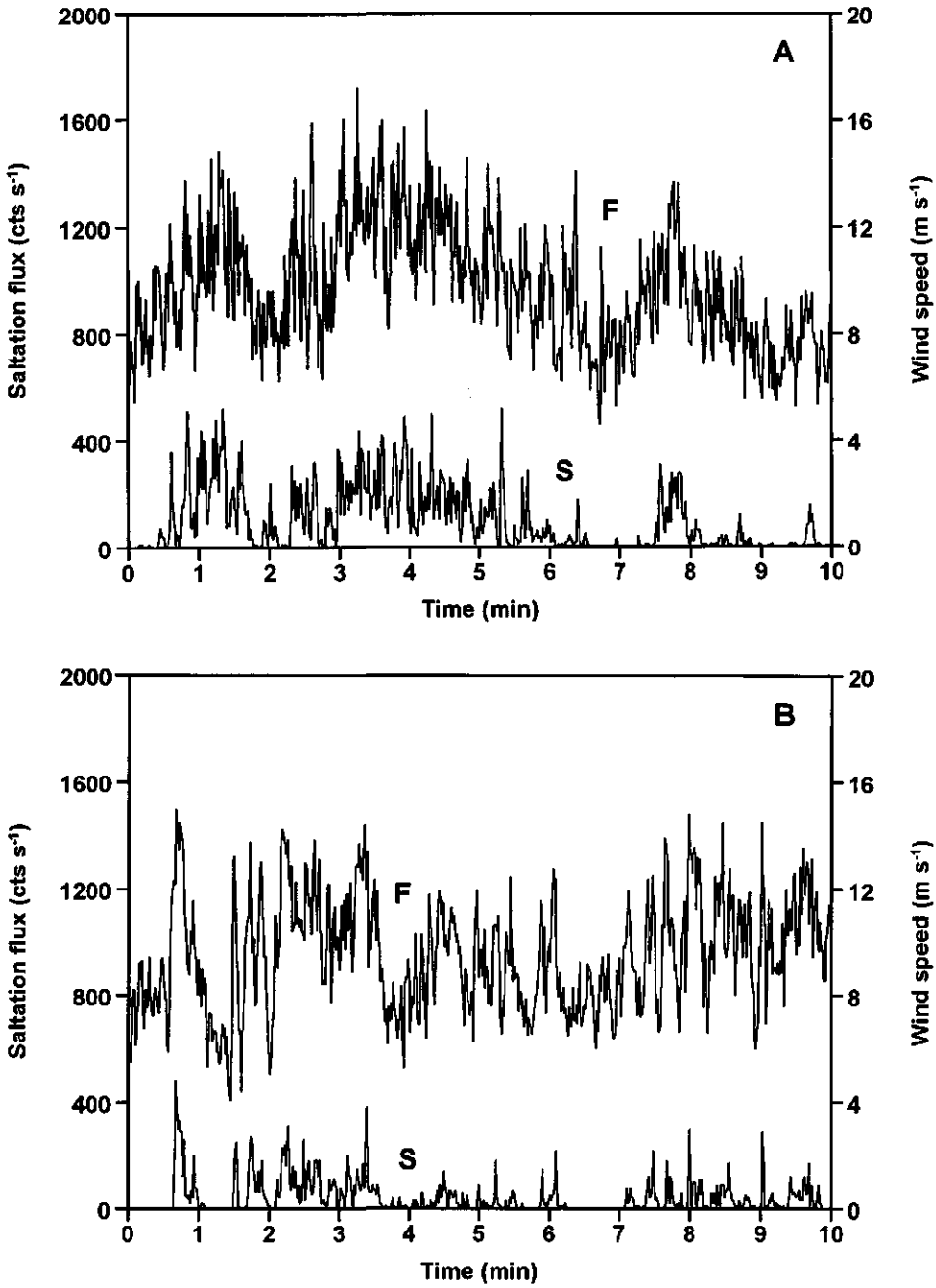

Figure 4. Records of wind speed (F) and saltation flux (S) for two Sahelian wind erosion events at ICRISAT Sahelian Center on (A) 27 June 1994 and (B) 25 June 1995.

of the average wind speed and the sampling period. For both storms, the minimum size is approximately 9.5 m. Hence, it is assumed that the smallest quasi-horizontal eddies detected at 3 m height were large enough to cause at the same time strong horizontal velocity fluctuations near the soil surface. A detailed analysis of the turbulent structures, i.e. a spectral analysis of the turbulent frequency spectrum, will be described in a separate paper. Here, emphasis is on the saltation response to wind speed and shear stress fluctuations.

The two plots in Fig. 4 clearly show that the saltation flux was intermittent in nature, with sporadic bursts of intense saltation transport immediately followed by periods without transport. The flow conditions during both storms were only slightly above threshold, and as a result saltation transport occurred only during gusts of varying durations. The saltation system responded quickly to wind speed fluctuations, and in general, a good relationship between instantaneous wind speed and saltation flux exists. Correlation coefficients (r) for the two storms are 0.65 and 0.57, respectively. The correlation is slightly better when the saltiphone recordings are assumed to lag 1 s behind wind speed (0.71 and 0.65). With an assumed lag of 2 s the r-values are 0.64 and 0.60, respectively, and decrease rapidly with increasing lag. The better correlation at a lag of 1 s indicates that the response time of the saltation system is in the order of 1 s due to inertia effects. This result is in accordance with the response time as it was calculated from numerical simulations by Anderson and Haff (1988), and was confirmed by experiments of Butterfield (1991).

From the data, the threshold wind speed conditions for initiation and cessation of saltation transport could be determined. The threshold wind speed at initiation of saltation was defined by Bagnold (1973) as the fluid threshold, i.e. the threshold at which sand movement starts owing to the direct force of the fluid only. The threshold wind speed at which saltation ceases is similar to Bagnold's impact threshold, which was defined as the threshold wind speed at which an initial disturbance of the sand becomes a continuous movement downwind. In other words, the wind alone is insufficient for continuous saltation transport, but saltation is sustained by the combined action of the wind force and the impacts of descending grains.

During both storms, periods of continuous saltation transport alternated with periods of no transport (Fig. 4). By selecting each isolated period of continuous saltation, the wind velocities at initiation and cessation of saltation transport were determined. On average, saltation started at 8.48 m s^{-1} (fluid threshold) and ceased at 7.66 m s^{-1} (impact threshold) during the first storm. During the second storm, the average fluid threshold was 9.60 m s^{-1} and the impact threshold was equal

to 8.45 m s^{-1}. The higher threshold conditions during the second storm can be explained by wetting of the topsoil due to a light rain (2.0 mm) some 36 h earlier. Soil moisture causes water films surrounding the soil particles that create cohesive forces between the particles. The wind force required to lift particles from a moist surface is therefore higher than during dry conditions (Chepil, 1956). This also explains the lower average saltation flux during the second storm (Table 2).

The instantaneous contributions to the average kinematic stress for both storms are shown in Fig. 5. The average stress is the result of short but intense positive contributions, superposed on negative and weaker positive contributions. The instantaneous stress levels could be 10 to 20 times stronger than the average stress level, but they occurred only during a very limited period of time. This intermittency in stress production occurs despite the fact that u' and v' are approximately Gaussian distributed (Table 2) and randomly fluctuating quantities when taken separately. The small deviations from the normal distribution cause a non-normal distribution of the kinematic stress, which is typical for turbulence (Panofsky and Dutton, 1984). The kinematic stress distribution is characterized by a positive skew (Table 2), indicating a relatively frequent occurrence of extreme values.

The kinematic stress events that exceeded the average value by at least one standard deviation were classified as turbulent flow structures according to Fig. 3. Some characteristics of the structures are given in Table 3. Of the average stress at sensor level, the classified structures accounted for 63.5% during the first storm, and 56.0% during the second storm. The percentage of time during which the structures were active was only 20.6% for the first, and 15.8% for the second storm. Sweeps and ejections were 25% more frequent than the inward and outward interactions. Also, the positive contributions to the shear stress by sweeps and ejections were about 70% stronger than the negative stress contributions, resulting in an overall positive shear stress.

A well defined relationship between the instantaneous kinematic shear stress and saltation flux does not exist. The correlation coefficients for both storms are 0.12 and 0.14, respectively, and when the saltation flux is assumed to lag 1 s behind kinematic stress, the coefficients are 0.05 and 0.15, respectively. Also, no correlation between kinematic shear stress and saltation flux exists when only the time periods with classified turbulent structures are considered. However, mean saltation fluxes for the four classified structures (Table 3) reveal that sweeps (class 4) and outward interactions (class 1) were associated with high saltation fluxes, whereas their stress contributions were positive and negative, respectively. Ejections (class 2) and inward interactions (class 3) were

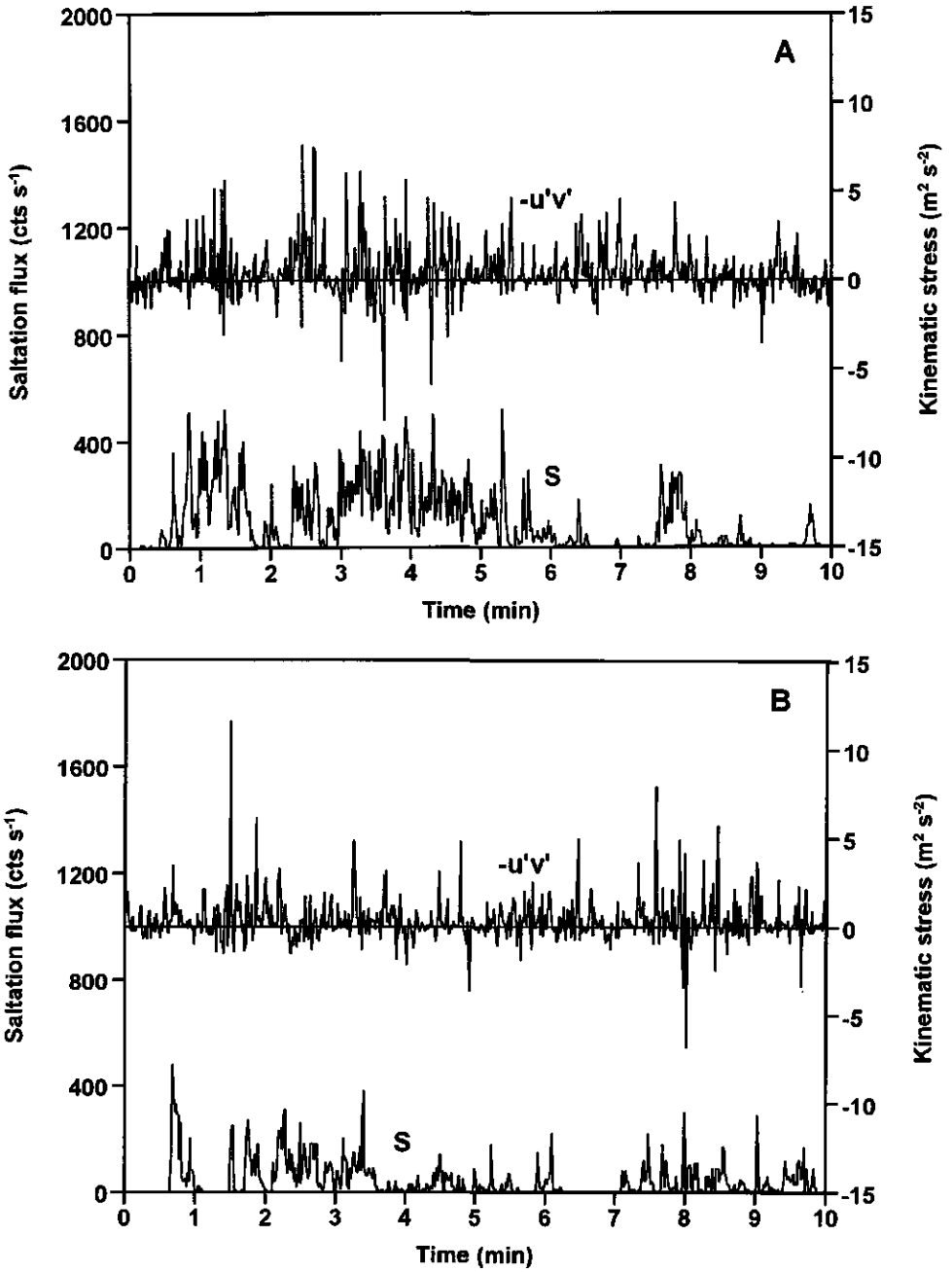

Figure 5. Plots of instantaneous kinematic stress (-u'v') and saltation flux (S) for two Sahelian wind erosion events at ICRISAT Sahelian Center on (A) 27 June 1994 and (B) 25 June 1995.

Table 3. Characteristics of four classified turbulent structures.

Date	Number of events				Mean duration				Mean stress				Contribution to average stress				Mean saltation flux			
					s				$m^2 s^{-2}$				%				cts s^{-1}			
	1†	2†	3†	4†	1	2	3	4	1	2	3	4	1	2	3	4	1	2	3	4
27-6-1994	19	24	21	31	1.32	1.42	1.10	1.35	-2.33	2.91	-1.54	3.65	-23.4	39.7	-14.3	61.5	256.8	23.2	19.6	241.7
25-6-1995	14	24	18	23	1.14	1.25	1.00	1.35	-1.92	2.67	-1.42	3.15	-14.2	36.9	-11.8	45.1	65.0	3.3	15.6	126.8

† 1 = outward interaction; 2 = ejection; 3 = inward interaction; 4 = sweep.

not capable of supporting appreciable saltation transport. Obviously, instantaneous contributions to the shear stress were of little significance in terms of saltation transport.

Sweeps and outward interactions have in common that u′ is positive (Fig. 3), meaning that the instantaneous horizontal wind speed is higher than average. Ejections and inward interactions have negative u′ values, or lower than average horizontal wind speeds. Correlation coefficients between u′ and saltation flux are exactly the same as the earlier given correlation coefficients between wind speed (F) and saltation flux (0.65 and 0.57), whereas the correlation between v′ and saltation flux is weak (-0.18 and -0.22). This is also illustrated in Fig. 6, where u′, v′, and the saltation flux during the first 3 min of the second storm are given. The close correspondence between u′ and the saltation flux is clear. The value of v′ tended to be negative during periods with saltation transport, but many exceptions can be found as well. These results suggest that the horizontal velocity fluctuations are of much more importance for saltation transport than the vertical velocity fluctuations.

In the foregoing analysis, instantaneous saltation flux was related to shear stress fluctuations measured at 3 m, assuming similar shear stress fluctuations being active near the soil surface at the same time. It is doubtful whether this assumption is correct. A similar assumption was made

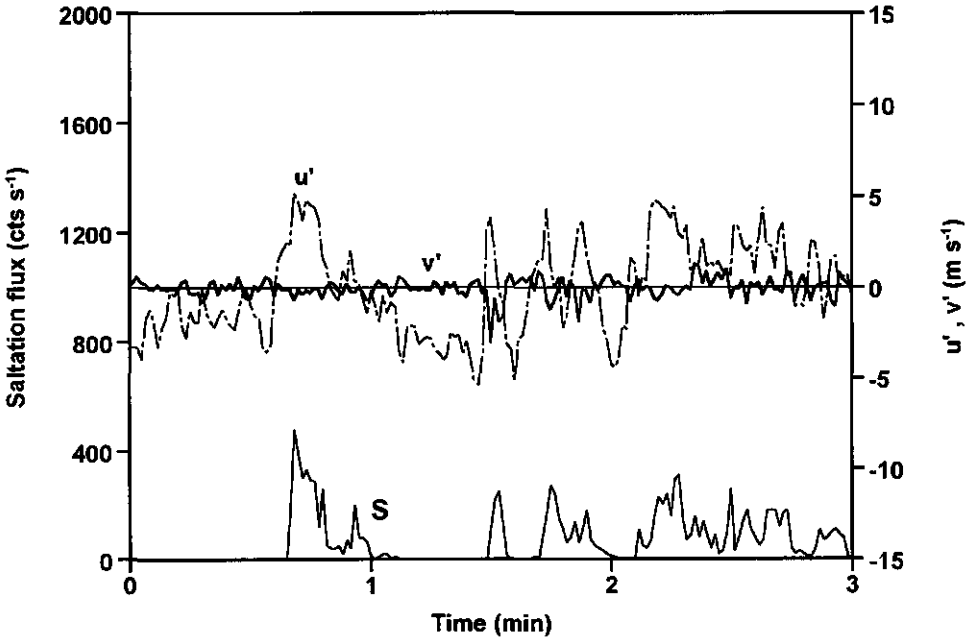

Figure 6. Saltation flux (S) in relation to the horizontal (u′) and vertical (v′) turbulent velocity fluctuations during the first 3 min of a storm event at ICRISAT Sahelian Center on June 25, 1995.

for the instantaneous wind speed, and the minimum size (9.5 m) of detectable quasi-horizontal eddies indicates that this assumption was correct. Hence, positive u′ values at 3 m were associated with positive values near the soil surface. A positive v′ at 3 m does not necessarily mean that v′ near the soil surface was positive as well. The vertical velocity fluctuations are produced by small eddies, the diameter of which are of the order of the height above the ground (Panofsky and Dutton, 1984). So, the observation of a downward moving eddy at 3 m does not necessarily mean that at the same time the shear stress created by the eddy was felt at the soil surface. Furthermore, such an eddy was moved horizontally with the average wind speed, which was an order of magnitude higher than the vertical wind speeds (Table 2), resulting in shear stress at the soil surface downwind of the anemometer. This uncertainty may have obscured the shear stress - saltation flux relationship. For instance, the data presented here do not show an exclusive role of sweeps for the initiation of saltation movement, as suggested by Grass (1983). More detailed measurements of instantaneous shear stress near the soil surface would possibly reveal that sweeps are the principal structures associated with initiation of saltation transport.

Despite the uncertainty in the shear stress - saltation flux relationship, it is concluded that for saltation transport the horizontal wind speed component is of much more significance than the vertical component. Turbulent structures with a positive u′ component, sweeps and outward interactions, are able to initiate and sustain saltation transport, whereas structures with a negative u′ component do not. Apparently, it is not the streamwise shear stress component but the horizontal drag force, which is proportional to u^2, is the driving force for saltation sand transport. The same was concluded for bed-load transport above a sea bed (Heathershaw and Thorne, 1985; Thorne et al., 1989). This conclusion suggests that saltation transport should not be predicted on the basis of shear stress (or friction velocity) alone, as most of the current transport equations do (Greeley and Iversen, 1985). It would be more useful if horizontal wind speed and its fluctuations, for instance described by the average and standard deviation, were incorporated in saltation transport models.

CONCLUSIONS

Measured fluxes of wind-blown saltation sand transport during two convective storms in the Sahelian zone of Niger showed a high degree of intermittency. Fluctuations in saltation flux were directly related to the gustiness of the wind. The best correlation between instantaneous wind speed and saltation flux was obtained when the measured saltation flux was assumed to lag 1 s behind

wind speed. This result confirms that the response time of the saltation system is in the order of 1 s, as it was calculated by Anderson and Haff (1988).

During the two storms, classified turbulent structures accounted in isolation for 60% of the average shear stress at sensor level, but the active time was only 18%. Of the four turbulent structures that were distinguished by the quadrant technique (Fig. 3), only sweeps and outward interactions were able to initiate and sustain saltation transport. Sweeps resulted in positive contributions to the average shear stress, whereas outward interactions contributed negatively to the average shear stress. The two structures have in common that the horizontal wind speed component was higher than average. Not the streamwise shear stress, therefore, but the horizontal drag force was primarily responsible for saltation sand transport. This result indicates that saltation transport models should incorporate the horizontal wind speed and its fluctuations as driving variables, instead of using the shear stress or friction velocity alone, as many of the current models do.

ACKNOWLEDGMENTS

The research was funded by the Netherlands Foundation for the Advancement of Tropical Research (WOTRO). The logistic support of the ICRISAT Sahelian Center is gratefully acknowledged. We thank Gijs van den Abeele of the Wageningen Agricultural University for his help with construction and installation of the electronic field equipment.

REFERENCES

Allen, J.R.L. 1994. Fundamental properties of fluids and their relation to sediment transport processes. p. 25-60. *In* K. Pye (ed.) Sediment transport and depositional processes. Blackwell Scientific Publications, Oxford, UK.

Anderson, R.S., and P.K. Haff. 1988. Simulation of eolian saltation. Science 24: 820-823.

Bagnold, R.A. 1973. The physics of blown sand and desert dunes. 5th ed., Chapman and Hall, London.

Bisal, F., and K.F. Nielsen. 1962. Movement of soil particles in saltation. Can. J. Soil Sci. 42: 81-86.

Braaten, D.A., K.T. Paw U, and R.H. Shaw. 1990. Particle resuspension in a turbulent boundary layer - observed and modeled. J. Aerosol Sci. 21: 613-628.

Butterfield, G.R. 1991. Grain transport rates in steady and unsteady turbulent airflows. Acta Mech. [Suppl] 1: 97-122.

Butterfield, G.R. 1993. Sand transport response to fluctuating wind velocity. p. 303-335. *In* N.J. Clifford et al. (ed.) Turbulence: Perspectives on flow and sediment transport. John Wiley & Sons, Chichester, UK.

Chepil, W.S. 1956. Influence of moisture on erodibility of soil by wind. Soil Sci. Soc. Am. Proc. 20: 288-292.

Dyer, K.R. 1986. Coastal and estuarine sediment dynamics. John Wiley & Sons, Chichester, UK.

Grass, A.J. 1983. The influence of boundary layer turbulence on the mechanics of sediment transport. p. 3-18. *In* B.M. Sumer and A. Müller (ed.) Mechanics of sediment transport. Proceedings Euromech 156. Balkema, Rotterdam, The Netherlands.

Greeley, R., and J.D. Iversen. 1985. Wind as a geological process on Earth, Mars, Venus and Titan. Cambridge University Press, Cambridge, U.K.

Hardisty, J. 1993. Frequency analysis of sand transport in a turbulent air flow. p. 295-304. *In* N.J. Clifford et al. (ed.) Turbulence: Perspectives on flow and sediment transport. John Wiley & Sons, Chichester, UK.

Heathershaw, A.D. and P.D. Thorne. 1985. Sea-bed noises reveal the role of turbulent bursting phenomenon in sediment transport by tidal currents. Nature 316: 339-342.

Lapointe, M. 1992. Burst-like sediment suspension events in a sand bed river. Earth Surf. Proc. and Landforms 17: 253-270.

Lee, J.A. 1987. A field experiment on the role of small scale wind gustiness in aeolian sand transport. Earth Surf. Proc. and Landforms 12: 331-335.

Lyles, L., and R.K. Krauss. 1971. Threshold velocities and initial particle motion as influenced by air turbulence. Trans. ASAE 14: 563-566.

Müller, A., A. Gyr, and T. Dracos. 1971. Interactions of rotating elements of the boundary layer with grains of the bed: A contribution to the problem of the threshold of sediment transportation. J. Hydraulic Res. 9: 373-411.

Nearing, M.A., and S.C. Parker. 1994. Detachment of soil by flowing water under turbulent and laminar conditions. Soil Sci. Soc. Am. J. 58: 1612-1614.

Panofsky, H.A., and J.A. Dutton. 1984. Atmospheric turbulence: Models and methods for engineering applications. John Wiley & Sons, New York.

Shao, Y., M.R. Raupach, and P.A. Findlater. 1993. The effect of saltation bombardment on the entrainment of dust by wind. J. Geophys. Res. 98: 12719-12726.

Spaan, W.P., and G.D. van den Abeele. 1991. Wind borne particle measurements with acoustic sensors. Soil Technology 4: 51-63.

Sterk, G. 1993. Sahelian wind erosion research project, Report III. Description and calibration of sediment samplers. Dep. of Irrigation and Soil & Water Conservation, Wageningen Agric. Univ., The Netherlands.

Sumer, B.M., and R. Deigaard. 1981. Particle motions near the bottom in turbulent flow in an open channel. Part 2. J. Fluid Mech. 109: 311-337.

Sumer, B.M., and B. Oguz. 1978. Particle motions near the bottom in turbulent flow in an open channel. J. Fluid Mech. 86: 109-127.

Sutherland, A.J. 1967. Proposed mechanism for sediment entrainment by turbulent flows. J. Geophys. Res. 72: 6183-6194.

Thorne, P.D., J.J. Williams, and A.D. Heathershaw. 1989. In situ acoustic measurements of marine gravel threshold and transport. Sedimentology 36: 61-74.

Wallace, J.M.H., H. Eckelmann, and R.S. Brodkey. 1972. The wall region in turbulent shear flow. J. Fluid Mech. 54: 39-48.

Chapter 3

Comparison of Models Describing the Vertical Distribution of Wind-Eroded Sediment

G. Sterk and P.A.C. Raats

Published in: Soil Science Society of America Journal 60: 1914-1919. (1996).

Reproduced by permission of the Soil Science Society of America.

Comparison of Models Describing the Vertical Distribution of Wind-Eroded Sediment

ABSTRACT

For the study of field wind erosion, detailed observations of wind-blown sediment transport in the field are needed. The objective of this study was to determine the best method to quantify the mass of wind-blown material moving past a fixed point during four storms. Twenty-one Modified Wilson and Cooke (MWAC) sediment catchers were installed in a pearl millet (*Pennisetum glaucum*) field in the Sahelian zone of Niger, on a sandy, siliceous, isohyperthermic Psammentic Paleustalf. Each catcher trapped materials at seven heights between 0.05 and 1.00 m. The vertical profiles of measured horizontal mass fluxes were described by two different models, a three-parameter power function and a five-parameter combined model, which is a combination of an exponential function and a power function. For all four storms, both models described accurately the mass fluxes between 0.05 and 0.26 m, but fitted mass fluxes at 0.50, 0.75, and 1.00 m deviated from measured fluxes. Deviations were 21.1, 45.2, and 60.6% for the power function, and 12.4, 18.5, and 38.0% for the combined model. Mass transport rates were calculated by integrating the mass flux profiles across height. The differences in calculated mass transport rates were small, but because of the better fit, the combined model was preferred. Correcting for the trapping efficiency of the MWAC catchers (0.49) and multiplying by the storm duration resulted in total mass transport values, which are equal to the mass of soil passing a strip of 1 m width perpendicular to the mean wind direction. The average mass transport values were 102.7, 15.5, 31.8, and 149.8 kg m^{-1}, respectively, for the four storms.

Wind erosion is a common phenomenon in arid and semi-arid areas, which are extensive and comprise about one-third of the world's land area (Lal, 1990). The frequent dust storms in these areas may have a very spectacular character, showing nature's power in moving soil particles; at the same time, they can be devastating for agricultural systems. Wind erosion may damage crops by abrasion and burial in sand. It also gives rise to soil degradation in the source areas by the loss of fertile topsoil. Deposition of wind-blown sand may create problems of sand dune formation in or at some distance from the source area.

In the wind erosion process, three different modes of transport can be distinguished: creep, saltation, and suspension (Bagnold, 1973). Particles transported by creep are too heavy to be lifted from the surface and so they roll or slide along the ground. Particles transported by saltation are

smaller than particles transported by creep. They move in series of short hops at heights generally well below 1 m. The smallest particles move in suspension. These particles may be carried with vertical winds to great heights and are subject to long range transport. Under typical conditions, Hudson (1973) suggests that particle diameters vary from 0.5 to 2 mm for creep, vary from 0.05 to 0.5 mm for saltation, and are smaller than 0.1 mm for suspension. The overlap in diameters for suspension and saltation indicates that certain particles may be moved by different transport modes, depending on the particle density and the wind speed. So, the amounts of material transported by the three modes depend on wind speed, particle density, and the texture of the topsoil. According to an estimate of Chepil (1945), the proportions vary from 50 to 75% in saltation, from 3 to 40% in suspension and from 5 to 25% in surface creep.

For the study of field wind erosion and the design and evaluation of wind erosion control techniques, detailed observations of wind erosion processes are needed. Wind-blown particle transport in the field is usually sampled with sediment catchers (e.g., Bagnold, 1973; Wilson and Cooke, 1980; Fryrear et al., 1991). Although the catchers described in the literature differ in size and shape, they generally consist of a vertical array of sediment traps. During a wind erosion event, each trap collects moving material at a certain height. From the weight of the trapped materials and the storm duration, horizontal mass fluxes are calculated. A mass transport rate at the point of observation is obtained by integrating the mass flux profile across height. Several models for the vertical distribution of horizontal mass flux were described in the literature.

According to Vories and Fryrear (1991), the relationship between horizontal mass flux and height can be described by:

$$q(z) = az^{-b} + c\exp(-dz) \qquad [1]$$

where q(z) (kg m^{-2} s^{-1}) is the mass flux at height z (m) and a, b, c, and d are regression coefficients. The first term at the right is considered to describe the suspension mass flux (Nickling, 1978), whereas the second term is supposed to describe the saltation mass flux, including creep (Fryrear and Saleh, 1993). A problem with the first term on the right side of Eq. [1] is that it causes the mass flux to go to infinity when z approaches zero, because the exponent in the power function is negative. Extrapolation to the soil surface gives unrealistic values of the mass flux near and at the soil surface (Vories and Fryrear, 1991). This problem can be solved by introducing a constant length α in the power function:

$$q(z) = a'(z + \alpha)^{-b'} + c\exp(-dz) \qquad (\alpha > 0) \qquad [2]$$

Equation [2] can be rewritten as:

$$q(z) = a''(\frac{z}{\alpha} + 1)^{-b'} + c\exp(-\frac{z}{\beta}) \qquad (\alpha > 0) \qquad [3]$$

where $a'' = a'\alpha^{-b'}$. Like c, the coefficient a'' has dimensions of mass flux (kg m^{-2} s^{-1}). The sum of the coefficients a'' and c represents the maximum mass flux at $z = 0$. The coefficient b' (dimensionless) and the length scale β (m) can be interpreted as measures of the decrease in mass flux with height.

Equation [3] is a general, combined mass flux model that describes the vertical distribution of horizontal mass fluxes from the soil surface to any height. It combines a modified power function and an exponential function. The exponential function was used in several wind tunnel studies to describe saltation mass flux profiles (e.g., Horikawa and Shen, 1960; Williams, 1964). Under natural conditions, with moving sediments being a mixture of saltation and suspension material, an exponential function is not sufficient, since it is restricted to saltation transport only (Fryrear and Saleh, 1993). The modified power function resembles the mass flux model first used by Zingg (1953):

$$q(z) = q_0(\frac{z}{\sigma} + 1)^{-p} \qquad [4]$$

where q_0 is the mass flux at $z = 0$, σ is a length scale, and p is a dimensionless exponent. Equation [4] is supposed to adequately describe the vertical profile of horizontal mass flux from the soil surface to any height (Zingg, 1953; Fryrear et al., 1991). On the other hand, the theoretically derived model of Scott et al. (1995) reveals that a power function is only valid for conditions where the mass per unit of volume of air containing the driving grains is constant in the vertical. This restricts the applicability of such a function to material moving in suspension, and thus they included a separate (logarithmic) saltation term to describe the full profile. Fitting their combined model to wind tunnel data showed, however, that the inclusion of the saltation term resulted in only a slight improvement in the fit compared with the more simple, power function. It was concluded that the extra term can be ignored as far as the concentration profile is concerned.

The purpose of this study is to quantify the wind-blown soil mass moving past a fixed point in a Sahelian pearl millet field, by using a simple, low cost, sediment catcher. Two mass flux profile

models, the combined mass flux model (Eq. [3]) and the modified power function (Eq. [4]), were applied for calculating mass transport rates. The models were tested on their performance of fitting the mass flux profiles through measured data.

MATERIALS AND METHODS

Sampling

Wilson and Cooke (1980) developed a wind erosion sampler that traps moving material at six heights between 0.15 m and 1.52 m. Each trap consists of a plastic bottle with an inlet and an outlet glass tube, mounted on a wind vane that rotates about a central pole. The vanes assure that the inlet tubes point into the wind. Wind-borne particles enter through the inlet, air escapes through the outlet, and the sediment is collected in the bottle.

Using the same principle, Kuntze et al. (1990) connected six similar traps to a frame of copper tubes, and named it the Modified Wilson and Cooke (MWAC) sediment catcher. The inlet and outlet tubes of the sample bottles are glass tubes with an internal diameter of 8.0 mm, resulting in an opening of 50.3 mm^2. The differences with the original Wilson and Cooke catcher are the horizontal position of the bottles, instead of a vertical position, and the use of only one large vane. The construction is simple and cheap, and operation in the field is easy. In this study, the MWAC catcher was used for field measurements. A seventh trap was added, and the intended measuring heights were 0.05, 0.12, 0.19, 0.26, 0.50, 0.75, and 1.00 m above the soil surface (Fig. 1), but these changed (5 - 20 mm) after soil surface changes. The height range assured that the trapped materials were a mix of saltation and suspension particles. Creep particles were not trapped.

Twenty-one MWAC catchers were installed in an experimental plot of 40 by 60 m within a pearl millet field at the International Crops Research Institute for the Semi-Arid Tropics (ICRISAT) Sahelian Center (ISC). The center is located at Sadoré (13°16'N;2°21'E) in southwest Niger, 45 km south of the capital Niamey. The climate at ISC is typical for the Sahelian zone of West Africa, with high temperatures all year round and one rainy season. Rainfall in the first half of the rainy season (May - July) is often preceded by short periods (typically 10 - 30 min) of strong winds, leading to severe erosion on unprotected soils.

The soil at the measurement field is a sandy, siliceous, isohyperthermic Psammentic Paleustalf of the Labucheri soil series (West et al., 1984), with 92.2% sand, 3.0% silt, and 4.8% clay. The size distribution of dry undispersed particles, including aggregates, of the topsoil (Table 1) is such

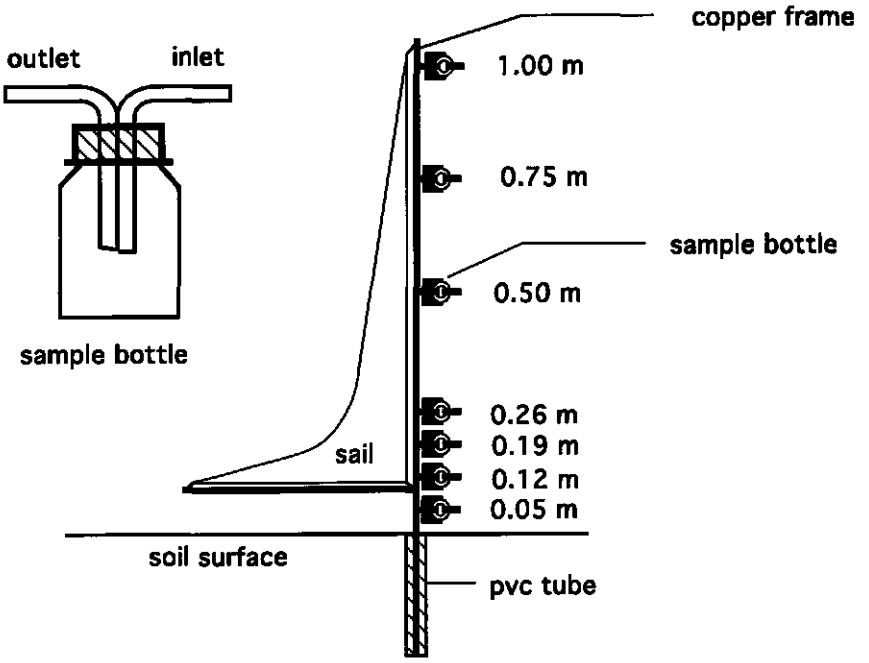

Figure 1. The Modified Wilson and Cooke sediment catcher (pvc = polyvinyl chloride).

Table 1. Aggregate size distribution† of topsoil at the ICRISAT Sahelian Center.

Size class	Mass
µm	%
< 63	3.1
63 - 125	18.2
125 - 250	35.7
250 - 500	32.8
500 - 1000	10.0
> 1000	0.2

† The size distribution of dry undispersed particles determined by dry sieving with a set of vibrating sieves.

that soil particles can be transported in either of three transport modes: creep, saltation, and suspension. The whole field was uniformly covered with millet stalks of the previous year crop. The amount of crop residues was equal to 800 kg ha^{-1}, corresponding to an estimated soil cover of 3.5%. The

field was surrounded by roads and other fields in which obstacles like trees and bushes were present. The distance from the experimental plot to upwind obstacles exceeded in all cases 20 times the height of the obstacle. Hence, it was assumed that the disturbance of the wind field in the plot was negligible during a storm. Saltating sand moving over the roads into the measurement field was not observed, but suspended dust was clearly entering the field during heavy storms.

Wind Tunnel Calibration

Before using the catcher in the field, it was tested and calibrated in the wind tunnel of the Research Institute for Agrobiology and Soil Fertility at Haren, The Netherlands (Sterk, 1993). The soil used for the calibration was from ISC. The overall trapping efficiency η of the MWAC catcher is defined as the ratio of measured (or calculated) mass transport rate, Q (kg m^{-1} s^{-1}) and total mass transport rate, Q_t (kg m^{-1} s^{-1}), measured in the wind tunnel:

$$\eta = \frac{Q}{Q_t} \qquad [5]$$

The measured mass transport rate was obtained by integrating the vertical profile of measured mass fluxes across height. The total mass transport rate was obtained by weighing the loss of soil from trays during simulation of a storm. The average overall trapping efficiency from 12 runs with wind speeds ranging from 9.9 to 11.5 m s^{-1} was 0.49, with a standard deviation of 0.03 (Sterk, 1993). The trapping efficiency showed no relation with wind speed. However, the efficiency of a wind erosion sampler may be particle size dependent because saltating sand grains are easier to trap than suspended dust (Shao et al., 1993). Therefore, a higher proportion of the moving material may be collected with the lowest traps compared with the highest traps, due to a relative increase in suspension-size particles with height. Apart from a lower trapping efficiency, the quantities of trapped material at 0.50, 0.75, and 1.00 m are very small, usually <1 g, which may potentially result in a large error in calculated fluxes. Nevertheless, it was assumed that (i) the overall trapping efficiency, as it was determined in the wind tunnel, may be used for calculating the total mass transport rate (Q_t), and (ii) the value of Q_t is not greatly influenced by the increase in experimental error with height since the low mass fluxes at the higher levels contribute little to the total mass transport rate.

Calculation of Total Mass Transport

From the weights of the trapped materials and the storm duration, mean horizontal mass fluxes, q(z) (kg m^{-2} s^{-1}), at height z (m) were calculated. Fitting Eq. [3] and [4] through the measured mass fluxes can be done with any nonlinear regression procedure. In this study, each sediment catcher provided seven data points, which is sufficient for fitting an equation with three regression coefficients, like Eq. [4]. It is questionable whether an equation with five regression coefficients, like Eq. [3], may be fitted from such a limited data set. Therefore, the number of coefficients in the regression analysis was reduced to four by fixing one. The coefficient α is a length parameter for shifting the curve across height, and it was assumed that it can be set at a constant length. As a first approximation α was set at 1 m. The sensitivity of the model for different values of α will be tested later in the paper. Equation [3] then reduces to:

$$q(z) = a''(z' + 1)^{-b'} + c\exp(-\frac{z}{\beta}) \qquad [6]$$

where $z'(=z\alpha^{-1})$ is a dimensionless height. The NONLIN module of the SYSTAT statistical package, which makes use of a quasi-Newton minimization method (Wilkinson, 1987), was applied for fitting Eq. [4] and [6] through the measured mass fluxes.

The curves were not extrapolated toward heights >1 m, since no observations of suspended mass fluxes above 1 m were available. It was assumed that the contribution of suspension transport above the 1 m level to the total mass transport is negligible. Integration of Eq. [4] and [6] across height (from z = 0 to z = 1 m) resulted in measured (or calculated) mass transport rates Q (kg m^{-1} s^{-1}) at the point of sampling. The total mass transport rate Q_t (kg m^{-1} s^{-1}) was obtained by dividing Q by the overall trapping efficiency η. Multiplying Q_t by the storm duration resulted in a total mass transport value M (kg m^{-1}), which is equivalent to the mass of soil passing a strip of 1 m width perpendicular to the mean wind direction.

RESULTS AND DISCUSSION

During the 1993 rainy season there were only four wind erosion events. Compared with the three previous years, with 21, 13, and 15 wind erosion events, respectively (Michels, 1994), the season represented a weak wind erosion season. The dates, durations, and wind conditions of the four storms are given in Table 2.

Table 2. Date, duration, and average values of wind speed and wind direction during four storms at ICRISAT Sahelian Center, 1993 rainy season.

Date	Duration	Wind speed†	Wind direction
	s	m s^{-1}	
13 June	1481	10.3	SE
27 June	1320	7.6	S
30 June	1321	8.9	SE
1 July	3004	9.2	SSE

† Mean wind speed measured at 2 m.

For every catcher and storm, a curve was fitted through the measured mass fluxes. Fitting of the modified power function (Eq. [4]) gave no problems, but the success of fitting Eq. [6] through the seven mass fluxes appeared to be dependent on the starting values for the regression coefficients in the NONLIN program. For obtaining a first estimate of the values of a'', b', c, and β, the method described by Fryrear and Saleh (1993) was used. Through measured fluxes from the four highest sample bottles (z = 0.26, 0.50, 0.75, and 1.00 m), a modified power function (Eq. [7]) was fitted resulting in two estimates (a''' and b'') of the regression coefficients a'' and b' in Eq. [6]:

$$q(z) = a'''(z' + 1)^{-b''} \qquad z' \geq 0.26 \qquad [7]$$

The estimates c' and β' of c and β (Eq. [6]) were obtained by fitting an exponential function through the fluxes measured at the three lowest positions (z = 0.05, 0.12, and 0.19 m):

$$q(z) = c' \exp(-\frac{z}{\beta'}) \qquad z < 0.26 \qquad [8]$$

The values of a''', b'', c' and β' were used as starting values for fitting Eq. [6] through the measured mass fluxes.

Comparing the modified power function (Eq. [4]) with the combined mass flux model (Eq. [6]) showed in nearly all cases a small difference between the two curves, which is illustrated in Fig. 2. Both models resulted in good fits of the measured mass fluxes at 0.05, 0.12, 0.19, and 0.26 m. At 0.50, 0.75, and 1.00 m, the calculated mass fluxes deviated more from the measured mass fluxes, perhaps reflecting the larger experimental error at these heights. The deviations were approximately two times larger with the modified power function than with the combined model (Table 3), and

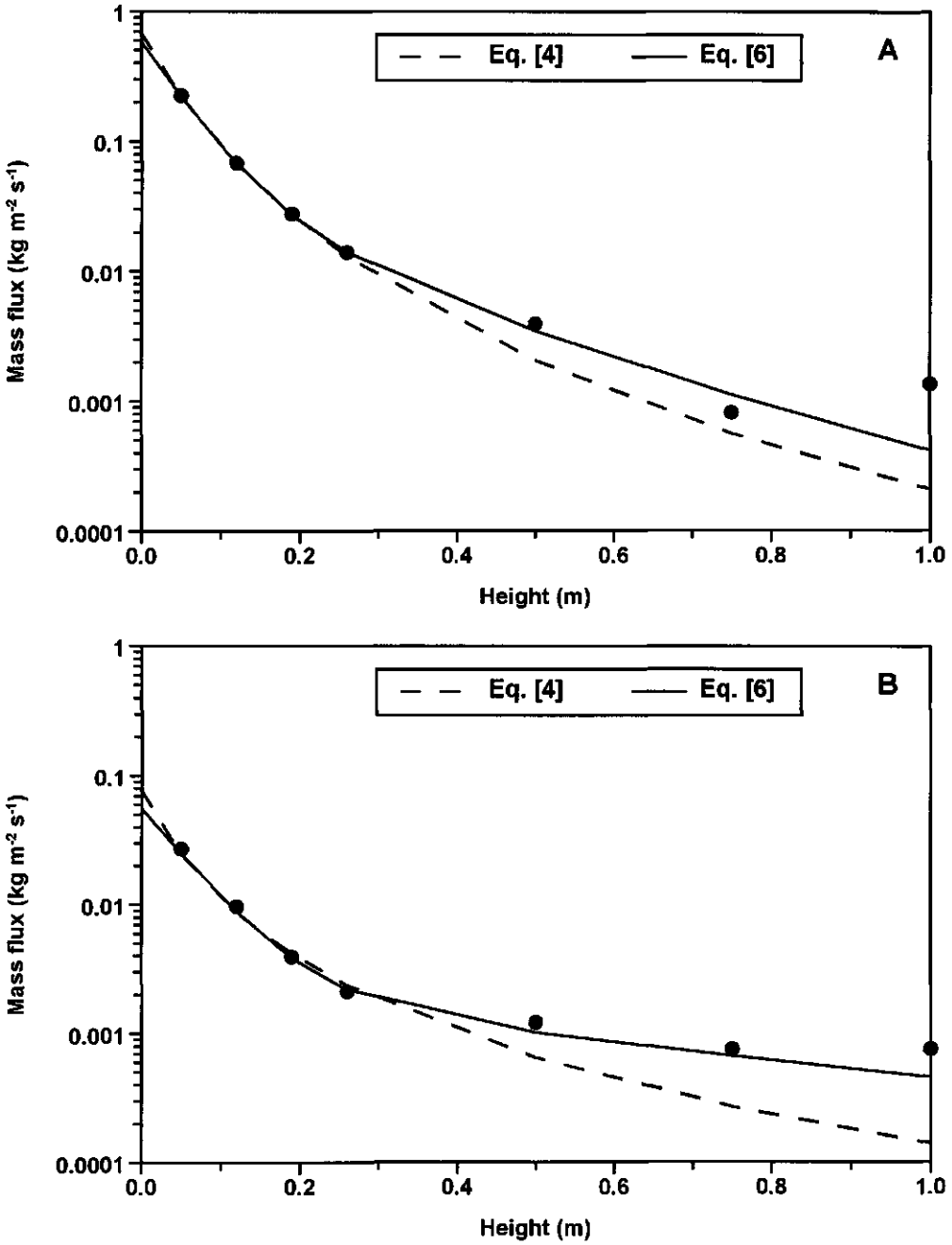

Figure 2. Fitted mass flux profiles through measured data for one catcher during two storms on (A) 13 June 1993 and (B) 27 June 1993.

Table 3. Average deviations between measured mass fluxes and mass fluxes calculated by two models† during four storms at ICRISAT Sahelian Center, 1993 rainy season.

Height	Model 1	Model 2
m	%	%
0.05	0.2	0.1
0.12	1.9	0.7
0.19	5.5	3.5
0.26	6.3	4.5
0.50	21.1	12.4
0.75	45.2	18.5
1.00	60.6	38.0

† Model 1 is the modified power function (Eq. [4]); Model 2 is the combined mass flux model (Eq. [6]).

generally, the modified power function slightly underestimated the mass fluxes, whereas the combined model was closer to the measured fluxes (Fig. 2). So, inclusion of the exponential term resulted in a small improvement of the curve fitting, which agrees with the results of Scott et al. (1995). Both models were used to calculate total mass transport rates (Q_t) and total mass transport values (M). The average values for Q_t and M show small differences between the two models (Table 4). Because of the slightly better performance for fitting the field data, the combined mass flux model is preferred and used in the continuation of this paper, although the simpler modified power function may be sufficient in many field studies.

Table 4. Summary statistics of total mass transport calculated by two mass flux profile models†, during four storms at ICRISAT Sahelian Center, 1993 rainy season.

		Model 1‡			Model 2		
Date	n	$\overline{Q}_t$	$\overline{M}$	CV	$\overline{Q}_t$	$\overline{M}$	CV
		g m^{-1} s^{-1}	kg m^{-1}	%	g m^{-1} s^{-1}	kg m^{-1}	%
13 June	20	71.8	106.3	31.8	69.3	102.7	35.9
27 June	21	12.5	16.5	37.1	11.8	15.5	33.5
30 June	21	26.6	35.2	42.8	24.1	31.8	46.6
1 July	21	56.3	169.2	32.9	49.9	149.8	34.5

† Model 1 is the modified power function (Eq. [4]); Model 2 is the combined mass flux model (Eq. [6]).
‡ n is the number of observations; $\overline{Q}_t$ is the average total mass transport rate; $\overline{M}$ is the average total mass transport value; CV is the coefficient of variation (similar for Q_t and M).

A measure of unit mass of material passing a unit width (M) is useful when soil losses from a certain area are studied. But when studying crop damage by wind erosion, a measure of mass passing a unit width per unit of time (Q_t) is more appropriate, since it is the blasting effect of sand that causes the greatest damage to crops (Wilson and Cooke, 1980). For example, during the fourth storm, the average total mass transport value was 46% higher than during the first storm, whereas the average total mass transport rate was 28% lower (Table 4). Thus, it is expected that crop damage during the first storm was more severe than during the fourth storm. In the measurement field, sowing was done after the first storm, but in other fields at ISC, where millet was sown one week earlier, severe crop damage was observed directly after the first storm. During the fourth storm, two weeks later, no crop damage in the measurement field and other fields was noticeable.

According to Vories and Fryrear (1991), integration of the separate terms of the combined mass flux model produces predictions of the suspension and saltation mass fluxes, respectively. It is evaluated now whether these predictions are correct. By sieving the trapped materials from two catchers, the mass percentages of saltation material (>63 μm) and suspension material (<63 μm) in each bottle were determined. Only the material from the five lowest bottles was used, because the quantity of trapped material in the two highest bottles was not sufficient for sieving. The measured percentages were compared with the model predictions (Table 5). The predicted percentages of saltation material decrease more rapidly with height than the measured percentages. Hence, the predicted saltation mass fluxes are too low compared with the measurements. As a consequence, the predicted suspension mass flux was overestimated by the model. Although the particle size of 63 μm is rather small for

Table 5. Predicted and measured mass percentages of suspension and saltation material.†

	Catcher 1				Catcher 2			
Height	$Su^{(p)}$	$Su^{(m)}$	$Sa^{(p)}$	$Sa^{(m)}$	$Su^{(p)}$	$Su^{(m)}$	$Sa^{(p)}$	$Sa^{(m)}$
m	%	%	%	%	%	%	%	%
0.05	4.7	2.7	95.3	97.3	4.6	2.3	95.4	97.7
0.12	19.6	5.8	80.4	94.2	17.0	6.0	83.0	94.0
0.19	55.1	14.5	44.9	85.5	47.2	15.4	52.8	84.6
0.26	86.3	27.3	13.7	72.7	79.9	31.4	20.1	68.6
0.50	99.9	48.7	0.01	51.3	99.9	50.0	0.01	50.0

† Su is suspension material; Sa is saltation material; (p) = predicted by the combined mass flux model (Eq. [6]); (m) = measured by dry sieving (63-μm mesh size) of trapped sediment with a vibrating sieve.

discriminating between saltation and suspension, it is concluded that the combined mass flux model does not actually predict saltation and suspension mass fluxes.

Since the coefficient α in Eq. [3] was arbitrarily set at 1 m, the sensitivity of the combined model for different values of α was tested by calculating Q for several values of α (Table 6). The same catcher as in Fig. 2 was used for the calculations. With values of α close to zero, the modified power function tends to increase sharply when z approaches zero, resulting in a high intercept q(0) and, obviously, in a high estimate of the mass transport rate Q. With α varying from 0.25 to 5.00 m, the calculated mass transport rates are very similar. The mass flux profile near the soil surface is mainly determined by the exponential term, which is in accordance with several wind tunnel studies (e.g., Horikawa and Shen, 1960; Williams, 1964; Sterk, 1993). When α is taken >5.00 m, Q deviates slightly from the values calculated with α between 0.25 and 5.00 m. Hence, it is concluded that setting α at 1 m was a reasonable assumption for extrapolation of the curve. Whether the

Table 6. Calculated mass transport rates for one catcher during four storms with different values for coefficient α in the combined mass flux model.

	Q†			
α	13 June	27 June	30 June	1 July
m	g m^{-1} s^{-1}	g m^{-1} s^{-1}	g m^{-1} s^{-1}	g m^{-1} s^{-1}
0.001	93.3	10.9	11.2	25.7
0.01	47.9	4.4	10.3	20.4
0.05	37.3	4.3	10.0	18.6
0.10	35.5	4.3	10.0	18.3
0.25	34.8	4.3	9.9	18.2
0.50	34.7	4.3	9.9	18.2
1.00	34.6	4.3	9.9	18.2
1.50	34.6	4.3	9.9	18.0
2.00	34.6	4.3	9.9	18.0
2.50	34.6	4.3	9.9	17.9
3.00	34.6	4.4	9.9	17.9
5.00	34.6	4.4	9.9	17.9
10.0	34.6	4.3	9.6	17.9
100.0	33.8	4.3	9.5	17.9

† Q is the mass transport rate calculated with Eq. [3].

extrapolation of Eq. [6] towards the soil surface is correct cannot be confirmed until we obtain mass flux measurements in this height range.

The total mass transport rate as determined by the MWAC catcher and the combined mass flux model is highly dependent on the overall trapping efficiency of the sampler. The efficiency was determined in a wind tunnel where, compared with the field, the wind is rather homogeneous and the degree of turbulence low. Rapid changes in wind direction are lacking, as well as vertical wind speeds that create the main lift forces for suspension transport. The character of the wind field in a wind tunnel may result in a trapping efficiency that is not correct for field conditions. So far, no techniques for determining the efficiency of samplers in the field exist and estimates of total mass transport rates have to be based on trapping efficiencies determined in wind tunnels. In the future, more studies on testing wind erosion samplers under field conditions should be done, with perhaps more attention paid to the particle size distribution as a function of height.

CONCLUSIONS

The quantity of soil material transported by the wind during four storms was measured with MWAC sediment catchers (Fig. 1), which are inexpensive and easy to construct. Wind-blown material was trapped at seven heights between 0.05 and 1.00 m. A three-parameter, modified power function (Eq. [4]) accurately described the measured mass fluxes below a height of 0.5 m. At the higher measurement levels, the calculated mass fluxes generally underestimated the measured fluxes. The two-term, combined mass flux model (Eq. [6]) described the measured mass fluxes at all heights more accurately than the modified power function. It is concluded that the combined model is better for fitting the vertical profile of horizontal mass flux, although the modified power function may be sufficient in many field studies of wind-blown sand transport.

The two separate terms in the combined mass flux model should not be used to predict the saltation and suspension mass fluxes, as claimed by Vories and Fryrear (1991). The predicted suspension mass fluxes from 0.05 to 0.50 m were approximately three times higher than the suspension mass fluxes that were determined by dry sieving the trapped sediments from two catchers. So, the model overestimates the suspension mass fluxes, and obviously, the saltation mass fluxes are underestimated.

Integration of the vertical mass flux profile across height from $z = 0$ m to $z = 1$ m resulted in a measured or calculated mass transport rate (Q) at the point of sampling. The total mass transport rate (Q_t) was obtained after correcting for the overall trapping efficiency of the MWAC catchers.

This trapping efficiency was determined in the wind tunnel and it is uncertain whether it is the same under field conditions. In a wind tunnel, wind is more homogeneous and less turbulent than in the field, which may result in a different efficiency.

ACKNOWLEDGMENTS

The research was funded by the Netherlands Foundation for the Advancement of Tropical Research (WOTRO). We thank the ICRISAT Sahelian Center for providing the necessary research facilities and for the assistance during the field experiments. The constructive comments, including some useful references, by three anonymous reviewers are gratefully acknowledged.

REFERENCES

Bagnold, R.A. 1973. The physics of blown sand and desert dunes. 5th ed., Chapman and Hall, London.

Chepil, W.S. 1945. Dynamics of wind erosion. I. Nature of movement of soil by wind. Soil Sci. 60: 305-320.

Fryrear, D.W., and A. Saleh. 1993. Field wind erosion: Vertical distribution. Soil Sci. 155: 294-300.

Fryrear, D.W., J.E. Stout, L.J. Hagen, and E.D. Vories. 1991. Wind erosion: Field measurement and analysis. Trans. ASAE 34: 155-160.

Horikawa, K., and H.W. Shen. 1960. Sand movement by wind: On the characteristics of sand traps. Tech. Mem. 119. Beach Erosion Board, U.S. Army, Washington D.C.

Hudson, N. 1973. Soil conservation. Batsford and Educational Ltd., London.

Kuntze, H., R. Beinhauer, and G. Tetzlaff. 1990. Quantification of soil erosion by wind, I. Final report of the BMFT project. Project nr. 0339058 A, B, C. Inst. of Meteorology and Climatology, Univ. of Hannover, Germany. (in German).

Lal, R. 1990. Soil erosion in the tropics: Principles and management. McGraw Hill Inc., New York.

Michels, K. 1994. Wind erosion in the southern Sahelian zone: Extent, control, and effects on millet production. Verlag Ulrich E. Grauer, Stuttgart, Germany.

Nickling, W.G. 1978. Eolian sediment transport during dust storms: Slims River Valley, Yukon Territory. Can. J. Earth Sci. 15: 1069-1084.

Scott, W.D., J.M. Hopwood, and K.J. Summers. 1995. A mathematical model of suspension with saltation. Acta Mech. 108: 1-22.

Shao, Y., G.H. McTainsh, J.F. Leys, and M.R. Raupach. 1993. Efficiencies of sediment samplers for wind erosion measurement. Aust. J. Soil Res. 31: 519-532.

Sterk, G. 1993. Sahelian wind erosion research project, Report III. Description and calibration of sediment samplers. Dep. of Irrigation and Soil & Water Conservation, Wageningen Agric. Univ., The Netherlands.

Vories, E.D., and D.W. Fryrear. 1991. Vertical distribution of wind eroded soil over a smooth, bare field. Trans. ASAE 34: 1763-1768.

West, L.T., L.P. Wilding, J.K. Landeck, and F.G. Calhoun. 1984. Soil survey of the ICRISAT Sahelian Center, Niger, West Africa. TropSoils, Texas A&M Univ., College Station, TX.

Wilkinson, L. 1987. SYSTAT: The system for statistics. Systat Inc., Evanston, IL.

Williams, G. 1964. Some aspects of the eolian saltation load. Sedimentology 3: 257-287.

Wilson, S.J., and R.U. Cooke. 1980. Wind erosion. p. 217-251. *In* M.J. Kirkby and R.P.C. Morgan (ed.) Soil erosion. John Wiley & Sons, Chichester, UK.

Zingg, A.W. 1953. Wind tunnel studies of the movement of sedimentary material. p. 111-135. *In* Proc. of the 5th Hydraul. Conf., State Univ. of Iowa Studies in Engineering Bull. 34.

Chapter 4

Mapping Wind-Blown Mass Transport by Modeling Variability in Space and Time

G. Sterk and A. Stein

Accepted for publication in: Soil Science Society of America Journal.

Reproduced by permission of the Soil Science Society of America.

Mapping Wind-Blown Mass Transport by Modeling Variability in Space and Time

ABSTRACT

Field observations of wind-blown particle transport are often characterized by a considerable spatial variation, which makes quantitative modeling of wind erosion difficult. This study examines how the horizontal distribution, or pattern, of mass transport can be determined from a limited number of point measurements. Twenty-one sediment catchers were installed in an experimental plot in the Sahelian zone of Niger, on a sandy, siliceous, isohyperthermic Psammentic Paleustalf. Mass transport values during four storms ranged from 24.0 to 213.6 kg m^{-1}, 7.2 to 26.0 kg m^{-1}, 9.6 to 68.9 kg m^{-1}, and 68.9 to 282.7 kg m^{-1}. Geostatistical theory was applied to produce storm based maps by modeling the spatial correlation structure with the variogram. To estimate the variogram from 21 observations, the four storms were treated as independent temporal replicates. Two geostatistical mapping techniques were applied. Kriging (a spatial interpolation technique) produced maps of mass transport providing the best possible estimates of net soil losses from the plot, which were 12.5, 2.0, 4.6, and 26.8 Mg ha^{-1}, respectively. To overcome smoothing, possible realizations of actual mass transport were created by stochastic simulations with simulated annealing. The simulated maps reproduced the statistical properties of the observations, and allowed a distinction between erosion and deposition areas within the experimental plot.

Wind erosion causes serious agricultural problems in many parts of the world, especially in regions with loose, dry, sandy soils, little vegetative protection of the soil, and periods of strong winds (Skidmore, 1988). Quantitative modeling of wind erosion in the field is difficult because of the different spatial scales on which the transport processes occur. Sediments can be carried across distances ranging from a few centimeters to thousands of kilometers, at a great range of heights, and in any direction (McTainsh et al., 1992).

On a field scale, observations of sediment transport often show a considerable spatial variation caused by differences in soil characteristics, surface roughness, topography, vegetation characteristics, and wind field (Wilson and Cooke, 1980; Fryrear et al., 1991). In practice, it is virtually impossible to measure and describe all factors at every point in the field to explain the variation in observed sediment transport. It may be doubted as well whether such detailed information is necessary for

wind erosion studies. An alternative approach is to produce storm based maps of sediment transport and to relate them to maps of soil erodibility factors. An extensive literature search made clear that studies of this kind are nonexisting in the wind erosion literature. In water erosion studies, it is more common to produce erosion maps (e.g., Schwing and Vogt, 1980; Morgan, 1986; Mellerowicz et al., 1994). These maps are usually constructed on the basis of aerial photographs, field survey, or model predictions using information on topography, soil type, management, etc. They show erosion features or the erosion hazard in a certain area, but do not show the horizontal distribution of actual, measured sediment transport.

Maps of a sampled property, or regionalized variable, are effectively obtained with geostatistics (Cressie, 1991). Geostatistical theory uses the concept of spatial correlation, which means that observations of a regionalized variable at any two points close to each other are more similar than observations at two points at a larger distance. By modeling the spatial correlation structure with the variogram, good quality maps of the regionalized variable are obtained by the spatial interpolation technique kriging. Alternatively, possible realizations of the regionalized variable may be reproduced by stochastic simulations.

In a wind erosion research project in Niger, West Africa, measurements of air-borne sediment were made in a pearl millet (*Pennisetum glaucum*) field (Sterk and Raats, 1996). During the 1993 wind erosion season, four storms were sampled with 21 sediment catchers. For each catcher and storm, a point measurement of particle mass transport was obtained. In this study, the resulting data sets are used to determine the horizontal distribution, or pattern, of mass transport in the field.

Maps of wind-blown sediment transport can be produced with geostatistics as long as a sufficient number of point observations is available to determine the variogram. Webster and Oliver (1992) investigated the confidence limits of variograms estimated from a varying number of observations. They concluded that variograms computed on fewer than 50 observations are of little value, and recommended that preferably 100 or more observations should be used. In this study, only 21 observations per storm were available. Therefore, the analysis of spatial variability is extended into the space-time domain by pooling the four storms to estimate the variogram. By using this procedure, storm based maps of sediment transport can be created with kriging and stochastic simulation.

Alternative mapping procedures such as splines and inverse distance calculations were considered as well, but not used. Both techniques are based on a model of the spatial correlation structure that is not verifiable by measurements. For instance, when using splines, the spatial correlation is

modeled by a linear trend with a logarithmic generalized covariance function (Cressie, 1991). Inverse distance interpolation assigns weights proportional to $d^{-\epsilon}$ to each neighboring observation, where d is the distance from a neighboring point to the prediction point and ϵ is a parameter. Hence, an assumption for the value of ϵ has to be made. The procedure that is proposed here has at least a certain degree of validation in field measurements, whereas the mentioned alternatives require more severe assumptions.

The objective of this study is to produce storm based maps of sediment transport by applying geostatistics. It is examined how the spatial correlation structure can be modeled with the variogram, when only four data sets of 21 observations are available.

THEORY

Regionalized variable theory is applied to model the spatial correlation structure with the variogram (Journel and Huijbregts, 1978). Each observation y is considered the realization of a regionalized variable Y(s), depending upon the measurement location s. The variability between any two quantities Y(s) and Y(s + h), at two points s and s + h separated by the vector h, is characterized by the variogram. The variogram $\gamma(h)$ as a function of the separation vector h, but independent of s, is defined as half the expectation of the squared differences of Y(s) and Y(s + h):

$$\gamma(h) = \frac{1}{2}E[Y(s) - Y(s+h)]^2 \qquad [1]$$

where E denotes the mathematical expectation. The variogram can be estimated by replacing the expectation with the mean value, taken for all pair differences of observations (y_i, y_{i+h}):

$$\hat{\gamma}(h) = \frac{1}{2n(h)}\sum_{i=1}^{n(h)}(y_i - y_{i+h})^2 \qquad [2]$$

where n(h) is the number of pairs (y_i, y_{i+h}) separated by the vector h, and the index i indicates the different spatial locations of the observations.

To overcome the lack of sufficient observations, the analysis is extended into the space-time domain by using observations from different storms. The main assumption to justify this step is that sediment transport in the experimental plot during the four storms can be characterized by a spatial correlation structure that is similar for each individual storm, irrespective of duration, wind speed, and wind direction of the storm. This implies that the spatial variability of mass transport

during different storms can be characterized by the same variogram model structure. It does not mean, though, that the spatial distribution of mass transport was the same for each storm.

Mass transport values were measured during four successive storms, denoted by y_{ij}, with $i = 1,..,21$, the spatial location, and $j = 1,..,4$, the storm number. To pool the spatial variation in mass transport, the storms are standardized to the mean mass transport value of all four storms:

$$y'_{ij} = y_{ij}\frac{\hat{\mu}_j}{\hat{\mu}_s} \qquad [3]$$

where y'_{ij} is the standardized mass transport at observation location i and for storm j, and $\hat{\mu}_j$ and $\hat{\mu}_s$ are the storm's mean mass transport and the standardized mean mass transport value, respectively. Lack of observations to estimate the variogram is circumvented by using the following equation:

$$\hat{\gamma}(h) = \frac{1}{2n(h)}\sum_{j=1}^{4}\sum_{i=1}^{n_j(h)}(y'_{ij} - y'_{i+h,j})^2 \qquad [4]$$

where y'_{ij} and $y'_{i+h,j}$ denote the ith pair of standardized observations at time j, separated by the vector h, of which there are $n_j(h)$. The total number of pairs of points for each vector h is equal to n(h). Since observations from different storms must not be subtracted from each other, n(h) is equal to the sum of the $n_j(h)$'s. In this way, each pair of observations within the same storm contributes to estimate the standardized variogram, irrespective of the time that the measurements were made.

In practice, pairs of observations with approximately the same separation vector h are grouped into classes. The basic unit of the distance class is the lag distance h_{lag}. For a finite number (m) of multiples of h_{lag}, m variogram values are obtained. Through all the pairs $[x,\hat{\gamma}(x)]$ with $x = k\,h_{lag}$, $k = 1,...,m$, a variogram model g(h) is fitted to facilitate interpretation, and to allow spatial interpolation (kriging) and stochastic simulations. Variogram models are characterized by two parameters: the sill and the range (Journel and Huijbregts, 1978). The sill is the limiting value of the variogram model g(h) as h increases. The range is the distance at which the variogram reaches its sill value. It gives the distance across which spatial dependencies exist. Beyond the range, two points in the field are no longer correlated. At the other end of the variogram, $\gamma(0) = 0$ by definition. However, in many studies, g(h) does not tend to zero when h approaches zero. This discontinuity at the origin is called the nugget effect and is caused by nonspatial variation such as measurement errors, and

the spatial variation that occurs at very small distances. Sometimes, the sill is equal to the nugget effect. Such a pure nugget effect corresponds to the total absence of spatial correlation.

A regionalized variable with a constant expectation (no trend) and for which the variogram exists is said to obey the intrinsic hypothesis. If true, the conditions for the geostatistical mapping techniques kriging and stochastic simulation are met (Journel and Huijbregts, 1978). Both techniques make use of the observations and the variogram, and are explained briefly here.

Kriging uses a linear combination of the observations to make unbiased predictions of an unsampled value with minimum error variance. It therefore provides the so-called best linear unbiased predictor (BLUP) of the regionalized variable (Stein and Corsten, 1991). Kriging estimates a stochastic variable, instead of a parameter, such as the expectation of an observation. Prediction is usually associated with a higher uncertainty. The information used for prediction consists of the observations and the variogram model. Although kriging provides a predictor with minimal variance of the prediction error at every position, it does not reproduce the statistical properties of the observations. Minimization of the prediction error variance involves a smoothing of the actual variability (Journel and Huijbregts, 1978), i.e., a loss of variation in the underlying stochastic field.

Stochastic simulation maintains the statistical properties of the observations but does not provide the best possible predictions (Journel and Huijbregts, 1978). When values are simulated on N grid nodes, these N simulated values have the same mean, variance, histogram, and variogram as the original set of observations. Simulation aims at reproducing the fluctuations that are present in the observations, instead of producing the best possible predictions. Moreover, the simulation is called conditional if the measurement values and the simulated values are the same at the measurement locations. Different conditional simulated fields will be different from each other, except at the measurement locations.

MATERIALS AND METHODS

Sampling

In the Sahel, severe wind erosion occurs mainly in the early rainy season (May - July). In that time of the year, heavy thunderstorms develop and bring the first rains of the new season. The thunderstorms are often accompanied by strong winds that result in severe erosion of unprotected soils before rainfall starts.

A field experiment was conducted at the International Crops Research Institute for the Semi-Arid Tropics (ICRISAT) Sahelian Center in southwest Niger (13°16'N;2°21'E), during the 1993 rainy season. The size of the measurement field was 170 by 90 m. The soil was classified as a sandy, siliceous, isohyperthermic Psammentic Paleustalf (West et al., 1984), with 92.2% sand, 3.0% silt, and 4.8% clay in the topsoil. The plant residues, millet stalks, of the previous crop were uniformly distributed across the field. The amount was ≈800 kg ha^{-1}, corresponding to an estimated soil cover of 3.5%. Pearl millet was sown on 14 June in planting holes spaced at 1 by 1 m (traditional sowing method). The field was characterized by an undulating topography. Distances between crests and depressions were from 25 to 50 m, with maximum height differences of ≈1 m.

Within the measurement field, an experimental plot of 40 by 60 m was selected such that the distance from the plot boundaries to the field boundaries exceeded 25 m in all directions. The plot was instrumented with 21 Modified Wilson and Cooke sediment catchers. A description of the catcher and a method for quantifying total mass transport (kilograms per meter) from trapped material

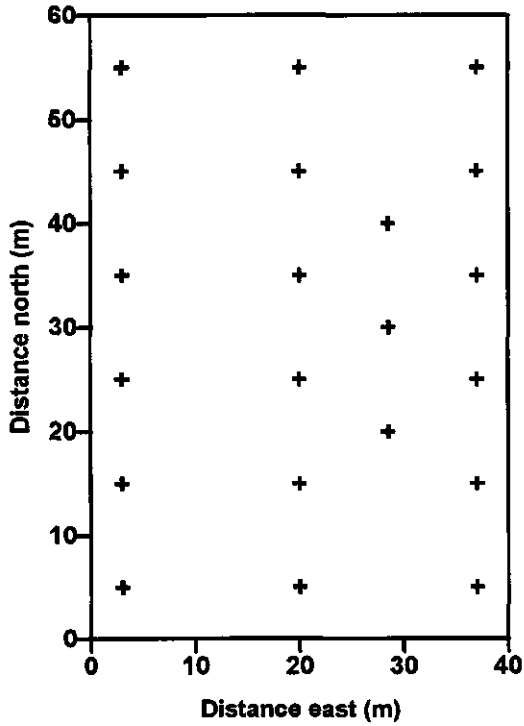

Figure 1. Experimental plot with the positions of 21 Modified Wilson and Cooke sediment catchers.

was given by Sterk and Raats (1996). Three rows of six catchers were regularly distributed in a north-south direction across the whole experimental plot (Fig. 1). Within a row, the distance between two neighboring catchers was 10 m and the distance between rows was 17 m. Between the second and third row, the three remaining catchers were placed in such a way that distances between these catchers and neighboring catchers was also ≈10 m. Distances from the plot boundaries to small (<1.25 m height) obstacles like bushes and fences exceeded 30 m in all directions. During storms, the distances to larger obstacles, mainly single trees with maximum heights of 5 m, in upwind direction of the experimental plot exceeded 100 m. Although the influence of obstacles on the wind field may extend in downwind direction to ≈40 times the height of the obstacle, the disturbances become very minor at a distance of ≈20 times the height (Jacobs, 1984). The influence of the obstacles on the wind field in the plot during a storm was therefore assumed to be negligible, and thus particles were moved at the maximum mass transport rate. During erosion events, suspended dust from surrounding areas was clearly entering the measurement field, but saltation or creep material moving into the field was not observed.

Variogram Model

Several models exist that can be used for fitting an estimation variogram. In this study, use was made of the spherical variogram model, which is defined as:

$$g(h) = \begin{cases} C_0[1 - \delta_k(h)] + C\left(\frac{3}{2}\frac{h}{a} - \frac{1}{2}\frac{h^3}{a^3}\right) & 0 \le h \le a \\ C_0 + C & h > a \end{cases} \qquad [5]$$

where the Kronecker delta function, $\delta_k(h)$, is 1 for h = 0 and vanishes elsewhere. The parameter C_0 is the nugget constant, C the sill parameter, and a is the range parameter of the spherical variogram model. The parameters C_0, C, and a were estimated with a weighted nonlinear regression procedure.

The spherical variogram model, estimated from the standardized data set, was converted to four variogram models, one for each storm. The range parameter of the model is the same for all storms, but the nugget constant (C_0) and the sill parameter (C) are dependent on the storm's mean mass transport. New values were calculated using the mean mass transport values of the four storms ($\hat{\mu}_j$) and the mean mass transport value of the standardized data set ($\hat{\mu}_s$):

$$C_{0,j} = C_{0,s}\left(\frac{\hat{\mu}_j}{\hat{\mu}_s}\right)^2 \qquad [6]$$

$$C_j = C_s\left(\frac{\hat{\mu}_j}{\hat{\mu}_s}\right)^2 \qquad [7]$$

where j denotes the storm number and s the standardized data set.

Mapping Procedures

Maps of wind-blown mass transport were produced with kriging and conditional stochastic simulations by using software from the Geostatistical Software Library (GSLIB) (Deutsch and Journel, 1992). For kriging, the program OKB2D was applied, which uses a two-dimensional ordinary kriging algorithm. It predicts a value of the regionalized variable (Y) at a certain location (s_0) on the basis of a number (p) of surrounding observations or neighborhood points. The predictor T for the value $Y(s_0)$ is a linear combination of the p observations $y_1,\ldots,y_p$:

$$T = \sum_{i=1}^{p} \lambda_i y_i \qquad [8]$$

The p weights λ_i are calculated such that T is unbiased and that the variance of the prediction error is minimal. This procedure requires information about the variogram of the regionalized variable. A detailed description of the calculation procedure can be found in geostatistical handbooks (e.g., Journel and Huijbregts, 1978; Cressie, 1991).

Several procedures are known to make conditional stochastic simulations. In this study, use was made of simulated annealing with the GSLIB program SASIM (Deutsch and Journel, 1992). Simulated annealing is a general technique for combinatorial optimization (Kirkpatrick et al., 1983) and has been adapted in the past to generate a field with a given variogram. The basic idea is that a field created with a noisy variogram is improved stepwise to a field with a well-structured, imposed, variogram. This is accomplished by assigning the observations to the N_{obs} grid nodes that are closest to the observation locations and random values to the $N - N_{obs}$ remaining grid nodes. The random values are drawn from the probability density function obtained from the user-specified histogram. A common approach is to use the histogram from the conditioning data (Deutsch and Journel, 1992).

The initial image is sequentially modified by swapping the values in pairs of grid nodes not involving conditioning data. A swap is accepted if the objective function O is lowered:

$$O = \sum_{h} \frac{[\gamma^*(h) - \gamma(h)]}{\gamma(h)^2} \qquad [9]$$

where $\gamma^*(h)$ is the variogram of the simulated realization, and $\gamma(h)$ is the specified variogram. Not all swaps that raise the objective function are rejected. The simulation is complete when further swaps do not lower the objective function or when a specified minimum objective function is reached.

RESULTS AND DISCUSSION

Although many thunderstorms occurred during the 1993 rainy season, only four were preceded by periods of strong winds resulting in erosion. In general, the thunderstorms move from east to west and, hence, the wind direction during a storm is usually easterly but can be variable, depending on the location relative to the center of the storm. The wind direction during the four sampled storms varied from southeast to south (Table 1). During the first event, one catcher was not functioning and was, therefore, not used for the analysis. The summary statistics of measured mass transport (Table 2) show that mean and median values are very similar for a particular storm, and that the coefficients of variation are low. This indicates that the distribution is close to the Gaussian distribution.

In terms of total mass transport, the four storms were very different in magnitude (Table 2). The second and third storm can be classified as weak storms, whereas the first and the fourth were strong storms. For all four storms, the range in mass transport values was large in comparison to

Table 1. Date, duration, and average wind speed and wind direction during four storms at ICRISAT Sahelian Center, 1993 rainy season.

Storm date	Duration	Wind speed†	Wind direction
	s	m s^{-1}	
13 June	1481	10.3	SE
27 June	1320	7.6	S
30 June	1321	8.9	SE
1 July	3004	9.2	SSE

† Mean wind speed measured at 2 m.

Table 2. Summary statistics† of wind-blown mass transport during four storms at ICRISAT Sahelian Center, 1993 rainy season.

Storm date	n	μ	σ	CV	Range	Median
		kg m^{-1}	kg m^{-1}	%	kg m^{-1}	kg m^{-1}
13 June	20	102.7	36.9	35.9	24.0 - 213.6	102.4
27 June	21	15.5	5.2	33.5	7.2 - 26.0	14.2
30 June	21	31.8	14.8	46.6	9.6 - 68.9	29.7
1 July	21	149.8	51.8	34.5	68.9 - 282.7	149.9

† n = number of observations; μ = mean; σ= standard deviation; CV = coefficient of variation.

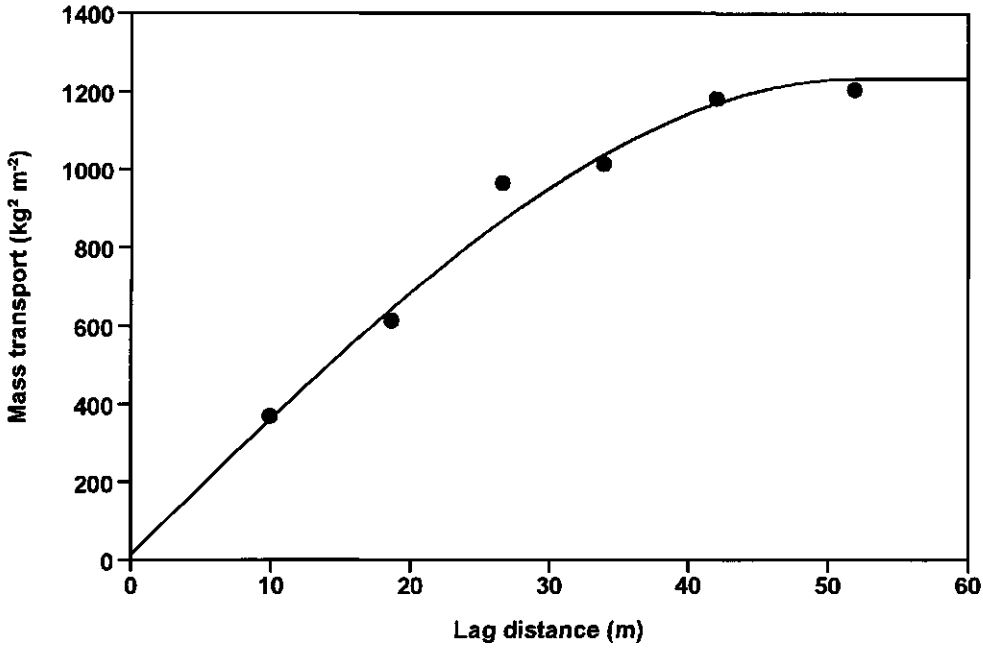

Figure 2. Calculated variogram of wind-blown mass transport and the fitted spherical model.

the mean, indicating that mass transport is indeed variable in space. The 83 observations were standardized with Eq. [3] to 75 kg m^{-1}, corresponding to the mean mass transport value of all four storms ($\hat{\mu}_s$). The resulting data set was used for the variogram calculations with Eq. [4]. The fitted spherical model (Eq. [5]) through the calculated variogram values (Fig. 2) has a range parameter (a) of 52.1 m, a nugget constant (C_0) of 15.1 kg^2 m^{-2}, and a sill parameter (C) of 1220 kg^2 m^{-2}. The low nugget/sill ratio (= 0.01) indicates that the variation due to measurement errors and other

Table 3. Parameters† of the spherical variogram model, used for kriging and stochastic simulations.

Storm date	C_0	C	a
	$kg^2 m^{-2}$	$kg^2 m^{-2}$	m
13 June	28.3	2287.6	52.1
27 June	0.7	52.1	52.1
30 June	2.8	222.1	52.1
1 July	60.3	4873.5	52.1

† C_0 = nugget constant; C = sill parameter; a = range parameter.

nonspatial sources is small compared with the spatial variation in wind-blown mass transport. The standardized variogram was converted to four spherical variograms with Eq. [6] and [7] (Table 3).

The intrinsic hypothesis, a necessary criterion for kriging and conditional stochastic simulations, is obeyed for three of the four storms since (i) the variogram exists, and (ii) no trend in mass transport values was found by a multiple linear regression analysis. The third storm, however, showed a trend in mass transport values, and, hence, the expectation is not constant but depends on the position. For this storm, it was assumed that the hypothesis of quasi-stationarity is fulfilled when the neighborhood size for kriging and stochastic simulation is sufficiently small (Journel and Huijbregts, 1978). In other words, the intrinsic hypothesis is not true for the whole plot, but in smaller neighborhoods, the expectation and variogram may be considered as stationary.

For kriging with the program OKB2D, the following input was used: the spherical variogram models (Table 3), the 21 observations, a minimum of 4 and a maximum of 16 (8 for the third storm) neighborhood points with a maximum search radius of 30. The kriging predictions for the four storms are presented in gray scale maps (Fig. 3). The SASIM simulations (Fig. 4) are based on the spherical variogram models (Table 3) and the 21 observations as well. For the user-specified histograms, the 21 conditioning data points (the observations) were taken, with the following specified ranges: storm 1: 0 to 240 kg m^{-1}; storm 2: 0 to 35 kg m^{-1}; storm 3: 0 to 75 kg m^{-1}; storm 4: 50 to 300 kg m^{-1}. Use was made of a two-part objective function and 100 lags for conditioning, which means that the experimental variogram is calculated from the 100 nearest grid points. The grid size for kriging and stochastic simulation was 41 × 61, hence, each grid cell in Fig. 3 and 4 corresponds to an area of 1 by 1 m in the experimental plot.

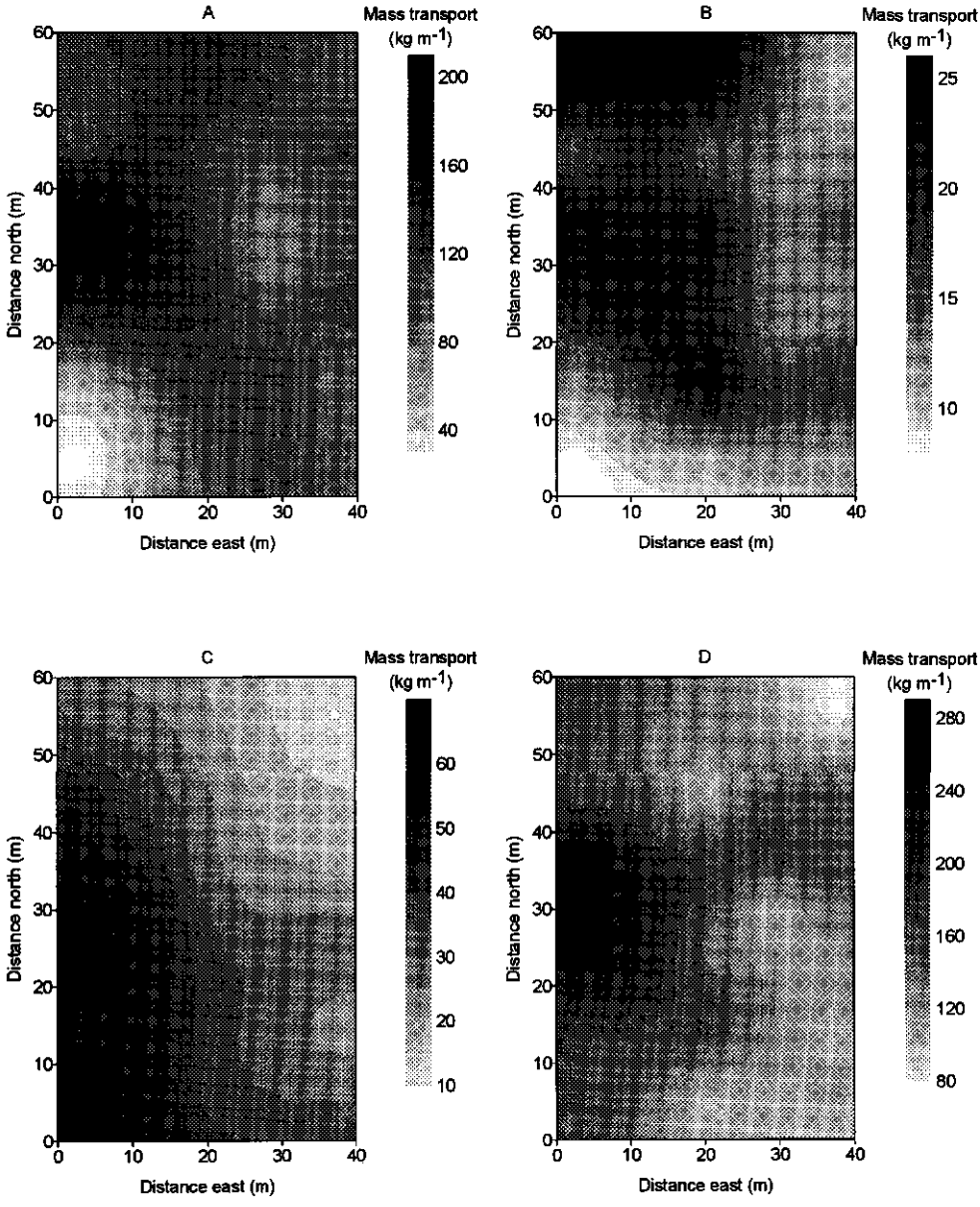

Figure 3. Maps of mass transport produced by kriging with the program OKB2D. Storm dates are (A) 13 June, (B) 27 June, (C) 30 June, and (D) 1 July 1993.

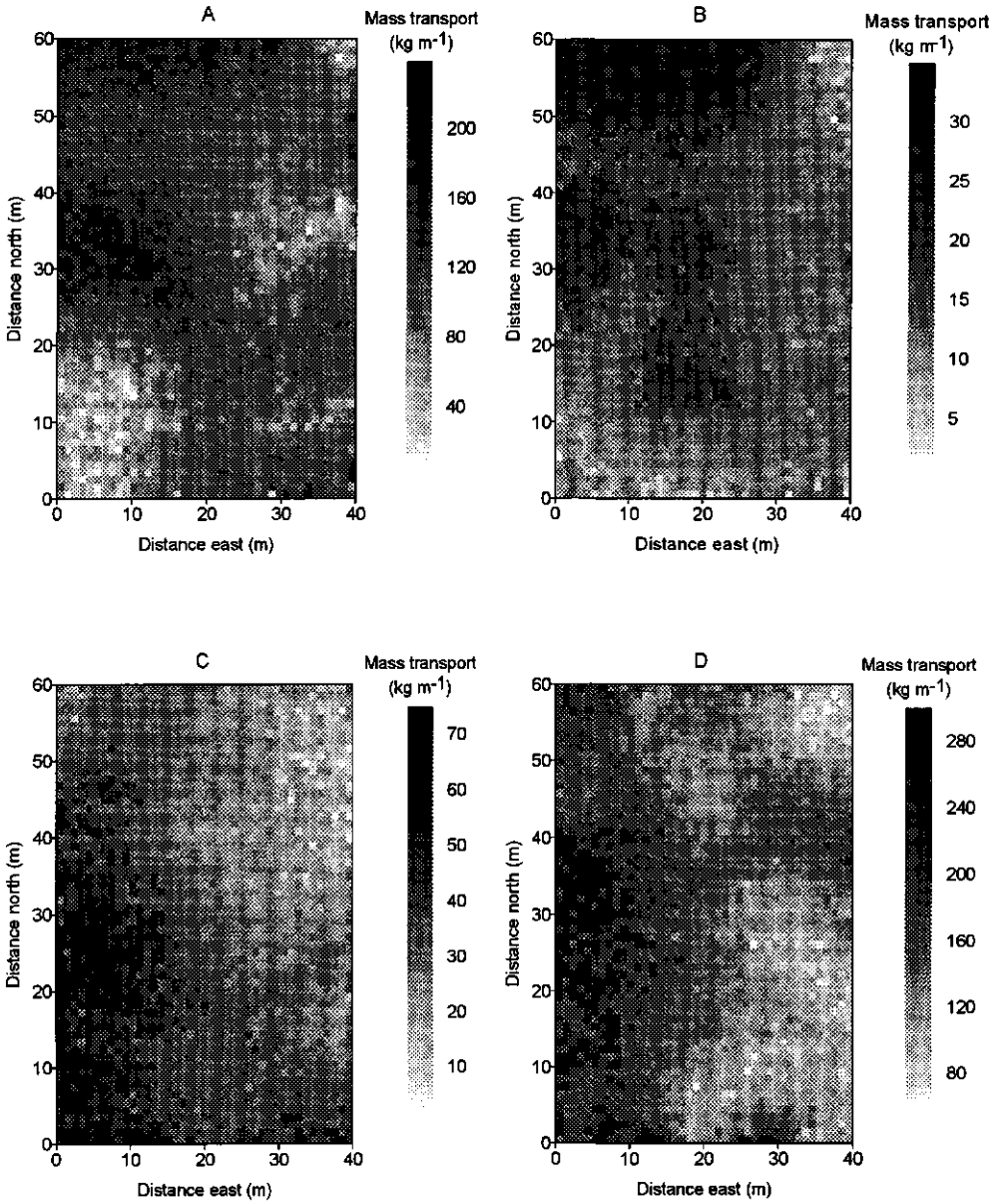

Figure 4. Maps of mass transport produced by simulated annealing with the program SASIM. Storm dates are (A) 13 June, (B) 27 June, (C) 30 June, and (D) 1 July 1993.

The interpolated maps (Fig. 3) show that the kriging algorithm tends to smooth out details and extreme values of the original data set. The variability that was present in the observations is not reproduced. However, kriging provides the best prediction of mass transport at each unsampled location at a given time and is therefore well suited for calculating net soil losses from the plot. For all four storms, a mass budget was determined by averaging the kriging predictions along the four boundaries of the experimental plot. The best possible estimate of net soil loss is obtained when the boundaries coincide with the outermost rows of sediment catchers, because the variance in prediction error is lowest along these rows. During the first, third, and fourth storms, the sediment moved into the plot across the eastern and southern boundaries and left the plot via the northern and western boundaries. During the second storm, only the southern and northern boundaries contributed to input and output of mass transport. The calculated soil losses by using kriging (Table 4) are compared with soil losses determined by averaging the measured mass transport values along the same boundaries (linear interpolation). The total soil loss from the plot as determined by kriging is slightly (5.8%) higher than the total soil loss calculated with linear interpolation. Comparing individual storms, however, shows that larger differences in net soil losses exist between the two calculation methods. Since kriging takes the spatial correlation structure of mass transport into account, it gives the better estimate of net soil losses from the experimental plot.

Stochastic simulations (Fig. 4) typically serve a different purpose than interpolated maps. Reproducing the variation that was present in the observations takes precedence over local accuracy. Although the overall patterns of mass transport are very similar in Fig. 3 and 4, the extreme values of mass transport, which create most soil and crop damage, are more distinct in the simulated maps. Furthermore, these maps emphasize the strong variation in mass transport across short distances.

Table 4. Calculated soil losses from the experimental plot.

	Net soil loss	
Storm date	Linear interpolation	Kriging
	Mg ha^{-1}	Mg ha^{-1}
13 June	8.4	12.5
27 June	2.0	2.0
30 June	6.6	4.6
1 July	26.4	26.8
Total	43.4	45.9

Because of this variation, the traditional method of describing soil loss per unit area (Table 4) becomes rather meaningless (Wilson and Cooke, 1980). It is more useful to distinguish erosion and deposition areas in the plot from downwind gradients in gray values. Positive gradients (from light to dark) are associated with erosion, negative gradients (from dark to light) with deposition, and zero gradients with transport only.

Multiple conditional simulations of one storm produce different realizations, and the differences among the alternative realizations provide a measure of spatial uncertainty (Deutsch and Journel, 1992). For each storm, five simulations were made and the correlation between all possible pairs of realizations was determined from 250 simulated values of each realization. For a particular storm, 10 correlation coefficients (r) were calculated, and the average correlation coefficients were 0.60, 0.74, 0.77, and 0.75, respectively, for the four storms. Although multiple simulations of one storm are expected to be correlated, the high degree of correlation suggests that the simulated patterns of mass transport represent the real, unknown sedimentation pattern. Hence, it is assumed that 21 sediment catchers was sufficient to characterize the spatial variation of mass transport in the experimental plot. Multiple simulations can be used as well to determine the minimum number of conditioning data points (or observations) needed for reproducing the reference spatial variability. In this way, sampling schemes can be statistically tested on their performance.

The interpolated and simulated maps are based on a variogram model that was estimated from four different storms, assuming a similar spatial correlation structure for the storms. To test the validity of this assumption by estimating a variogram for each storm would require a sampling scheme with at least 50, but preferably 100, catchers in the experimental plot (Webster and Oliver, 1992). In wind erosion studies, sampling at such a high density is usually not possible because of the high

Table 5. Results of cross-validations with the program XVOK2D.

Storm date	MAE†	RMAE‡
	kg m^{-1}	%
13 June	26.6	25.9
27 June	4.6	29.9
30 June	6.6	20.5
1 July	38.9	26.0

† MAE = mean absolute error.
‡ RMAE = relative mean absolute error (relative to the average mass transport value).

costs of equipment and labor. As an alternative, it is possible to test the quality of the variogram model by means of a cross-validation. To do so, the variogram model is used to re-predict the actual observations from neighboring observations. Cross-validation was done for all four storms with the GSLIB program XVOK2D (Deutsch and Journel, 1992), yielding the mean absolute error (MAE) and the relative mean absolute error (RMAE), which is the mean absolute error relative to the storm's mean mass transport value (Table 5). The mean deviations between predictions and actual observations are ≈25%, and it is concluded that the quality of the variogram was sufficient for the purpose of this study.

CONCLUSIONS

Maps of wind-blown mass transport were produced for four storms from 21 observations with kriging and conditional stochastic simulation. Both techniques require information about the spatial structure of mass transport, which was modeled with the variogram. To have sufficient observations for estimating the variogram, the four sampled storms were treated as independent temporal replicates. The obtained variogram model (Fig. 2) shows that the variation in the observations was mainly caused by spatial variability, whereas nonspatial variability was small.

Maps of storm based mass transport produced by kriging (Fig. 3) are useful for quantifying soil losses per unit area but less useful for the study of wind erosion processes within the field. Minimization of the variance of the prediction error resulted in a loss of the real, observational variation.

Maps obtained by conditional stochastic simulation (Fig. 4) reproduce the statistical properties of the observations and better show the spatial variability in mass transport. These maps can be used for detailed studies of erosion and deposition processes within the field. By using a geographical information system, the spatial information on erosion and deposition can be combined with information on soil erodibility, crusting, surface roughness, topography, and crop characteristics. This may lead to a better understanding of field wind erosion processes.

Producing five simulations for each storm resulted in good correlations between the different realizations of a particular storm, indicating that 21 observations was enough for a full characterization of the spatial variability of mass transport in the experimental plot.

ACKNOWLEDGMENTS

The research was funded by the Netherlands Foundation for the Advancement of Tropical Research (WOTRO). We thank the ICRISAT Sahelian Center for providing the necessary research facilities and for the assistance during the field experiments. The technical assistance of P.J.J.F. Torfs, G. Bier, and H. Stomphorst of the Wageningen Agricultural University for preparing this manuscript is gratefully acknowledged.

REFERENCES

Cressie, N.A.C. 1991. Statistics for spatial data. John Wiley & Sons, New York.

Deutsch, C.V., and A.G. Journel. 1992. GSLIB: Geostatistical software library and user's guide. Oxford University Press, New York.

Fryrear, D.W., J.E. Stout, L.J. Hagen, and E.D. Vories. 1991. Wind erosion: Field measurement and analysis. Trans. ASAE 34: 155-160.

Jacobs, A.F.G. 1984. Wind reduction near the surface behind a thin solid fence. Agric. For. Meteorol. 33: 157-162.

Journel, A.G., and Ch.J. Huijbregts. 1978. Mining geostatistics. Academic Press, London.

Kirkpatrick, S., C.D. Gelatt Jr., and M.P. Vecchi. 1983. Optimization by simulated annealing. Science 220: 671-680.

McTainsh, G.H., C.W. Rose, G.E. Okwach, and R.G. Palis. 1992. Water and wind erosion: Similarities and differences. p. 107-119. *In* H. Hurni and K. Tato (ed.) Erosion, conservation, and small-scale farming. Walsworth Publ. Co., Marceline, MS.

Mellerowicz, K.T., H.W. Rees, T.L. Chow, and I. Ghanem, 1994. Soil conservation planning at the watershed level using the Universal Soil Loss Equation with GIS and microcomputer technologies: A case study. J. Soil Water Conserv. 49: 194-200.

Morgan, R.P.C. 1986. Soil erosion and conservation. Longman Group, Essex, UK.

Schwing, J.F., and H. Vogt. 1980. An attempt at a large-scale non-experimental cartographic approach to the variability of erosion features and land sensitivity to erosion in the Alsace (France) vineyards. p. 207-214. *In* M. De Boodt and D. Gabriels (ed.) Assessment of erosion. John Wiley & Sons, Chichester, UK.

Skidmore, E.L. 1988. Wind erosion. p. 203-233. *In* R. Lal (ed.) Soil erosion research methods. Soil and Water Conserv. Soc., Ankeny, IA.

Stein, A., and L.C.A. Corsten. 1991. Universal kriging and cokriging as a regression procedure. Biometrics 47: 575-587.

Sterk, G., and P.A.C. Raats. 1996. Comparison of models describing the vertical distribution of wind-eroded sediment. Soil Sci. Soc. Am. J. 60: 1914-1919. (Chapter 3 in this volume).

Webster, R., and M.A. Oliver. 1992. Sample adequately to estimate variograms of soil properties. J. Soil Sci. 43: 177-192.

West, L.T., L.P. Wilding, J.K. Landeck, and F.G. Calhoun. 1984. Soil survey of the ICRISAT Sahelian Center, Niger, West Africa. TropSoils, Texas A&M Univ., College Station, TX.

Wilson, S.J., and R.U. Cooke. 1980. Wind erosion. p. 217-251. *In* M.J. Kirkby and R.P.C. Morgan (ed.) Soil Erosion. John Wiley & Sons, Chichester, UK.

Chapter 5

Wind-Blown Nutrient Transport and Soil Productivity Changes in Southwest Niger

G. Sterk, L. Herrmann and A. Bationo

Published in: Land Degradation & Development 7: 325-335. (1996).

Reproduced by permission of John Wiley & Sons.

Wind-Blown Nutrient Transport and Soil Productivity Changes in Southwest Niger

ABSTRACT

This study was conducted to quantify nutrient losses by saltation and suspension transport. During two convective storms, mass fluxes of wind-blown particles were measured in a pearl millet (*Pennisetum glaucum*) field in southwest Niger, on a sandy, siliceous, isohyperthermic Psammentic Paleustalf. The trapped material at three heights (0.05, 0.26 and 0.50 m) and a sample of vertically deposited dust were analyzed for total element (TE) contents of K, C, N, and P. The nutrient content of the material at 0.05 m was similar to the nutrient content of the topsoil. At 0.50 m, the material was three times richer in nutrients than the topsoil, whereas the deposited dust, trapped at 2.00 m, was 17 times richer. For all four elements, a TE mass flux profile was fitted throughout the observations. From the TE profiles, the following nutrient losses from the experimental plot were estimated: 57.1 kg ha^{-1} K, 79.6 kg ha^{-1} C, 18.3 kg ha^{-1} N, and 6.1 kg ha^{-1} P. The TE profiles showed a maximum value in the saltation layer. The suspended TE mass fluxes above the saltation layer were an order of magnitude lower than the saltation fluxes, but extended to greater heights. Therefore, saltation and suspension are both able to transport significant quantities of nutrients. While saltation results in only a local redistribution of nutrients, suspension may transport dust over thousands of kilometers, resulting in a regional loss of nutrients.

Rainfall in the Sahel has shown a general decline since the 1960's (Sivakumar, 1992). In the 1970's and early 1980's, droughts and several years of crop failure occurred. At the same time, rapid population growth, with growth rates close to 3% per year during recent decades, has resulted in an expansion of the cropped area onto more marginal land which was previously utilized for communal grazing. The use of the fallow system, which was traditionally applied for restoring soil fertility, has been dramatically reduced and crop yields have declined (Ramaswamy and Sanders, 1992). Consequently, the combination of drought and over-exploitation has caused desertification on a large scale. The land degradation processes include erosion by water and wind and deposition elsewhere, long term reduction in the amount and diversity of natural vegetation, and salinization of soils (Dregne et al., 1991).

In the Sahel, severe wind erosion occurs mainly in the first half of the rainy season (May - July). Then the rainfall occurs in heavy thunderstorms that are often preceded by violent winds, which

result in severe erosion of unprotected soils. Agricultural damage is twofold: (i) young seedlings, which are sown after the first rains, are damaged by sand blasting and burial, forcing farmers to resow several times in some years; (ii) decreasing soil productivity due to the loss of fertile topsoil. During the dry season (October - April), strong winds may also result in moderate wind erosion (Michels, 1994), whereas the Harmattan winds in the second half of the dry season (January - March) transport dust from remote areas in the Sahara towards the Sahel, where part of it is deposited, enriching the soils with fine particles (Drees et al., 1993).

In the wind erosion process three transport modes can be distinguished: creep, saltation and suspension (Bagnold, 1973). Creep particles are large and too heavy to be lifted by the wind. They roll or slide over the surface. Saltation particles bounce over the soil surface, reaching maximum heights of about 1 m, but the bulk of saltation particles moves just above the soil surface. The smallest particles are held aloft by the wind as suspended dust. This distinction in particle size classes for the different transport modes is only arbitrary. At the transition of two modes, particles of a particular size may be moved by both modes, depending on differences in density and wind speed. Here, the following size classes are used: suspension material, <63 μm; saltation particles, from 63 to 500 μm; and creep particles, >500 μm. During a particular event, creep can transport particles horizontally from a few centimeters up to several meters. The saltation range is from a few meters up to a few hundred meters, whereas suspended dust may travel up to thousands of kilometers.

The loss of plant nutrients from soils is usually attributed to losses by suspension (e.g., Zobeck and Fryrear, 1986a; Leys and McTainsh, 1994). Suspension selectively removes the finest soil particles that contain disproportionately greater concentrations of plant nutrients (Young et al., 1985). Although there seems to be a consensus among scientists that soil losses by suspension are the major cause of decreasing soil fertility in the source area, no information is available on nutrient losses by saltation and creep. Saltation, however, moves the main mass of wind-blown particles (Chepil, 1945), and thus may be an important cause of losses of plant nutrients. Creep is considered not to result in significant nutrient losses. Creep mainly transports coarse sand, which is usually rich in silicon and poor in plant nutrients.

The objective of this study was to quantify nutrient losses from a Sahelian pearl millet field by wind erosion. The distinction between losses by saltation and suspension is emphasized. The contributions of these two transport modes to changes in soil productivity are discussed.

MATERIALS AND METHODS

A field experiment was conducted at the International Crops Research Institute for the Semi-Arid Tropics (ICRISAT) Sahelian Center, abbreviated hereafter to ISC, during the 1993 rainy season. The center is located in southwest Niger, at Sadoré, 45 km south of the capital, Niamey. A field was selected for the experiment that had been cropped with pearl millet (*Pennisetum glaucum*) during the previous three years. The whole field was planted with pearl millet on 14 June. Sowing was done in planting holes spaced 1 m by 1 m apart. Plant residues (millet stalks from the previous crop) were uniformly distributed over the field, corresponding to a soil cover of 800 kg ha^{-1}. Within the field, an experimental plot of 40 by 60 m was chosen. The distances from the plot boundaries to obstacles in the upwind direction during storms exceeded 20 times the height of the obstacle in all cases. Hence, it was assumed that during storms (i) the wind field in the plot was not significantly disturbed by those obstacles, and (ii) wind-eroded material was moving at the maximum transport rate. The soil at the selected field is a sandy, siliceous, isohyperthermic Psammentic Paleustalf (West et al., 1984), with 92.2% sand, 3.0% silt, and 4.8% clay in the topsoil. The aggregate size distribution of the topsoil (Table 1), determined by dry sieving of soil samples, shows that the bulk of soil mass is in the saltation size range.

For the measurements of wind-blown mass transport, 21 Modified Wilson and Cooke (MWAC) catchers (Sterk and Raats, 1996) were installed in the experimental plot (Fig. 1). The MWAC catcher has one large vane that ensures that the catcher is positioned facing into the wind. Seven erosion traps are attached on a central pole at heights of 0.05, 0.12, 0.19, 0.26, 0.50, 0.75, and 1.00 m. Each trap consists of a small (100 ml) PVC sample bottle, closed with a cap through which inlet

Table 1. Aggregate size distribution of the topsoil at the experimental plot.

Size class	Mass
µm	%
< 63	3.1
63 - 125	18.2
125 - 250	35.7
250 - 500	32.8
500 - 1000	10.0
> 1000	0.2

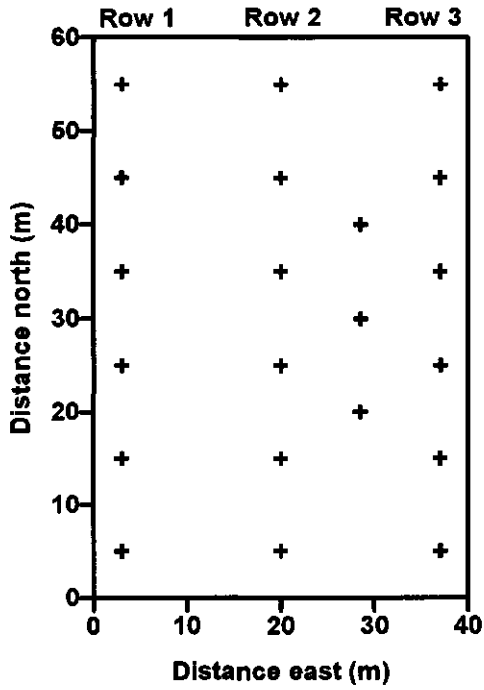

Figure 1. Positions of 21 MWAC catchers on the experimental plot.

and outlet tubes enter the bottle. These are glass tubes with an internal diameter of 8 mm, and are each bent at 90° outside the bottle but in opposite directions.

The efficiency of the MWAC catcher for trapping soil at ISC was determined in a wind tunnel (Sterk, 1993). The overall trapping efficiency was defined as the ratio of measured mass transport rate, determined with the MWAC catcher (see next section), and the total mass transport rate. The total mass transport rate was obtained by weighing the soil in trays before and after simulation of a storm. The average overall trapping efficiency from 12 runs, with wind speeds varying from 9.9 to 11.5 m s^{-1} was 0.49. The efficiency showed no relation to wind speed. Whether the trapping efficiency is particle size dependent is not known.

From the weight of the trapped materials and the duration of the storm, mean horizontal mass fluxes q(z) (kg m^{-2} s^{-1}) at the sampling height z (m) were calculated. The relationship between horizontal mass flux and height was best described by a two-term mass flux model (Sterk and Raats, 1996):

$$q(z) = a(\frac{z}{\alpha} + 1)^{-b} + c\exp(-\frac{z}{\beta}) \quad [1]$$

where a, α, b, c and β are regression coefficients. The model describes the vertical profile of horizontal mass flux from the soil surface (z = 0) to any height z. It therefore includes creep, saltation, and suspension transport. For each catcher and storm, Eq. [1] was fitted through the mass flux observations by nonlinear regression. In this study, Eq. [1] was only used to describe the mass flux profile from z = 0 to 1 m, since no observations were available at greater heights. Integration over height (from 0 to 1 m) resulted in a measured mass transport rate Q (kg m^{-1} s^{-1}) at the point of sampling. The total mass transport rate Q_t at each observation location was obtained by correcting for the overall trapping efficiency of the MWAC catcher.

Samples for nutrient measurements were taken at each row of six MWAC catchers (rows 1, 2, and 3 in Fig. 1). The trapped materials were collected at three height levels, the lowest level (0.05 m), the fourth sampling level (0.26 m), and the fifth sampling level (0.50 m). Samples from the same height in each separate row were grouped so that there were nine samples per storm. Soil samples were also taken from the topsoil in the experimental plot. Some soil was taken from the top layer (0 - 0.02 m) next to each catcher. One soil sample was made for each row of six catchers by grouping the six samples.

Apart from horizontal particle transport at the millet field, vertically oriented dust deposition was measured over the same period. Two rectangular bulk deposition samplers were installed at 2 m height in a fallow area at ≈1 km from the measurement field. These samplers have a collection surface of 0.18 m^2 and are covered with a polyethylene mesh (mesh size 2 mm). The mesh prevents birds and insects from entering, and also avoids resuspension of dust once it has settled. Dust deposition during the sampling period mainly took place as rain wash-out (Herrmann et al., 1996). Therefore, the deposition rate at the fallow site is approximately equal to the deposition at the millet site.

For all samples, the total element (TE) contents of potassium (K), phosphorus (P), nitrogen (N), and carbon (C) were determined. Total K and P were measured by X-ray fluorescence (Siemens SRS 200). The samples were ground (<20 μm), mixed 1:1 with Mowiol (polyvinyl alcohol), pressed into tablets, and measured against standards using a Cr-anode. Total C and N were measured with a gas chromatograph (Carlo Erba NA 1500). In this procedure, ground samples (20 - 50 mg) are burnt. Then C is oxidized to CO_2 by Cr_2O_3 and Co_3O_4 at 1020°C, and N is reduced to N_2 by Cu

at 600°C. The resulting CO_2 and N_2 are quantified by thermal conductivity against a reference gas (He).

According to Zobeck and Fryrear (1986a), the extractable cation content of wind-eroded material as a function of height can be described with a simple power function:

$$X(z) = pz^q \qquad [2]$$

where X is the extractable cation content (mg kg^{-1}), and p and q are (positive) regression coefficients. The equation showed good correlations between fitted and measured extractable cation contents of Na, Ca, Mg, and K. Leys and McTainsh (1994) have published data of the contents of organic C, total N, and total P in wind erosion samples at seven heights. Comparison with these data showed that Eq. [2] accurately described the vertical profiles of C, N, and P (R^2 = 0.88, 0.98, 0.97, respectively), and therefore Eq. [2] was used in this study as a model for the vertical distribution of the TE content with height. In this model, the TE content is zero at the soil surface, suggesting that creep is not transporting plant nutrients. Multiplication of Eq. [1] and Eq. [2] yields an equation that describes the vertical profile of TE mass flux:

$$f(z) = pz^q[a(\frac{z}{\alpha} + 1)^{-b} + c\exp(-\frac{z}{\beta})] \qquad [3]$$

where f(z) is the horizontal mass flux (mg m^{-2} s^{-1}) of a certain element at height z. The TE mass flux profiles were numerically integrated over height from z = 0 to 1 m. The total TE mass transport rates F_t (mg m^{-1} s^{-1}) were obtained by correcting measured TE mass transport rates for the overall trapping efficiency of the MWAC catcher.

RESULTS

In general, thunderstorms in the Sahel move from east to west. The wind direction during a storm is usually easterly, but may vary from north to south depending on the location relative to the center of the storm. Although many thunderstorms occurred during the 1993 rainy season, only four were preceded by periods of strong winds resulting in wind erosion (Table 2). The wind direction during the storms varied from southeast to south.

For each MWAC catcher and storm, Eq. [1] was fitted through the measured mass fluxes at seven heights. In general, the fitted mass flux profiles showed good agreement with observations.

Table 2. Descriptive statistics of four storms at ICRISAT Sahelian Center, 1993 rainy season.

Date	Duration	Wind speed†	Wind direction	$\overline{Q}_t$‡	Soil loss§
	s	m s^{-1}		g m^{-1} s^{-1}	Mg ha^{-1}
13 June	1481	10.3	SE	69.3	12.5
27 June	1320	7.6	S	11.8	2.0
30 June	1321	8.9	SE	24.1	4.6
1 July	3004	9.2	SSE	49.9	26.8

† Mean wind speed measured at 2 m.
‡ Average value of 21 total mass transport rates.
§ For calculation procedure see Sterk and Stein (1997).

Average deviations between measured and calculated mass fluxes increased from 0.1% at the lowest sampling level to 38.0% at the highest level (Sterk and Raats, 1996). Figure 2 shows two fitted mass flux profiles for one catcher during the storm events of 13 June and 1 July. Note the underestimation of measured mass fluxes at 0.75 and 1.00 m during the erosion event of 13 June.

From the fitted mass flux profiles, the total mass transport rates (Q_t) per catcher were calculated. The average values (Table 2) show that in terms of mass transport the magnitude of the storms was variable. Soil losses from the experimental plot were calculated from storm based maps of mass transport (Sterk and Stein, 1997). The losses were rather different, showing that high mass transport rates do not necessarily lead to high soil losses. The storm duration and the spatial distribution of mass transport also have important effects on the resulting soil loss.

The storms of 13 June and 1 July were strong enough to provide sufficient quantities of trapped material for chemical analyses. Two dust samples were collected on 9 July, and were grouped into one sample. This represented the deposition from 7 June until 9 July at the fallow site. The total dust deposition over this period was equal to 0.24 Mg ha^{-1}.

The TE contents of the topsoil (Table 3) do not show any significant differences between rows. Therefore, the average values of the three rows were used for comparison with the TE contents of the wind-blown material. The values obtained are very similar to those reported by West et al. (1984), who described soil profiles and topsoil properties on different fields at ISC. The TE contents of the material trapped with the MWAC catchers show only slight differences between the three rows. Between the two storms, some differences were manifest, mainly at the 0.50 m level. In general, the TE contents increased with height. However, during the first storm some exceptions were found.

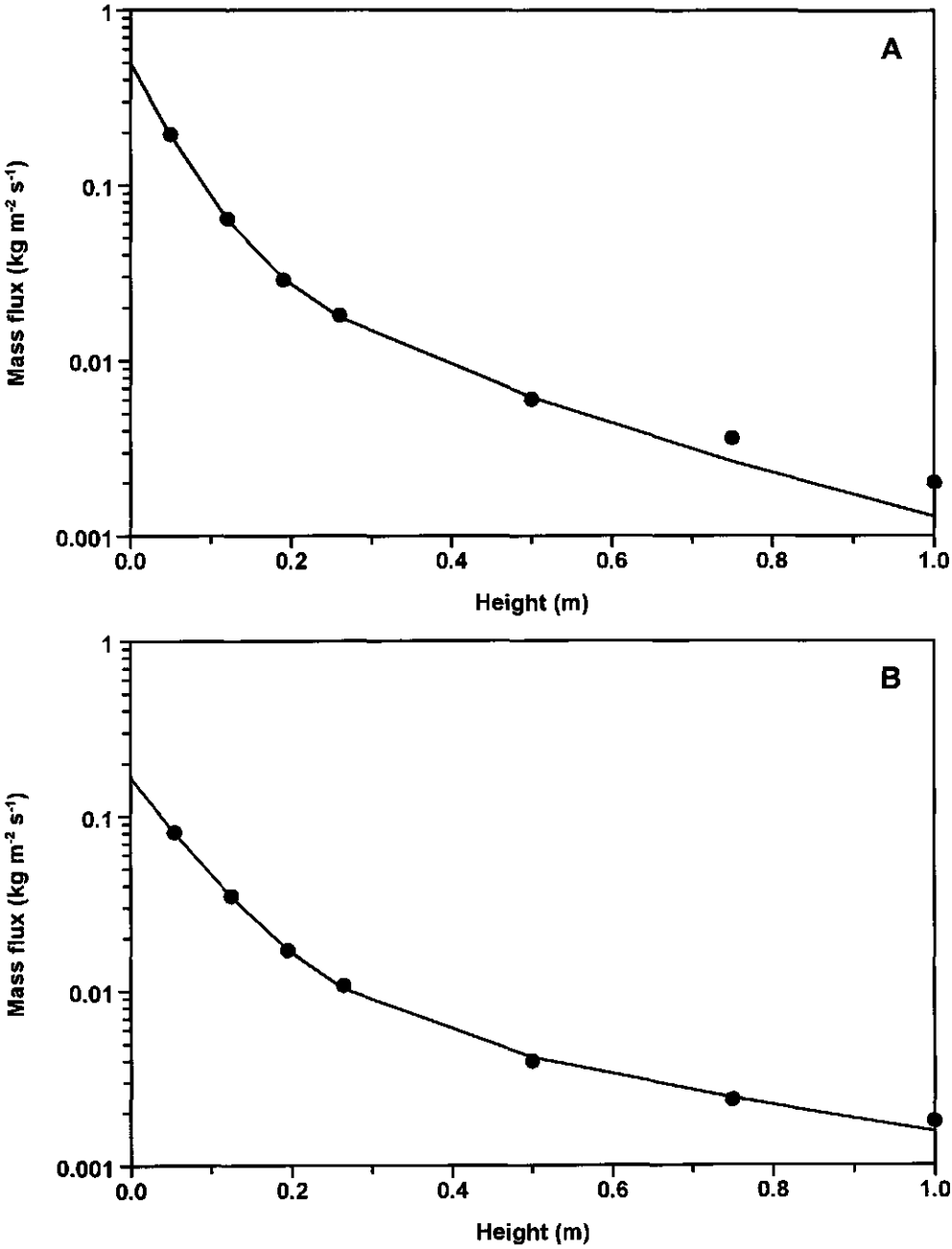

Figure 2. Fitted profiles through measured mass fluxes for one MWAC catcher during the wind erosion events of (A) 13 June and (B) 1 July 1993.

Table 3. Total element contents of the topsoil in the experimental plot, a dust deposition sample in a fallow site, and the materials trapped with 18 MWAC catchers during two storms at ICRISAT Sahelian Center, 1993 rainy season.

	Row	Height	K	C	N	P
		m	%	%	%	mg kg^{-1}
Topsoil	1	0	0.10	0.15	0.05	145
	2	0	0.12	0.19	0.04	144
	3	0	0.12	0.18	0.04	146
	AVG	0	0.11	0.17	0.04	145
Dust sample	-	2.00	1.10	5.36	0.79	728
13 June	1	0.05	0.13	0.19	0.03	130
	2	0.05	0.12	0.26	0.04	137
	3	0.05	0.14	0.23	0.03	160
	1	0.26	0.20	0.50	0.07	176
	2	0.26	0.19	0.36	0.04	153
	3	0.26	0.24	0.36	0.06	150
	1	0.50	0.21	0.40	0.08	140
	2	0.50	0.23	0.61	0.09	161
	3	0.50	0.24	0.53	0.08	193
1 July	1	0.05	0.15	0.23	0.04	151
	2	0.05	0.14	0.26	0.03	134
	3	0.05	0.13	0.26	0.03	110
	1	0.26	0.29	0.47	0.06	203
	2	0.26	0.28	0.47	0.05	227
	3	0.26	0.28	0.40	0.05	177
	1	0.50	0.46	0.70	0.10	389
	2	0.50	0.44	0.83	0.08	234
	3	0.50	0.47	0.89	0.09	238

For example, the C content in the first row was lower at 0.50 m than at 0.26 m. This is probably due to the relatively larger measurement errors for the low quantities trapped at 0.50 m.

The ratio of the amount of a particular element in the transported material to the amount of that element in the parent soil is defined as the enrichment ratio (ER). Average ER values for both storms (Table 4) indicate that at the lowest level (0.05 m) the chemical composition of the erosion

Table 4. Average enrichment ratios of a dust sample and trapped erosion materials for two storms at ICRISAT Sahelian Center, 1993 rainy season.

		Enrichment ratio†			
	Height	K	C	N	P
	m				
Dust sample	2.00	10.00	31.53	19.75	5.02
13 June	0.05	1.18	1.33	0.83	0.98
	0.26	1.91	2.39	1.42	1.10
	0.50	2.06	3.02	2.08	1.14
1 July	0.05	1.27	1.47	0.83	0.91
	0.26	2.58	2.63	1.33	1.40
	0.50	4.15	4.74	2.25	1.98

† Ratio of the TE content of the eroded material to the TE content of the topsoil.

material was very similar to that of the topsoil. The material at the highest sampling level (0.50 m) was about three times richer in nutrients than the topsoil, whereas the sample of deposited dust was 17 times richer.

Fitting Eq. [2] to all TE contents resulted in four pairs of regression coefficients for each storm and row of MWAC catchers. The fitted model described the measured values reasonably well, with mean R^2 values of 0.97, 0.90, 0.88, and 0.71 for K, C, N, and P, respectively. Use of the regression coefficients of Eq. [1] and Eq. [2] in Eq. [3] resulted in the mass flux profile, f(z), of each element in the transported material. Figure 3 shows two fitted curves of potassium for the same catcher as in Fig. 2. The fitted curves for the other elements resulted in similar shapes.

Nutrient losses from the experimental plot were estimated from the total TE mass transport rates (F_t). A mass budget (ΔF_t) for the plot was determined for both storms (Table 5). The total TE mass transport rates along the four plot boundaries were averaged. For this purpose, the outermost rows with MWAC catchers were chosen as boundaries. The mean wind direction of a storm determined the boundaries that contributed to input ($F_t \downarrow$) and the ones that contributed to output ($F_t \uparrow$) of erosion material. During both storms, the material moved into the plot over the eastern and southern boundaries, and left the plot via the northern and western boundaries. Multiplying ΔF_t with half the circumference of the plot and the storm duration resulted in the nutrient losses from the plot, which were converted to kilograms per hectare.

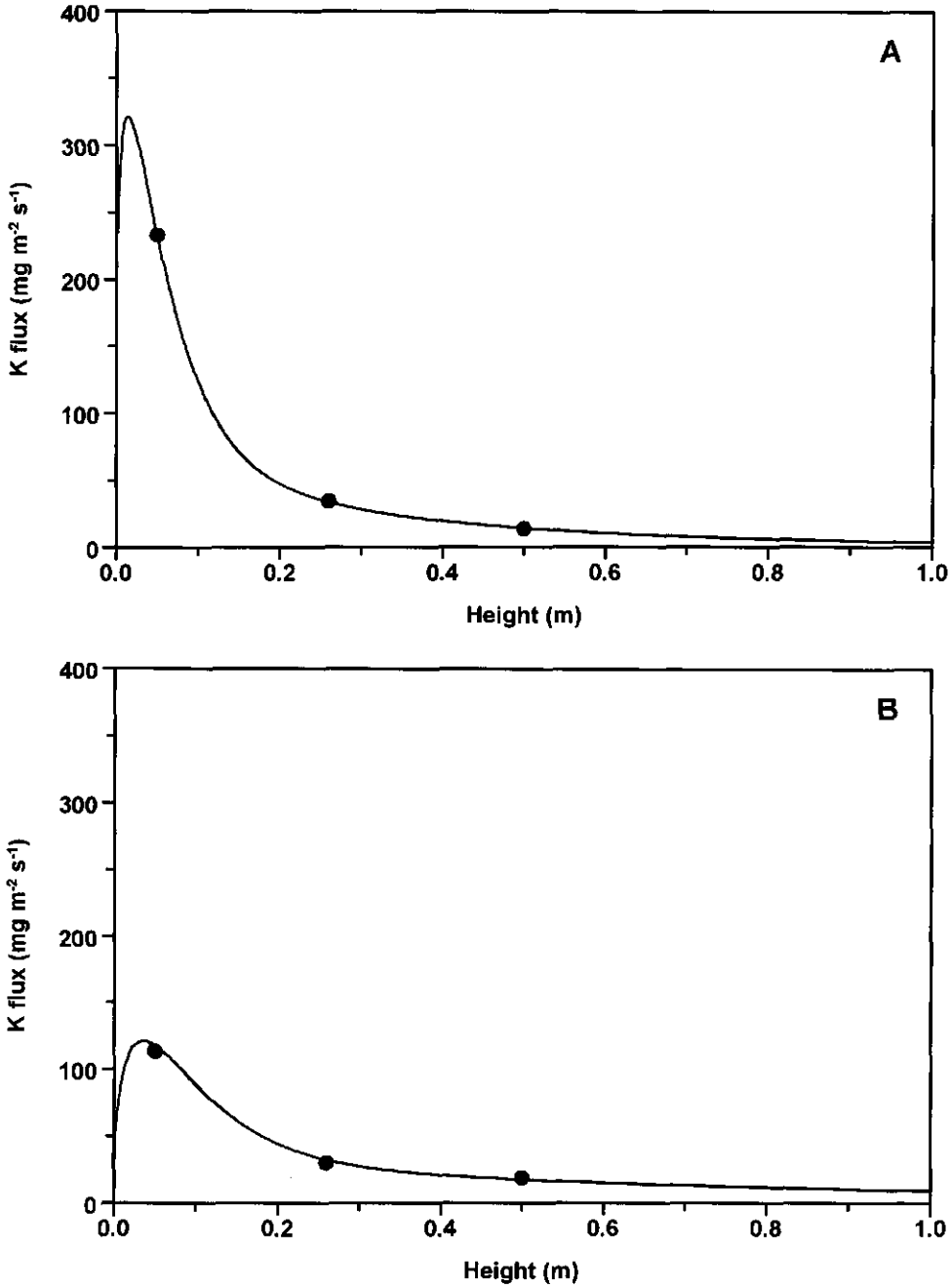

Figure 3. Fitted profiles through measured potassium mass fluxes for one MWAC catcher during the storm events of (A) 13 June and (B) 1 July 1993.

Table 5. Estimated nutrient losses from the experimental plot during two storms at ICRISAT Sahelian Center, 1993 rainy season.

Date	Element	$F_t\downarrow$ †	$F_t\uparrow$ ‡	ΔF_t §	Nutrient loss
		mg m^{-1} s^{-1}	mg m^{-1} s^{-1}	mg m^{-1} s^{-1}	kg ha^{-1}
13 June	K	93.9	109.2	-15.3	11.2
	C	157.2	188.9	-31.7	23.2
	N	22.0	28.6	-6.6	4.9
	P	9.9	11.1	-1.2	0.9
1 July	K	68.4	99.3	-30.9	45.9
	C	120.3	158.3	-38.0	56.4
	N	14.6	23.7	-9.1	13.4
	P	5.3	8.8	-3.5	5.2

† $F_t\downarrow$ = average incoming TE mass transport rate.
‡ $F_t\uparrow$ = average outgoing TE mass transport rate.
§ $\Delta F_t = F_t\downarrow - F_t\uparrow$ = TE mass budget.

Compared with the amounts of nutrients present in the first 0.10 m of the topsoil, which were calculated from the TE contents of the topsoil (Table 3) and a dry bulk density of 1650 kg m^{-3} (Klaij and Hoogmoed, 1989), the estimated nutrient losses were equal to 3.2%, 2.8%, 2.8%, and 2.6% of the total for K, C, N, and P, respectively. Nutrient input by dust deposition in the fallow site over the same period was simply calculated by multiplying the total dust input by the TE contents of the sample (Table 3), resulting in inputs of 2.5 kg ha^{-1} K, 13.0 kg ha^{-1} C, 1.9 kg ha^{-1} N, and 0.2 kg ha^{-1} P.

DISCUSSION

The horizontal mass flux of wind-blown material decreases strongly with height (Fig. 2). Just above the soil surface, saltation is the dominant transport mode, whereas suspension becomes dominant around the 1 m level. At 0.50 m, saltation and suspension are equally important (Sterk and Raats, 1996). The following (arbitrary) height classes were distinguished: (1) 0 - 0.15 m, where saltation is dominant; (2) 0.15 - 0.85 m, where saltation and suspension are both important; (3) 0.85 - 1.00 m, where suspension is dominant; (4) >1.00 m, where there is only suspension transport.

As stated earlier, it is not known whether the efficiency of the erosion traps is particle size dependent. Saltation particles are generally easier to trap than particles moving in suspension (Shao et al., 1993). If this is also true for the MWAC catcher, the measured suspension mass fluxes were

underestimated, which is irrelevant in the first height class, but not in the second and third height classes.

The calculated TE mass flux profiles (Fig. 3) show that the main mass of nutrients is transported in height class (1), where saltation is dominant. These high TE mass fluxes can be explained by the presence of small aggregates. The aggregate size distribution of the topsoil (Table 1) shows that only 3.1% is <63 μm, whereas dispersed particle size analysis revealed that there is 7.8% of silt and clay in the topsoil. So, much of the fine, nutrient-rich material is not present as dispersed particles, but has formed particle bonds. The larger aggregates are transported by saltation, whereas the very small aggregates still can be transported by suspension (Zobeck and Fryrear, 1986b). In the second height class, the TE mass flux decreases with height, first sharply and then more gradually as suspension becomes more important. In the third and fourth height classes, the gradual decrease of the TE mass flux continues.

In general, suspended dust is richer in nutrients than the coarser saltation material (Table 3), owing to a higher percentage of clay and silt particles (Zobeck and Fryrear, 1986b). The suspension particle mass fluxes, however, are much lower than the saltation mass fluxes, even when they are underestimated by the MWAC catcher. The resulting TE mass fluxes moved by suspension are an order of magnitude lower than the saltation TE mass fluxes, but are extended to a height of several hundred meters, and thus suspension can also transport considerable amounts of plant nutrients.

Saltation transport can only result in a local redistribution of soil particles and nutrients. Once picked up by the wind, saltating soil particles are moved in a downwind direction until they are deposited near some obstacle such as trees, bushes, fences, etc. In southwest Niger, the landscape is dominated by old laterite plateaus and a parkland, with scattered trees and bushes, on the sand plains between the plateaus. The parkland is dominated by millet fields in which the shrubs are usually cut down at the beginning of the growing season, but regrow after the crop is harvested. Although there is much less than a few decades ago, there is also fallow land with a denser vegetation of bushes, grasses, and herbs. Therefore, saltation leads to short range transport, with the main sources of soil particles and nutrients being the bare millet fields in the dry season and early rainy season, and the main sinks being the fallow areas with good vegetation cover. The fertility status of a fallow site is improved at the expense of decreasing soil productivity in the surrounding millet fields. This situation has two implications. First, the nutrient losses from the cropped areas mean a restricted cropping period relative to the potential. Second, the crop-fallow system functions only with a

sufficient area of fallow land, otherwise the regional budget of saltation particles and nutrients becomes negative. The first indications of such a negative budget were given for the Maradi region in south Niger and were explained by agricultural over-use (Mainguet and Chemin, 1991).

The function of fallow vegetation in trapping soil particles can be simulated by adequate mulch cover. Geiger et al. (1992) measured differences of 0.15 to 0.20 m in surface elevation between mulched and bare millet plots at ISC in only five years. They concluded that the elevated surface was due to entrapment of wind-blown material, and the stabilization of the original soil surface against wind erosive forces. Applying mulches on degraded surfaces may even result in regeneration of the soil. Trapping of wind- and water-deposited sediments by tree branches on a barren, crusted surface resulted in natural revegetation of the surface after a few months in the rainy season. This revegetation was related to better fertility and improved water infiltration (Chase and Boudouresque, 1987). On a smaller scale, individual obstacles, especially shrubs, act as sinks for saltation particles from the surrounding source areas. The trapped sediments tend to accumulate around the bases of the shrubs, forming micro-dunes. These dunes are known to farmers as having the best productivity after the shrubs have been cut down. Similar observations of nutrient-rich deposits near obstacles have been reported from Australia (Ludwig and Tongway, 1995).

The sinks and sources for saltation transport are not stable, but change with time. Millet fields that have been cultivated for many years may be turned into fallow land, becoming a sink for saltation material, and fallow sites will be used for crop production again after a few years. If these new fields are not well protected against wind erosion, the sites will change from sinks into sources for saltation material. Furthermore, mulch covers on a particular field may change from year to year due to the limited availability of mulches. Crop residues are the most easily available mulch material, but are also needed for fuel, construction, and fodder. In addition, applied residues are subject to decomposition by termites. Therefore, millet fields usually have insufficient mulch cover, or the mulch is concentrated on just one field, leaving other fields unprotected.

The fine suspended dust which is raised from the field by a convective storm may be carried over long distances, resulting in a loss of fine particles and nutrients from the area and thus enhancing regional soil degradation. For example, Prospero et al. (1970) were able to trace dust arriving at Barbados from across the Atlantic Ocean to a severe storm that originated in West Africa five days earlier. Similar observations of dust crossing the Atlantic Ocean were reported by Carlson and Prospero (1972) and Westphal et al. (1988). Apart from losses, there are also inputs of dust. During the

Harmattan season, fine suspended dust is transported towards the Sahel, where it partly settles. During the early rainy season, some of the dust raised by a convective storm is deposited again by gravity or rain wash-out. Drees et al. (1993) measured 50% of the total annual dust input at ISC in the early rainy season, whereas the contribution of the Harmattan season to the total was only 15%. Whether there is a net loss or gain of dust due to suspension transport in the Sahel is unclear. Soil surfaces that are well protected against erosion by good vegetation cover can only benefit from dust deposits. For example, we measured 0.24 Mg ha^{-1} of dust deposition in the fallow site at ISC during the 1993 early rainy season, whereas soil losses by wind erosion from this site were negligible owing to dense vegetation that gave adequate protection to the soil surface. In areas with inadequate protection against strong winds, soils probably lose more fine particles than they gain. The calculated total soil loss from the experimental plot during the four storms was equal to 45.9 Mg ha^{-1} (Table 2). Using the rough assumption that the loss due to suspension transport was 3.1% (= mass percentage of aggregates <63 μm in Table 1) of the total, the dust input in the fallow was equal to only 17% of the suspension loss from the plot.

The estimated nutrient losses (Table 5) from the experimental plot during the two storm events show that wind erosion can remove significant quantities of plant nutrients. Compared with the nutrient inputs in the fallow site during the same period, the estimated nutrient losses were 10 to 30 times higher. The actual nutrient losses from the experimental plot during the 1993 early rainy season were even higher than the estimated values because of (i) the storm events of 23 June and 30 June, and (ii) the suspension losses above the 1 m level. Furthermore, the possible underestimation of the suspension mass fluxes may have resulted in a lower estimate of the nutrient losses.

In other years, the soil and nutrient losses from millet fields are probably much higher than the numbers presented here. The 1993 rainy season, with only four storms, was classified as a weak wind erosion season. During the rainy seasons of the previous three years, 21, 13, and 15 wind erosion events, respectively, were recorded at ISC (Michels, 1994). Considering the quantities of soil mass and plant nutrients that can be removed by a single storm, the negative impact of wind erosion on soil productivity in southwest Niger can be very serious in some years.

CONCLUSIONS

The two modes of transport of wind-eroded particles, saltation and suspension, have different consequences for soil productivity in the Sahel. On a local scale, saltation moves soil particles and

nutrients over short distances, from bare, unprotected soils towards areas with sufficient vegetation or mulch cover, or individual obstacles like bushes. In the source areas, soil productivity is declining, whereas the sinks are enriched and hence soil productivity is enhanced. On a regional scale, saltation does not normally result in a net loss of nutrients. It merely causes a redistribution of soil particles and nutrients from bare, arable fields to fallow land. When the area under fallow becomes too small, saltation may lead to a negative particle and nutrient budget.

Suspension may transport nutrient-rich dust from the Sahel for thousands of kilometers, exporting nutrients to other parts of the world. At the same time, the Sahel benefits from dust depositions during the Harmattan season and the early rainy season. Areas with a good vegetation cover, like fallow sites, particularly benefit from dust depositions. Unprotected surfaces, however, lose more fine soil and nutrients by suspension transport than they gain from dust inputs. The data presented are not sufficient to permit any final conclusions to be drawn, but they indicate that a single convective storm can lead to a loss of nutrients from an arable field that exceeds the total annual input by dust. Since more land has been turned into cropland in the last few decades, it is likely that nowadays there is a net loss of fine soil particles and nutrients by suspension transport in the Sahel.

As far as soil fertility and agricultural production are concerned, the emphasis should be on (i) the protection of fields against erosive winds caused by convective storms in the early rainy season, and (ii) reduction of saltation transport within fields during the dry season. Soil and nutrient conservation in the rainy season allows a prolonged and more effective cropping on the low fertility soils in southwest Niger. Reduction of saltation transport in the dry season prevents irregular distribution of nutrients in the field, making crop stands less heterogeneous by improving nutrient availability. With the current farming practices in Niger, soil conservation can only be achieved by effective use of crop residues as mulch cover. However, the present biomass production is not sufficient for soil protection. Further research is needed to explore the possibilities of alternative mulch material and to increase biomass production.

ACKNOWLEDGMENTS

The authors gratefully acknowledge the financial support of the Netherlands Foundation for the Advancement of Tropical Research (WOTRO). The assistance and cooperation of the ICRISAT Sahelian Center during the field experiment is much appreciated. The nutrient analyses were conducted at the Soil Science Department of the University of Hohenheim. We thank L. Stroosnijder and

P.A.C. Raats of the Wageningen Agricultural University for their constructive comments on an earlier version of the manuscript.

REFERENCES

Bagnold, R.A. 1973. The physics of blown sand and desert dunes. 5th ed. Chapman and Hall, London.

Carlson, T.N., and J.M. Prospero. 1972. The large-scale movement of Saharan air outbreaks over the northern equatorial Atlantic. J. Appl. Meteorol. 11: 283-297.

Chase, R., and E. Boudouresque. 1987. Methods to stimulate plant regrowth on bare Sahelian forest soil in the region of Niamey, Niger. Agric. Ecosyst. Environ. 18: 211-221.

Chepil, W.S. 1945. Dynamics of wind erosion. I. Nature of movement of soil by wind. Soil Sci. 60: 305-320.

Drees, L.R., A. Manu, and L.P. Wilding. 1993. Characteristics of aeolian dusts in Niger, West Africa. Geoderma 59: 213-233.

Dregne, H.E., M. Kassas, and B. Rozanov. 1991. A new assessment of the world status of desertification. Desertification Control Bull. 20: 6-18.

Geiger, S.C, A. Manu, and A. Bationo. 1992. Changes in a sandy Sahelian soil following crop residue and fertilizer additions. Soil Sci. Soc. Am. J. 56: 172-177.

Herrmann, L., K. Stahr, and M.V.K. Sivakumar. 1996. Dust deposition on soils of southwest Niger. p. 35-47. *In* B. Buerkert et al. (ed.) Wind erosion in West Africa: The problem and its control. Proc. Int. Symp., Stuttgart, Germany. 5-7 Dec. 1994. Margraf Verlag, Weikersheim, Germany.

Klaij, M.C., and W.B. Hoogmoed. 1989. Crop response to tillage practices in a Sahelian soil. p. 265-275 *In* Soil, crop, and water management in the Sudano-Sahelian zone. Proc. Int. Worksh., Niamey, Niger. 11-16 Jan. 1987. ICRISAT, Patancheru, India.

Leys, J., and G. McTainsh. 1994. Soil loss and nutrient decline by wind erosion - cause for concern. Aust. J. Soil Water Conserv. 7: 30-35.

Ludwig, J.A., and D.J. Tongway. 1995. Spatial organisation of landscapes and its function in semi-arid woodlands, Australia. Landscape Ecology 10: 51-63.

Mainguet, M., and M.C. Chemin. 1991. Wind degradation on the sandy soils of Mali and Niger and its part in desertification. Acta Mech. [Suppl] 2: 113-130.

Michels, K. 1994. Wind erosion in the southern Sahelian zone: Extent, control, and effects on millet production. Verlag Ulrich E. Grauer, Stuttgart, Germany.

Prospero, J.M., E. Bonatti, C. Schubert, and T.N. Carlson. 1970. Dust in the Caribbean atmosphere traced to an African dust storm. Earth Planetary Sci. Letters 9: 287-293.

Ramaswamy, S., and J.H. Sanders. 1992. Population pressure, land degradation and sustainable agricultural technologies in the Sahel. Agric. Systems 40: 361-378.

Shao, Y., G.H. McTainsh, J.F. Leys, and M.R. Raupach. 1993. Efficiencies of sediment samplers for wind erosion measurements. Aust. J. Soil Res. 31: 519-532.

Sivakumar, M.V.K. 1992. Climate change and implications for agriculture in Niger. Climatic Change 20: 297-312.

Sterk, G. 1993. Sahelian wind erosion research project, Report III. Description and calibration of sediment samplers. Dep. of Irrigation and Soil & Water Conservation, Wageningen Agric. Univ., The Netherlands.

Sterk, G., and P.A.C. Raats. 1996. Comparison of models describing the vertical distribution of wind-eroded sediment. Soil Sci. Soc. Am. J. 60: 1914-1919. (Chapter 3 in this volume).

Sterk, G., and A. Stein. 1997. Mapping wind-blown mass transport by modeling variability in space and time. Soil Sci. Soc. Am. J. (in press). (Chapter 4 in this volume).

West, L.T., L.P. Wilding, J.K. Landeck, and F.G. Calhoun. 1984. Soil survey of the ICRISAT Sahelian Center, Niger, West Africa. TropSoils, Texas A&M Univ., College Station, TX.

Westphal, D.L., O.B. Toon, and T.N. Carlson. 1988. A case study of mobilization and transport of Saharan dust. J. Atmos. Sci. 45: 2145-2175.

Young, R.A., A.E. Olness, C.K. Mutchler, and W.C. Moldenhauer. 1985. Chemical and physical enrichments of sediment from cropland. p. 107-116. *In* Erosion and Soil Productivity. ASAE Publication No. 8-85.

Zobeck, T.M., and D.W. Fryrear. 1986a. Chemical and physical characteristics of windblown sediment II. Chemical characteristics and total soil and nutrient discharge. Trans. ASAE 29: 1037-1041.

Zobeck, T.M., and D.W. Fryrear. 1986b. Chemical and physical characteristics of windblown sediment I. Quantities and physical characteristics. Trans. ASAE 29: 1032-1036.

Chapter 6

Wind Erosion Control with Crop Residues in the Sahel

G. Sterk and W.P. Spaan

Accepted for publication in: Soil Science Society of America Journal.

Reproduced by permission of the Soil Science Society of America.

Wind Erosion Control with Crop Residues in the Sahel

ABSTRACT

Mulching for wind erosion control in Sahelian farming systems is limited by low biomass production and use of crop residues for other purposes. The aim of this study was to test the effectiveness in soil protection created by two low amounts of crop residues. A field experiment was conducted in southwest Niger, on a Psammentic Paleustalf (sandy, siliceous, isohyperthermic) during the early rainy seasons of 1994 and 1995. Particle mass transport was quantified in two plots of 55 by 70 m. During the first storms of both seasons, the plots were without a mulch cover. Afterward, one plot was covered with flat pearl millet (*Pennisetum glaucum*) stalks. The application rates were 1500 and 1000 kg ha^{-1} during the first and second seasons, respectively. To quantify the mulch effect, mass transport rate differences between the two bare plots were quantified with a multiple linear regression model ($R^2 = 0.89$), using wind speed (7.4 - 12.3 m s^{-1}), wind direction, and storm duration (464 - 3835 s). Total mass transport rates were reduced from 365.2 to 132.9 g m^{-1} s^{-1} (63.6%) with 1500 kg ha^{-1}, and from 325.1 to 188.0 g m^{-1} s^{-1} (42.2%) with 1000 kg ha^{-1} of crop residues. Soil protection tended to decrease with increasing wind speed. Linear regression indicated that the reduction in mass transport becomes zero at wind speeds of 11.1 and 16.0 m s^{-1} for the 1000 and 1500 kg ha^{-1} covers, respectively. The 1000 kg ha^{-1} cover even enhanced sediment transport by 6.5% during one storm with a wind speed of 11.3 m s^{-1}. The 1500 kg ha^{-1} mulch cover reduced sediment transport from 49.7 to 80.2% during five storms with wind speeds varying from 8.3 to 10.6 m s^{-1}, and is therefore recommended as the better application rate for wind erosion control in the Sahel.

Wind erosion is a common phenomenon on sandy soils of the African Sahel. During the dry season (October - April), strong Harmattan winds blow from the northeast and cause moderate erosion (Michels et al., 1995a). The main erosion period, however, is during the early rainy season (May - July), when severe but short duration (10 - 30 min) wind storms create spectacular dust clouds. These storms are gust fronts, formed by strong downdrafts of cold air in cumulonimbus clouds, or thunderstorms, that bring the first rains of the new rainy season. Agricultural damage by wind erosion is twofold. It may damage seedlings that are sown at the beginning of the rainy season (Michels et al., 1995b), and it causes land degradation by the loss of nutrient-rich soil material (Sterk et al., 1996a).

Mulching is one of the cheapest and most effective measures to protect the soil against erosive winds. Furthermore, mulches help reduce water erosion, reduce intense solar radiation, suppress extreme fluctuations of soil temperatures, and reduce water loss through evaporation, resulting in more stored soil moisture. These effects help to create improved conditions for plant growth in many circumstances (Morgan and Rickson, 1995).

Testing the efficacy of mulch material in reducing wind erosion has mainly been done in wind tunnels (e.g., Siddoway et al., 1965; Lyles and Allison, 1981; Fryrear, 1985). Wind tunnels have the advantage that experimental conditions like wind speed, wind direction, and storm duration can be controlled. Moreover, a certain storm can be repeated as often as necessary. The main disadvantage of using wind tunnels is the homogeneous and less turbulent flow compared with the atmospheric boundary layer, making it uncertain whether the laboratory results can be translated to natural conditions. In the field, it is much more complicated to do similar experiments. With real storms, the number, duration, average wind speed, and wind direction cannot be controlled. Also, when testing a certain quantity of mulch material, the measured soil erosion is compared with an unprotected control plot. The soils of the control and the test plots must be equally erodible, the wind field during storms similar, and there should be no mutual influence of the mulched and the unprotected plots.

For the Sahelian farming systems, it is of special interest to test the efficacy of small quantities of crop residue in reducing wind erosion. Although the benefits are obvious, mulching is not widely practiced. Stalks of pearl millet (*Pennisetum glaucum*), which is the main crop grown by Sahelian farmers, are by far the most available mulch material, but are also needed for other purposes, like fodder, fuel, and construction material (Lamers and Feil, 1993). The availability of millet residues for soil protection is therefore limited.

A Sahelian field experiment with flat millet stalks revealed that a soil cover of 500 kg ha^{-1} does not result in an overall decrease of particle mass flux during early rainy season storms (Michels et al., 1995a). However, clear differences existed between individual storms. Sediment transport was as often enhanced as it was reduced. A much better protection of the soil surface was obtained with an amount of 2000 kg ha^{-1}, which reduced the particle mass flux on average by 47%.

Under the current biomass production levels, with an average millet stover production of 2200 kg ha^{-1} (Manu et al., 1991), crop residue amounts of 2000 kg ha^{-1} for soil conservation are not realistic in the Sahel. Therefore, the effect of lower quantities on wind erosion was studied. The

objective was to determine the reduction in wind-blown mass transport created by 1000 and 1500 kg ha^{-1} of flat millet stalks during early rainy season storms.

MATERIALS AND METHODS

A field experiment was conducted at the International Crops Research Institute for the Semi-Arid Tropics (ICRISAT) Sahelian Center (ISC) in southwest Niger, during the 1994 and 1995 rainy seasons. The location of ISC (13°16'N;2°21'E) is 45 km south of the capital, Niamey. Thunderstorms in the early rainy season generally move westward, and the resulting wind direction during a storm is usually east. Therefore, a field was selected at the eastern side of the center to reduce disturbance of the wind field by obstacles like fences, buildings, and experimental wind breaks that are present at ISC. The roughness of the terrain eastward of the measurement field resembled the situation in the region, with scattered trees and bushes. The height of these obstacles ranged from 0.5 to 5 m. Distances of the main obstacles to the center of the field were sufficiently large to assume that the wind profile in the field was only negligibly disturbed.

The soil at the measurement field is classified as a sandy, siliceous, isohyperthermic Psammentic Paleustalf according to the U.S. soil taxonomy (West et al., 1984). The texture of the topsoil consists of 92.2% sand, 3.0% silt, and 4.8% clay. The dry aggregate size distribution of the topsoil is given in Table 1.

The sandy Sahelian soils often have a strong structural crust, formed by high-intensity rainfall in the early rainy season. Structural crusts typically have two layers (Valentin and Bresson, 1992).

Table 1. Aggregate size distribution† of topsoil at the ICRISAT Sahelian Center.

Size class	Mass
µm	%
< 63	3.1
63 - 125	18.2
125 - 250	35.7
250 - 500	32.8
500 - 1000	10.0
> 1000	0.2

† The size distribution of dry undispersed particles determined by dry sieving with a set of vibrating sieves.

At a depth of a few millimeters, a thin and dense plasmic layer is formed by the clay and silt particles that are washed out from the top layer by raindrops. The plasmic layer is covered by loose, cohesionless sand, which is easily eroded by wind or water. During both seasons, the crust was broken twice by weeding, but returned immediately during the next rain.

Prior to installation of equipment, the whole field was cleared by removing weeds and residues from the previous crop. Pearl millet was sown on 17 June during the 1994 rainy season, and on 21 June of the following year. Sowing was similar to the traditional method, with planting holes, or pockets, spaced at the corners of squares of 1 by 1 m. In each pocket, 50 to 100 seeds were thrown, and 2 weeks after emergence the number of plants was manually reduced to three. The low plant density and the late sowing dates assured that young millet plants did not have a significant influence on the wind field during the experiments. The soil surface between the millet pockets was kept clear of weeds by hoeing at 3 and 6 weeks after sowing.

The size of the field was 170 by 90 m, and within the field two experimental plots with a size of 55 by 70 m were selected. Both plots were equipped with ten sediment catchers that were uniformly distributed over the whole area of the plot (Fig. 1). In the center of Plot II (north), three acoustic saltation sensors, or saltiphones (Spaan and Van den Abeele, 1991), and a meteorology mast were placed. The meteorological measurements included precipitation, wind speed, and wind direction. Precipitation was measured with a tipping bucket rain gauge, wind speed with a fast-response cup anemometer at 2 m height, and wind direction was determined from the three orthogonal velocity components measured with a three-dimensional propeller anemometer at 3 m.

The saltiphone records impacts of saltating sand grains with a microphone with a membrane of 201 mm^2. The microphone is placed inside a steel tube (diameter = 0.05 m, length = 0.13 m) that protects it from severe weather conditions. The tube is mounted on a ball bearing and has two vanes at the back to keep it oriented into the wind.

During erosion, part of the saltating sand grains moving through the tube hits the microphone and creates high frequency signals. By amplifying these signals and filtering low-frequency signals, saltating sand can be distinguished from other noises like those created by wind and rain. Every amplified signal, or pulse, is cut off after 1 ms, so, theoretically, a maximum number of 1000 grains per second can be recorded. The actual number of impacts may be higher due to overlap of particle impacts during the 1 ms pulse duration.

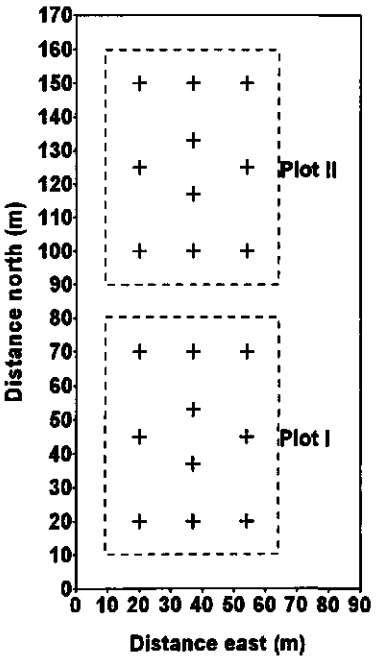

Figure 1. Layout of the measurement field, with two experimental plots and the positions of the Modified Wilson and Cooke (MWAC) sediment catchers.

The three saltiphones were installed with the center of the microphones positioned at 0.10 m height. The created pulses were continuously recorded and stored with a sampling frequency of 1 Hz. The output, in counts per second, shows the temporal variability of the saltation flux, which was used to determine the exact starting time and duration of storms.

The mass of soil particles moved by the wind was quantified with Modified Wilson and Cooke (MWAC) sediment catchers (Sterk and Raats, 1996). The catcher consists of a central pole with seven sediment traps attached between 0.05 and 1.00 m. A large vane at the back keeps the catcher oriented into the wind. Each trap has a 100 ml PVC bottle, with two glass tubes, an inlet and an outlet, entering the bottle through the cap. The tubes have an internal diameter of 8 mm, and are bent 90° in opposite directions on the outside. During a storm, dust-laden wind enters the bottles through the inlet, air escapes through the outlet, and the soil particles are trapped in the bottles.

After each storm, the material in the bottles was collected, dried, and weighed. Dividing the particle mass in each bottle by the storm duration and the area of the opening of the inlet tube resulted

in seven horizontal mass fluxes for each catcher. Through the vertical profile of horizontal mass fluxes, the following model was fitted with a nonlinear regression procedure (Sterk and Raats, 1996):

$$q(z) = a(\frac{z}{\alpha} + 1)^{-b} + c\exp(-\frac{z}{\beta}) \qquad [1]$$

where q(z) is the horizontal mass flux (kg m^{-2} s^{-1}) at height z (m), and a, α, b, c, and β are regression coefficients. Integrating the profiles across height resulted in measured (or calculated) mass transport rates Q (kg m^{-1} s^{-1}) at the sampling point. Theoretically the upper limit for integration could be taken at infinity. However, no measured mass fluxes above 1 m height were available to calibrate the model in that height range. Given the strong decrease of particle mass flux with height, it is assumed that the mass of sediment moving above 1 m is negligible compared with the mass below 1 m. Therefore, the limits for integration were taken at z = 0 and 1 m. Dividing Q by the trapping efficiency of the MWAC catcher, equal to 0.49 for this Sahelian soil (Sterk, 1993; Sterk and Raats, 1996), resulted in a total mass transport rate Q_t at the point of sampling. The value of Q_t is equal to the total mass of particles below 1 m height that passed, per unit of time, a strip 1 m wide and perpendicular to the mean wind direction.

In both seasons, the plots were left bare for the first 3 weeks after installation of the equipment. This was done to make a comparison between the two plots possible and to evaluate whether the plots were equally eroded during storms. Afterward the southern plot (Plot I) was covered with millet stalks. Length of stalks ranged from 0.5 to 1.5 m, with diameters ranging from 10 to 20 mm. The application rates were equal to 1500 kg ha^{-1} in 1994, and 1000 kg ha^{-1} in 1995, corresponding to estimated soil covers of 7.1 and 4.7%, respectively. The residues were uniformly distributed without a specific orientation of the stalks, and redistributed every time after weeding. The weight of the material was sufficiently high to assure that stalks were not blown away during storms.

Under bare conditions, the soil surface was smooth and without any roughness other than that created by the soil particles themselves, characterized by a roughness length of approximately 0.001 m. Only just after weeding the roughness length increased to approximately 0.01 m, but in both seasons no wind storms occurred during these periods. Covering the soil surface with millet stalks resulted in an increase in roughness length to estimated values of 0.02 and 0.03 m for the 1000 and 1500 kg ha^{-1} rates, respectively.

RESULTS AND DISCUSSION

Compared with the 1993 rainy season, when four erosive storms occurred (Sterk et al., 1996a), the 1994 and 1995 rainy seasons were characterized by many erosion events. In total 20 storms occurred, which were rather variable in terms of wind speed, wind direction, and duration (Table 2). This variability can be explained by the local character of the thunderstorms. The most severe conditions are expected near the center of the cumulonimbus cloud, where a forward, i.e., eastward, outflow of cold air occurs (Cotton and Anthes, 1989). Away from the center, conditions are less severe with lower wind speeds and a wind direction that is shifted either northward or southward. Furthermore, the duration of wind storms is likely to change with position relative to the center of the cloud. The probability of rain decreases away from the center, which may cause an extended wind erosion period at the northern and southern limits compared with the center. Hence, the characteristics of a storm at a certain location depend on the distance to the center of the cloud.

The simultaneous recording of wind speed and saltation flux with one saltiphone during a typical Sahelian storm (Fig. 2) clearly illustrates the alternation of quiet periods, with little activity, and intense bursts of saltation transport. A good correlation between instantaneous wind speed and

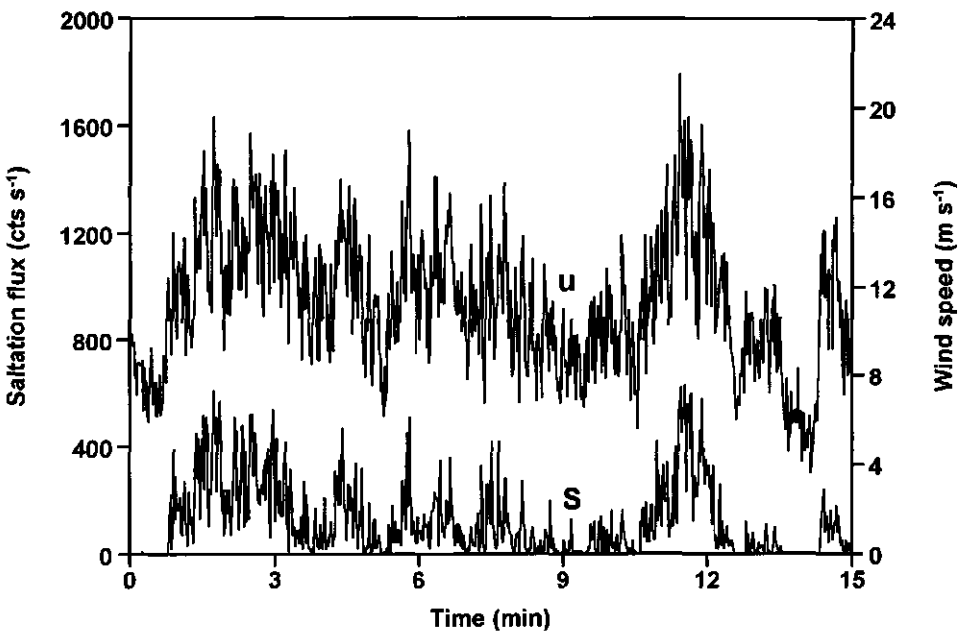

Figure 2. Graph of instantaneous wind speed (u) and saltation flux (S) vs. time for a typical Sahelian wind erosion event on 13 July 1995.

Table 2. Characteristics† of storms during the 1994 and 1995 rainy seasons at ICRISAT Sahelian Center.

				Plot I			Plot II		
Date	$\bar{u}$	Wdir	Dur	Cover	$\bar{Q}_t$	CV	Cover	$\bar{Q}_t$	CV
	m s^{-1}	degr	s	kg ha^{-1}	g m^{-1} s^{-1}	%	kg ha^{-1}	g m^{-1} s^{-1}	%
1994									
7 June	7.7	180.0	3835	0	12.8	63.5	0	17.6	39.1
10 June	12.3	37.8	464	0	196.1	20.6	0	153.9	25.2
14 June	7.4	107.5	2007	0	12.7	33.7	0	7.0	29.2
15 June	15.8	47.4	942	0	nd‡	nd	0	nd	nd
18 June	10.7	94.4	1209	0	56.6	17.4	0	50.8	21.0
27 June	9.4	118.1	515	1500	43.6	38.1	0	71.9	24.8
1 July	8.4	150.9	584	1500	16.6	105.9	0	71.7	27.7
4 July	10.6	81.2	838	1500	39.3	37.6	0	78.0	16.5
9 July	8.3	94.5	822	1500	10.2	58.2	0	21.6	27.2
12 July	9.4	75.7	902	1500	23.2	19.0	0	40.3	18.5
1995									
28 May	8.6	160.4	1983	0	97.7	34.1	0	137.1	16.4
5 June	9.0	175.2	2157	0	21.5	69.4	0	52.7	15.1
13 June	9.1	153.8	600	0	117.2	21.6	0	119.5	14.4
14 June	11.1	37.6	1086	0	132.8	15.5	0	107.8	14.1
17 June	9.4	173.3	1893	0	63.7	34.2	0	99.0	18.4
20 June	8.8	160.4	1662	0	68.8	37.7	0	104.9	18.3
25 June	9.6	86.9	415	1000	41.7	33.9	0	74.0	22.7
8 July	9.3	131.1	1092	1000	20.2	37.7	0	65.0	16.8
13 July	11.3	91.7	723	1000	118.2	17.5	0	123.8	16.1
16 July	8.9	175.6	1034	1000	7.9	96.0	0	54.0	28.6

† $\bar{u}$ = average wind speed; Wdir = average wind direction (0° = north); Dur = storm duration; $\bar{Q}_t$ = average total mass transport rate; CV = coefficient of variation.
‡ nd = not determined.

saltation flux exists (r = 0.76). The best correlation, however, is obtained if a time lag of 1 s between saltation flux and wind speed (r = 0.79) is assumed, indicating that the response time of saltating sand grains to wind speed fluctuations is in the order of 1 s (Sterk et al., 1996b).

For all storms but one, Eq. [1] was fitted through the measured mass fluxes of each catcher. The data of the storm of 15 June 1994 were not used for the analysis. This storm was immediately followed by 25 mm of rain in only 35 min. Although the average rain intensity was moderately high (42.9 mm h^{-1}), the instantaneous value exceeded 100 mm h^{-1} several times, and created much splash erosion while the instantaneous wind speed exceeded 20 m s^{-1}. Part of the splash material entered the sediment traps and got mixed with wind-blown material. This problem did not occur during the other events, although several wind storms were immediately followed by rain. During some of those events splash material had clogged the inlet tubes of the lowest traps, but it was never observed to have entered the bottles.

The average total mass transport rates ($\overline{Q}_t$; Table 2) show that significant differences between the two plots existed when both plots had a bare soil surface. The difference is not consistent, but changes from storm to storm, which partly can be explained by avalanching (Chepil and Woodruff, 1963). During an erosion event, the mass transport rate Q_t as a function of the distance downwind from a nonerodible boundary increases from zero at the boundary toward a maximum transport rate. With an easterly wind, the downwind distance from the nonerodible boundary, i.e., a dirt road, to both plots is similar. Hence, no big differences in average mass transport rates are expected, except for differences caused by spatial variability in mass transport. With a southerly or northerly wind, the situation is different, with one plot being much closer to the nonerodible boundary than the other plot. For instance, during the storm of 5 June 1995 the average total mass transport rate in Plot I (south) was 60% lower than in Plot II while the wind came from the south. During the storm of 10 June 1994 the wind direction was north-northeast and the total mass transport rate was then 27% higher in Plot I.

To determine the effect of millet residues on sediment transport, the difference in average total mass transport rates when both plots were bare needs to be quantified. Although wind direction is one of the key parameters, linear regression revealed that differences cannot entirely be explained by wind direction only ($R^2 = 0.49$). Therefore, a multiple linear regression analysis was carried out, and a three-parameter model, using average wind speed ($\overline{u}$), average wind direction (Wdir), and storm duration (Dur), was obtained ($R^2 = 0.89$; n = 10):

$$\Delta = 420.158 - 29.275\overline{u} - 0.995\,\mathrm{Wdir} - 0.013\,\mathrm{Dur} \qquad [2]$$

where Δ is the difference (%) in average total mass transport rates ($\overline{Q}_t$)between the two plots, relative to Plot II:

$$\Delta = 100\frac{\overline{Q}_{t,I} - \overline{Q}_{t,II}}{\overline{Q}_{t,II}} \quad [3]$$

The effect of millet residues on sediment transport was determined by using the regression model and the average total mass transport rates in the two plots. First, Δ was calculated with Eq. [2] from measured wind speed, wind direction, and storm duration. Then the average mass transport rate in Plot I when the surface would have been bare ($\overline{Q}'_{t,I}$) was estimated by:

$$\overline{Q}'_{t,I} = \overline{Q}_{t,II}(\frac{\Delta}{100} + 1) \quad [4]$$

The reduction in average total mass transport rates, Red (%), caused by the millet stalks is now equal to:

$$\text{Red} = 100\frac{\overline{Q}'_{t,I} - \overline{Q}_{t,I}}{\overline{Q}'_{t,I}} \quad [5]$$

The calculated values of Red are given in Table 3.

By summing the values of $\overline{Q}_{t,I}$ and $\overline{Q}'_{t,I}$, the average reductions in mass transport during five (1994) and four (1995) events, respectively, were calculated. The total mass transport rates were reduced by 42.2%, from 325.1 to 188.0 g m^{-1} s^{-1}, with a cover of 1000 kg ha^{-1}, and by 63.6%, from 365.2 to 132.9 g m^{-1} s^{-1}, with a soil cover of 1500 kg ha^{-1}. It can, therefore, safely be assumed that soil losses from the protected plot were significantly lower than from the unprotected plot.

Compared with the results of Michels et al. (1995a), who measured an average reduction of 47.1% in particle mass flux with a soil cover of 2000 kg ha^{-1}, better soil protection with lower crop residue amounts was obtained in our study. They used the same field at ISC and similar mulch material, but their experimental setup was entirely different. They divided the field into two rows of nine plots of 19 by 45 m, with three replications of 0 (control), 500, and 2000 kg ha^{-1} treatments in each row (cross-over design). Such a setup has the disadvantage of different treatments influencing each other. Particle transport in the control plots with protected plots in the upwind direction was reduced

Table 3. Reductions in average total mass transport rates caused by two different soil covers of flat pearl millet stalks.

Date	Cover	Δ†	$\overline{Q}'_{t,I}$‡	Red§
	kg ha^{-1}	%	g m^{-1} s^{-1}	%
1994				
27 June	1500	20.5	86.7	49.7
1 July	1500	17.2	84.0	80.2
4 July	1500	19.4	93.2	57.9
9 July	1500	74.0	37.7	73.0
12 July	1500	57.7	63.6	63.5
1995				
25 June	1000	47.6	109.2	61.8
8 July	1000	3.1	66.9	69.8
13 July	1000	-10.4	111.0	-6.5
16 July	1000	-29.6	38.0	79.1

† Δ = difference in average total mass transport rates when both plots would have been bare, as calculated with Eq. [2].
‡ $\overline{Q}'_{t,I}$ = average total mass transport rate in Plot I if the soil would have been bare.
§ Red = reduction in average total mass transport rates caused by the mulch cover.

due to the shelter created by the mulch, resulting in a low incoming mass transport rate. In contrast, when a protected plot is downwind of a control plot, the incoming particle mass flux is relatively high and the measured particle mass flux inside the plot could be higher than in the situation with two protected plots following each other. So, it is likely that the measured reduction in sediment transport created by 2000 kg ha^{-1} of millet stalks did not reflect the potential reduction. On the other hand, such an experimental setup has the advantage of every single storm actually contributing to the estimate of the reduction in sediment transport. With the experimental setup used in this study, about half of the erosion events were needed to quantify differences in sediment transport rates between the two plots. However, it is believed that quantifying differences between experimental plots prior to testing mulches gives better information, irrespective of the number of data points.

The reductions in total mass transport rate (Table 3) show a clear tendency of decreasing soil protection with increasing average wind speed of the storm. This is illustrated in Fig. 3, where the following linear regression models were fitted through the data for 1000 ($R^2 = 0.99$; n = 4) and 1500 kg ha^{-1} ($R^2 = 0.74$; n = 5), respectively.

$$Red = 420.49 - 37.78\bar{u} \quad [6]$$

$$Red = 152.02 - 9.47\bar{u} \quad [7]$$

Although the R^2 values indicate good correlations between reduction and wind speed, the number of data points was not sufficient for a proper analysis. Hence, the models may only be used to give an indication of the relation between wind speed and reduction in mass transport.

The difference in protective quality of the two mulch covers becomes apparent with the strength of a storm. During weak storms, defined as events with wind speeds varying from 7.5 to 10.0 m s^{-1}, both quantities gave a good protection to the soil surface. During strong storms, with wind speeds exceeding 10.0 m s^{-1}, the 1000 kg ha^{-1} of millet residues was not sufficient. According to the linear regression model (Eq. [6]), the reduction in sediment transport becomes zero at an average wind speed of 11.1 m s^{-1}. With stronger storms, erosion may actually be enhanced (Fig. 3). Although this observation is based on only one storm, it is supported by the data of Michels et al. (1995a),

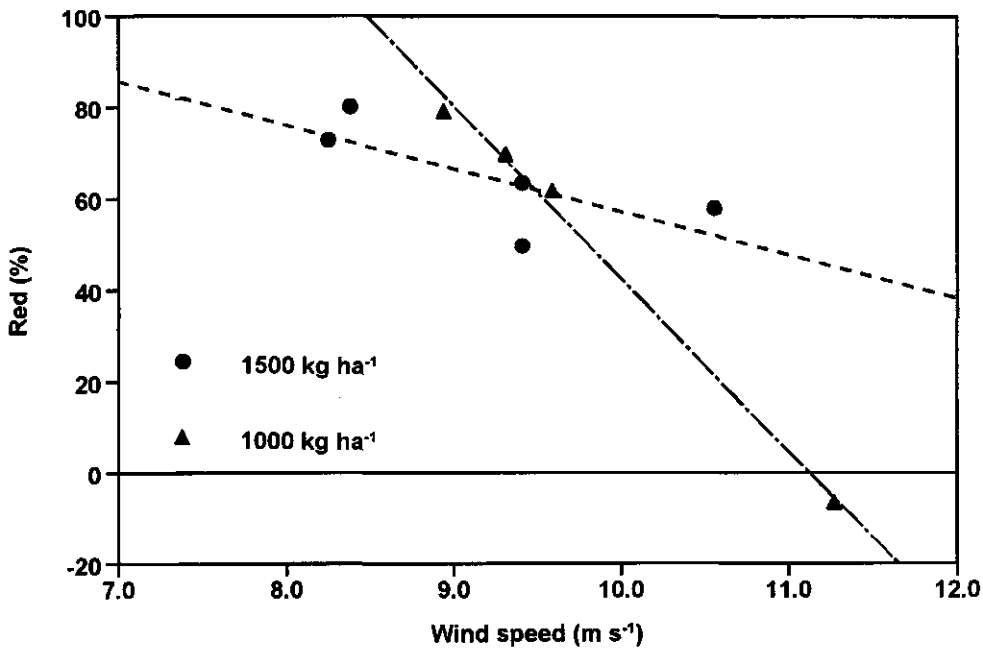

Figure 3. Relationship between average wind speed and the reduction in average total mass transport rates caused by mulch covers of 1500 and 1000 kg ha^{-1} of flat pearl millet stalks.

and by the wind tunnel study of Enninga (1994), who obtained a strong enhancement of erosion at low soil cover rates. Of the 20 storms during the rainy seasons of 1994 and 1995, only six strong storms occurred (Table 2), which indicates that sediment transport would have been reduced effectively during at least 14 storms.

A mulch cover of 1500 kg ha^{-1} can reduce sediment transport effectively during strong storms as well. The regression model (Eq. [7]) suggests that the reduction becomes zero at a wind speed of 16.0 m s^{-1}. However, it remains uncertain at which wind speed sediment transport is actually reduced, since there were not enough strong storms to calibrate the regression model for high average wind speeds. Based on the recorded storms (Table 2), it is concluded that the mulch cover would have sufficiently protected the soil surface from severe erosion during at least 19 of the 20 storms.

The relationship between wind speed and reduction in sediment transport was also observed by Siddoway et al. (1965) and Bilbro and Fryrear (1994). Unfortunately, in neither of the two studies was this relationship discussed in any detail. A physical explanation of the decreasing efficacy in soil protection with increasing wind speed was not found in the wind erosion literature. For instance, an often-applied technique to quantify the effects of roughness elements on threshold wind speed for erosion is drag or stress partitioning (Raupach et al., 1993). The overall drag force F can be partitioned into a force F_r exerted on the roughness elements, i.e., the millet stalks, and a force F_s exerted on the bare soil surface between the roughness elements:

$$F = F_r + F_s \qquad [8]$$

A decrease in efficacy of soil protection with increasing average wind speed would suggest that the ratio F_r/F_s is not constant, but decreases, resulting in a relatively higher stress at the bare soil surface. However, in the literature no evidence exists for the F_r/F_s ratio to decrease significantly with increasing wind speed when the soil cover is not changing, which was the case in this study. It certainly cannot explain why the average mass transport rate during the event of 13 July 1995 was even 6.5% higher in the protected plot than in the bare plot. This implies a negative F_r/F_s ratio, which is not realistic, and thus, a different explanation has to be given.

One of the simplifications of the stress partitioning theory is that it avoids direct consideration of the nature of turbulence close to the surface (Raupach et al., 1993). Lyles et al. (1971) presented wind tunnel data that show an important effect of roughness elements on turbulent velocity fluctuations. Roughness lowers mean wind speed near the surface and shelters erodible grains. But,

at the same time, increasing roughness substantially increases velocity fluctuations in the mean flow direction. In other words, the relative turbulence intensity T_u, defined as (Hinze, 1975):

$$T_u = \frac{\sigma_u}{\bar{u}} \qquad [9]$$

where σ_u (m s^{-1}) is the root mean square (RMS) of the fluctuating velocity component, and $\bar{u}$ is the average wind speed, is higher for a rough surface than for a smooth surface. Furthermore, T_u is independent of wind speed for a certain roughness, but decreases with height above the surface.

Based on these findings, it is possible to explain the reduced efficacy in soil protection with increasing wind speed. On a rough surface, the average wind speed near the surface is reduced, but the probability distribution of velocity fluctuations is much wider than on a smooth surface. This is explained by the higher RMS value, which is approximately equal to the standard deviation of velocity fluctuations. Hence, the probability that high instantaneous velocities, relative to the average wind speed, occur is higher above a rough surface than above a smooth surface. The effect is enhanced by the large and positive skewness of the streamwise velocity fluctuations over rough surfaces (Raupach et al., 1991), whereas above smooth surfaces the velocity fluctuations are approximately Gaussian distributed (Sterk et al., 1996b).

Near the threshold wind speed for erosion, equal to 8 m s^{-1} for this soil, roughness reduces the average wind speed below the threshold wind speed, but enhances turbulence. Only those gusts that exceed the threshold wind speed are able to erode soil particles. With increasing average wind speed, the probability distribution of velocity fluctuations shifts toward the threshold wind speed. The positive skewness results in relatively more strong gusts, which are the main events causing particle transport (Fig. 2). Hence, the benefits from roughening are being lost by the increasing gustiness of the wind. This effect is stronger for low mulch covers than for high covers, since the average wind speed near the soil surface is reduced less.

CONCLUSIONS

Covering the soil surface with 1500 kg ha^{-1} of flat millet stalks gave good protection against erosive winds. On average, sediment transport was reduced by 63.6% during five storms. The protective quality of a mulch cover of 1000 kg ha^{-1} was less, but still reduced sediment transport by 42.2% during four storms.

In general, the efficacy in reducing sediment transport decreased with increasing average wind speed of a storm. This effect can be explained by an increase in the relative turbulence intensity (Eq. [9]) due to the roughness elements. The decrease in protection with wind speed was stronger for the 1000 kg ha^{-1} cover since it reduces less the average wind speed compared with the 1500 kg ha^{-1} cover.

Both quantities of millet stalks protected the soil surface sufficiently during weak storms, with wind speeds between 7.5 and 10.0 m s^{-1}. During strong storms, with wind speeds exceeding 10 m s^{-1}, the 1000 kg ha^{-1} mulch application was not sufficient, and even caused an increase of 6.5% in sediment transport during one storm with a wind speed of 11.3 m s^{-1}. The 1500 kg ha^{-1} mulch application did still result in a 57.9% reduction of sediment transport during a strong storm with a wind speed of 10.6 m s^{-1}. However, some uncertainty exists as to which wind speed level this application will still lead to a reduction in sediment transport.

Finally, it is concluded that the better application rate of millet residues for wind erosion protection in the Sahel is 1500 kg ha^{-1}. A quantity of 1000 kg ha^{-1} may protect soils against erosion during weak storms, but involves the risk of increasing erosion during strong storms. In years with many strong storms, the reduction obtained during weak storms could be nullified during strong storms.

ACKNOWLEDGMENTS

This research was funded by the Netherlands Foundation for the Advancement of Tropical Research (WOTRO), and was conducted in close cooperation with the ICRISAT Sahelian Center. The logistic support from ISC and the assistance of Habibou Halidou and Boubacar Soumana with the field work is gratefully acknowledged. We like to thank L. Stroosnijder and P.A.C. Raats for their comments on a draft of this paper.

REFERENCES

Bilbro, J.D., and D.W. Fryrear. 1994. Wind erosion losses as related to plant silhouette area and soil cover. Agron. J. 86: 550-553.

Chepil, W.S., and N.P. Woodruff. 1963. The physics of wind erosion and its control. Advances in Agron. 15: 211-302.

Cotton, W.R., and R.A. Anthes. 1989. Storm and cloud dynamics. Academic Press, San Diego, CA.

Enninga, F. 1994. The wind erosion protection of flat maize residues on a sandy Sahelian soil. M.S. thesis, Dep. of Irrigation and Soil & Water Conservation, Wageningen Agric. Univ., The Netherlands.

Fryrear, D.W. 1985. Soil cover and wind erosion. Trans. ASAE 28: 781-784.

Hinze, J.O. 1975. Turbulence. 2nd ed., McGraw-Hill, New York.

Lamers, J.P.A., and R.P. Feil. 1993. The many uses of millet residues. ILEIA Newsl. 9: 15.

Lyles, L., and B.E. Allison. 1981. Equivalent wind erosion protection from selected crop residues. Trans. ASAE 24: 405-408.

Lyles, L., L.A. Disrud, and R.K. Krauss. 1971. Turbulence intensity as influenced by surface roughness and mean velocity in a wind-tunnel boundary layer. Trans. ASAE 14: 285-289.

Manu, A., A. Bationo, and S.C. Geiger. 1991. Fertility status of selected millet producing soils of West Africa. Soil Sci. 152: 315-320.

Michels, K., M.V.K. Sivakumar, and B.E. Allison. 1995a. Wind erosion control using crop residue I. Effects on soil flux and soil properties. Field Crops Res. 40: 101-110.

Michels, K., M.V.K. Sivakumar, and B.E. Allison. 1995b. Wind erosion control using crop residue II. Effects on millet establishment and yields. Field Crops Res. 40: 111-118.

Morgan, R.P.C., and R.J. Rickson. 1995. Slope stabilization and erosion control: A bioengineering approach. Chapmann & Hall, London.

Raupach, M.R., R.A. Antonia, and S. Rajagopalan. 1991. Rough-wall turbulent boundary layers. Appl. Mech. Rev. 44: 1-25.

Raupach, M.R., D.A. Gillette, and J.F. Leys. 1993. The effect of roughness elements on wind erosion threshold. J. Geophys. Res. 98: 3023-3029.

Siddoway, F.H., W.S. Chepil, and D.V. Armbrust. 1965. Effect of kind, amount, and placement of residue on wind erosion control. Trans. ASAE 8: 327-331.

Spaan, W.P., and G.D. van den Abeele. 1991. Wind borne particle measurements with acoustic sensors. Soil Technol. 4: 51-63.

Sterk, G. 1993. Sahelian wind erosion research project, Report III. Description and calibration of sediment samplers. Dep. of Irrigation and Soil & Water Conservation, Wageningen Agric. Univ., The Netherlands.

Sterk, G., L. Herrmann, and A. Bationo. 1996a. Wind-blown nutrient transport and soil productivity changes in southwest Niger. Land Degradation Developm. 7: 325-335. (Chapter 5 in this volume).

Sterk, G., A.F.G. Jacobs, and J.H. van Boxel. 1996b. The effect of turbulent flow structures on saltation sand transport in the atmospheric boundary layer. Submitted to: Earth Surf. Proc. and Landforms. (Chapter 2 in this volume).

Sterk, G., and P.A.C. Raats. 1996. Comparison of models describing the vertical distribution of wind-eroded sediment. Soil Sci. Soc. Am. J. 60: 1914-1919. (Chapter 3 in this volume).

Valentin, C., and L.M. Bresson. 1992. Morphology, genesis and classification of surface crusts in loamy and sandy soils. Geoderma 55: 225-245.

West, L.T., L.P. Wilding, J.K. Landeck, and F.G. Calhoun. 1984. Soil survey of the ICRISAT Sahelian Center, Niger, West Africa. TropSoils, Texas A&M Univ., College Station, TX.

Chapter 7

Farmers' Knowledge of Wind Erosion Processes and Control Methods in Niger

G. Sterk and J. Haigis

Submitted to: Agricultural Systems.

Farmers' Knowledge of Wind Erosion Processes and Control Methods in Niger

ABSTRACT

On-station research on wind erosion processes in Sahelian Africa has revealed that wind-blown particle transport forms a constraint for local crop production systems. This paper describes the results of an on-farm survey on wind erosion processes and soil conservation practices. Interviews were held with 138 farmers from seven villages in southern Niger. Of the interviewed farmers, 63% consider wind-blown particle transport as damaging to their cropping systems. In their view, seedlings are damaged by scouring sand grains, or are lost when buried in sand deposits. Production was said to be negatively influenced by retarded growth and development of the crop. Nearly all farmers reported to observe differences between fields with respect to wind erosion. Fields that are mainly eroded were said to lose fertility and produce less, whereas deposition of material results in a better fertility and production. These differences occur also on a smaller scale, with erosion and deposition spots in the same field. Most farmers (96%) are familiar with techniques to reduce wind erosion, and 92% applied one or more of those techniques in the field. The indigenous soil conservation techniques are application of manure and mulching with crop residues or tree branches. New techniques are tree planting, natural regeneration of woody vegetation, and application of *zai*, a method of soil preparation from Burkina Faso. These techniques have been introduced in two villages by an agricultural development project. The farmers who have applied these measures reported to have less wind erosion problems in their fields. It is concluded that the stimulation of regeneration of natural, woody vegetation is the most promising measure to reduce wind erosion problems in Niger.

Land degradation and the consequent reduction of crop production potential is a serious problem throughout the Sahelian zone of Africa. Increasing population pressure and competing uses for land have resulted in reduced fallow periods and an expansion of the cropped area into marginal land (Taylor-Powell, 1991). Infertile sandy soils common to the region are susceptible to degradation by wind and water erosion, particularly when the natural vegetation cover has been depleted. Water erosion is mainly a problem on the slopes of low mountains, or plateaus, which occupy only a minor fraction of the area. Wind erosion, however, is a widespread phenomenon throughout the Sahel, especially in the early rainy season (May - July) when erosive storms occur locally (Sterk et al., 1996).

Despite the wide recognition of the potential problems associated with wind erosion, it did not get much scientific attention till the late 1980's. Since then, a few field experiments, mostly on-station, were done to determine the effects of wind erosion on crops and soils, and to test methods for wind erosion control. These studies have revealed that sand transport may severely damage young crops (Klaij and Hoogmoed, 1993; Michels, 1994; Michels et al., 1995a; Gaouna, 1996), and soil productivity declines when fertile topsoil is being removed by wind (Mainguet and Chemin, 1991; Sterk et al., 1996). Wind erosion can be counteracted by technical control measures. Several studies have shown that particle transport is sufficiently reduced by leaving crop residues as a mulch on the soil surface (Michels et al., 1995b; Buerkert et al., 1996; Sterk and Spaan, 1997), or by planting living wind breaks perpendicular to the predominant wind direction during storms (Renard and Vandenbelt, 1990; Banzhaf et al., 1992; Michels, 1994; Mohammed et al., 1995). Also, tillage operations that create ridges at the soil surface may reduce soil particle transport (Klaij and Hoogmoed, 1989).

One aspect that was never considered in any of the mentioned studies is the farmers' opinion about wind erosion processes and their need for control measures. However, any discussion and planning on wind erosion control must take into account farmers' views (Rinaudo, 1996). Understanding traditional land management should be one of the references for improving or designing wind erosion control measures that fit into the local farming systems (Ben Salem, 1991). For instance, Neef et al. (1996), who studied the influence of land right systems on the adoption of erosion control measures in southwest Niger found that customary tenure does not allow non-owners of land to plant trees on borrowed fields. This creates an important constraint when agroforestry systems like tree wind breaks should be introduced.

Only two reports of on-farm studies were found in the literature that included wind erosion as a perceived agricultural problem in the Sahel. In a survey in the Hamdallaye watershed, southwest Niger, nearly all interviewed farmers mentioned that wind erosion causes losses of fertile topsoil, and reduces yields when eolian sediments bury crop seedlings (Taylor-Powell, 1991). To cope with these problems, the farmers reported to have changed crop residue management by using millet stalks as a protective mulch after harvest. Rinaudo (1996) reported results of a long-term project in the Maradi region, southern central Niger. In general, conventional wind erosion control methods were not adopted by farmers. Good results were obtained, though, with farmer-managed natural regeneration of woody species, which is a cheap method that fits easily into local farming systems.

In this study, Sahelian farmers were interviewed to ascertain their knowledge of wind erosion processes and control techniques. The objectives were (i) to evaluate the impact of wind-blown particle transport on local crop production systems, and (ii) to determine the techniques for wind erosion control applied by farmers.

SURVEY METHODOLOGY

A survey was conducted in southern Niger, during the 1995 rainy season (May - September). Semi-structured interviews were held with local farmers for data collection. This method is partly in accordance with the topical Rapid Rural Appraisal concept, that includes data collection from other sources as well (Conway and Barbier, 1990). A total of 138 farmers from seven villages was interviewed. The names, locations, and other characteristics of the selected villages are given in Table 1.

The sedentary farming systems combine pastoral activities with rainfed crop production. The main crop is pearl millet (*Pennisetum glaucum*), often intercropped with cowpea (*Vigna unguiculata*). Other crops grown by farmers from the selected villages are sorghum (*Sorghum bicolor*), sorrel (*Hibiscus sabdarifa*), and groundnut (*Arachis hypogaea*). Sowing is generally done after the first good rain event in the early wet season. In millet intercropping systems, the second crop is not sown until 2 to 3 weeks after the millet (Spencer and Sivakumar, 1987).

Table 1. Characteristics of selected villages in the survey.

Village name	Location	Sample size	Main ethnic group	Project	
				Name	Period
Sounga-Dossado	12°52'N;2°26'E	19	Djerma	Energy II	since 1994
Kirtachi-Seybou	12°47'N;2°28'E	20	Djerma	Energy II	since 1994
Chical	14°15'N;3°26'E	20	Haussa	SAA†	1974 - 1987
Boulkass	13°49'N;3°05'E	19	Djerma	GTZ‡	1992 - 1994
Serkin Hatchi	13°36'N;7°16'E	27	Haussa	MIDP§	since 1981
Dan Ido	13°44'N;6°58'E	13	Haussa	MIDP	since 1981
Liboré	13°25'N;2°13'E	20	Djerma	-	-

† Service Arrondissemental d'Agriculture.
‡ Gesellschaft für Technische Zusammenarbeit.
§ Maradi Integrated Development Project.

Before starting the actual interviews, a pre-survey was held with 15 farmers to test the questionnaire, and to get an idea about the possible answers given by farmers. The used questionnaire was semi-structured, with a mixture of open-end questions and questions with codified answers. It consisted of three parts. The first part dealt with crop damage caused by wind-blown particle transport. A distinction was made between plant losses due to burial in sand and plant damage by abrasion. Abrasion damage is caused by scouring sand grains that can damage leaves and stems of plants but does not necessarily kill plants. Burial of seedlings in deposited sand is often harmful, since high soil temperatures during daytime may kill the plants (Michels, 1994). In the second part, farmers were asked to describe the effects of erosion and deposition on soil fertility at different scales. Farmers had to indicate differences between entire fields that either gain or lose soil, and between erosion and deposition spots within the same field. The third part dealt with the techniques used by farmers to reduce wind erosion damage, including the influence of natural vegetation on erosion intensity.

Because farmers in the selected villages only speak local languages, the interviews were held with the help of experienced interpreters. Interviews were generally held at the farmers' compounds, usually early in the evening. The resulting database was analyzed for farmers' perceptions of the three main topics, i.e. crop damage, soil fertility aspects, and control measures. In general, no distinction between the seven different villages was made. Only when farmers from certain villages gave significantly different answers compared with the rest, these differences were taken into account and are discussed.

RESULTS AND DISCUSSION

Crop Damage

Nearly all farmers reported to observe plant losses during the first weeks of the rainy season (Table 2). Seedlings are mainly lost by livestock browsing, but wind-blown sand and drought were also mentioned as important reasons. Plants buried in sand often die because of reduced photosynthesis, the weight of the sand deposits, and the very high soil temperatures during daytime, resulting in a lower plant density. In extreme cases, farmers are forced to resow their fields, which results in late development of the crop and, therefore, a lower production. Crops reported to be very susceptible to sand coverage are millet and cowpea. Sorghum and sorrel are less susceptible, whereas groundnut is the most resistant crop (Table 3). The differing susceptibility to sand coverage is possibly caused by the difference in sowing dates. Millet and cowpea are usually sown during the early rainy season,

Table 2. Farmers' perceptions of plant losses and plant damage in the early growth stages.

Observation	Reason	Yes	No	n†
		%	%	
Plant losses		89	11	138
	Animals	57	43	123
	Drought	33	67	123
	Sand transport	46	54	123
	Other	48	52	123
Plant damage		80	20	138
	Animals	40	60	111
	Drought	32	68	111
	Sand transport	59	41	111
	Other	38	62	111

† n = number of farmers interviewed on specific question.

Table 3. Susceptibility of five crops to losses or damage due to wind-blown sand transport.

	Observation of losses				Observation of damage			
Crop	VO†	ST†	NV†	n‡	VO	ST	NV	n
	%	%	%		%	%	%	
Millet	70	26	4	57	54	41	5	66
Cowpea	54	37	9	54	73	19	8	63
Sorghum	44	23	33	43	29	33	38	55
Groundnut	27	19	54	41	40	23	37	43
Sorrel	41	29	30	49	42	33	25	57

† VO = very often; ST = sometimes; NV = never.
‡ n = number of farmers planting the specific crops.

when erosion activity is most severe. The other crops are sown later in the rainy season, when erosion is usually less intense.

Apart from loosing entire plants, most farmers also reported to observe damaged plants in the early growth stages (Table 2). Abrasion damage by sand transport was given as the main reason. Animals, i.e. livestock browsing and insects, and drought were considered important reasons as well. The farmers described the damage caused by blowing sand as burnt parts on the crop seedlings,

particularly on leaves, but also on stems. It influences their production by retarding growth and development of the crop. Also, plants are weaker, but in good rainfall years the influence on the total production was said to be limited. As with sand burial, millet and cowpea are the most susceptible crops. Sorghum, groundnut, and sorrel are less susceptible, but can also be damaged (Table 3).

The observations on millet are partly supported by research results, but no information about wind erosion damage on the other crops exists. Michels (1994) concluded that millet seedlings are particularly damaged by burial in sand, but are very resistant against abrasion. Of all farmers, 26% mentioned both kinds of damage, 37% reported to have only one kind of damage, and 37% did not mention sand transport at all as a reason of production losses. Hence, 63% of the interviewed farmers consider wind erosion a potential threat for their crop production systems.

Soil Fertility Aspects

Wind-blown soil is transported from one location to another. Depending on wind speed, soil material is either eroded from unprotected areas, where wind speed is at its maximum, or deposited at locations where wind speed is reduced by obstacles or roughness of the soil surface. Farmers were asked to point out differences in soil fertility, or production potential, between areas with deposition of soil material and areas from which soil is generally eroded.

Nearly all farmers indicated to observe differences in soil particle transport between fields (Table 4). Only 6% of the farmers said to observe neither erosion, nor deposition in their fields. In general, it is believed that sediment is traveling limited distances; from or to neighboring fields, although some farmers think that the material may also travel across longer distances. Differences between fields were said to be caused by topographic differences, and the presence or absence of trees and soil conservation measures.

Of the farmers that reported to have deposition of wind-blown material in one or more fields, 98% indicated that soil fertility, and thus production potential, of the entire field is improved. Several farmers (14%) also mentioned improved soil moisture characteristics.

Contrary to improved soil fertility by deposited material, soil losses are considered to result in decreasing soil fertility. Of the farmers that reported to have eroded fields, 97% said that either soil fertility or production potential is reduced in those fields. Few farmers (5%) also mentioned worse soil moisture properties.

Table 4. Farmers' observations of wind erosion and deposition processes (n = 138).

Observation	Yes	No
	%	%
Deposition in entire field	87	13
Loss from entire field	89	11
Transport within field	86	14

Apart from differences between fields, 86% of the farmers said to observe redistribution of soil material within the same field (Table 4). Again, erosion spots are considered to result in reduced fertility and lower production, whereas deposition areas are considered to become richer in nutrients and have a higher production potential.

The farmers' perceptions of soil productivity changes by wind-blown particle transport are in agreement with the research results of Sterk et al. (1996). In that study it was shown that wind-blown sand may transport considerable quantities of nutrients over limited distances. They concluded that nutrients are either eroded from unprotected fields and deposited in protected fields, or are redistributed within the same field.

Control Measures

Before questioning farmers about their techniques for wind erosion control, they were asked whether they consider wind erosion a problem for their crop production. Most farmers (81%) do consider it a problem, mainly because of decreasing soil fertility and, to a lesser extent, crop damage. The farmers that do not think that erosion is a problem reported earlier to have mainly deposition in their fields, and hence, they believe to benefit from nutrient-rich soil deposits.

Most farmers (96%) know techniques to reduce wind erosion, and 92% applied one or more of those in the field during the 1995 rainy season (Table 5). Several techniques like mulching with branches were more practiced than they were mentioned as wind erosion control measures. This indicates that some farmers do not consider those specific techniques to reduce wind erosion. For instance, farmers use branches of trees and shrubs on bare, crusted spots for soil regeneration. The organic material attracts termites that break the crust, but at the same time, the mulch material may trap blowing sand and thus it also reduces wind erosion (Chase and Boudouresque, 1987). None of the farmers mentioned wind breaks or ridging as possibilities to reduce wind erosion.

Table 5. Knowledge and application of wind erosion control measures in Niger (n = 138).

Wind erosion control measure	Known	Practiced
	%	%
Mulching with millet residues	80	78
Mulching with branches	46	52
Tree planting	32	25
Regeneration of vegetation	26	29
Application of manure	30	33
Application of *zai*†	7	23

† A soil tillage method from Burkina Faso, using pits filled with compost for sowing crops.

Mulching increases soil roughness, which gives a reduction of the surface wind speed. If an adequate mulch quantity is used, it is very effective in reducing wind erosion. However, the quantity of millet residues available in the low input farming systems is generally not sufficient for soil protection (Michels et al., 1995b; Sterk and Spaan, 1997). Although not studied, it is likely that the same is true for branches, given the widespread degradation of woody species in the Sahel.

Planting of trees and natural regeneration of vegetation are measures that have an influence on the wind field in a certain area. They are particularly effective when applied on a village scale or larger scales. Then, the trees and shrubs act as roughness elements and reduce wind speeds in the whole area (Stigter et al., 1993). Furthermore, shrubs with dense canopies starting near the soil surface may trap wind-blown particles and protect the soil from erosion (Sterk et al., 1996). In addition, more trees and shrubs enhance the availability of mulch material.

Application of manure and *zai* are not real wind erosion control measures but merely cultural practices to improve soil fertility. Fertilization results in better growth and development of crops, making plants more resistant against damage caused by sand transport (Buerkert et al., 1996). Moreover, biomass production will be greater and thus more mulch material will be available after harvest. However, application of manure and *zai* are also limited by insufficient availability of manure and organic material for *zai* pits (Lamers and Feil, 1995).

The knowledge of the different wind erosion control measures was obtained from several sources (Table 6). Tree planting, natural regeneration of (woody) vegetation, and *zai* are measures that have been introduced and promoted by agricultural projects. These three techniques were mainly

Table 6. Sources of knowledge of different wind erosion control measures.

	Source of knowledge					
	Father	Other Farmer	Extension officer	Project agent	Other	n†
	%	%	%	%	%	
Mulching with millet residues	37	11	3	39	10	108
Mulching with branches	32	7	0	60	1	72
Tree Planting	0	0	0	94	6	34
Regeneration of vegetation	0	0	0	95	5	40
Application of manure	40	7	2	13	38	45
Application of *zai*‡	0	0	0	100	0	32

† n = number of farmers practicing the specific wind erosion control measure.
‡ A soil tillage method from Burkina Faso, using pits filled with compost for sowing crops.

applied in the two villages where the Maradi Integrated Development Project (MIDP) is active (Table 1). Although some farmers from other village have knowledge about these new techniques, only very few applied them in the field. Application of manure and mulching with crop residues and tree branches are the indigenous techniques for controlling wind erosion. The latter two measures have been promoted by projects as well. Only four farmers reported to have obtained knowledge about wind erosion control from extension officers, which indicates that the extension service of Niger is either not advocating soil conservation measures, or has not been active in the seven villages.

Most farmers (84%) believe that the wind erosion intensity changes from year to year. Exactly half of them said that wind erosion is becoming less every year, whereas the other farmers believe that erosion is increasing nowadays. The former group consisted mainly of farmers from the two MIDP villages (Table 1), where wind erosion control measures have been successfully adopted (Rinaudo, 1996). The main reason given for the decrease in particle transport is more and better woody vegetation. The other farmers from villages where wind erosion problems were said to be increasing blame drought and the removal of trees for firewood. All of them are aware that the natural vegetation can help to reduce wind erosion but they apparently do not have possibilities to stimulate regeneration of the vegetation. According to Rinaudo (1996), theft of trees for wood is such a serious problem, that farmers have no other possibilities than to chop down the trees themselves. Furthermore, competition with crops for moisture and nutrients is often a reason to remove young trees and shrubs from arable fields.

CONCLUSIONS

Farmers from seven villages in southern Niger view wind erosion as a serious constraint for their crop production systems. In general, the interviewed farmers have a good knowledge of wind erosion and its effects on crops and soils. In their view, crops are damaged, and often die because of wind-blown particle transport. Moreover, soil productivity is negatively influenced by erosion, whereas deposition results in a better productivity. These observations are in accordance with results from on-station wind erosion research.

Traditional techniques to combat wind erosion are application of manure, and mulching with millet residues or tree branches. Application of these measures is limited by the insufficient availability of manure and mulch material. Measures that have been promoted by an agricultural development project in two villages include tree planting, regeneration of woody vegetation, and application of *zai*. According to the farmers that apply these measures, they are very successful in soil conservation and crop protection.

Natural regeneration of trees and shrubs was also indicated by the other farmers as a possibility to reduce wind erosion. However, they apparently do not have the means or possibilities to stop the current degradation of the natural vegetation. It is recommended that future research should concentrate on developing strategies to regenerate natural vegetation on farm and village scales. An important requirement is that the species of trees and shrubs in farmers fields may not compete strongly with crops, otherwise it is not acceptable for farmers. Selecting species should therefore be done in cooperation with farmers.

REFERENCES

Banzhaf, J., D.E. Leihner, A. Buerkert, and P.G. Serafini. 1992. Soil tillage and windbreak effects on millet and cowpea: I. Wind speed, evaporation, and wind erosion. Agron. J. 84: 1056-1060.

Ben Salem, B. 1991. Prevention and control of wind erosion in arid regions. Unasylva 164: 33-39.

Buerkert, A., J.P.A. Lamers, H. Marschner, and A. Bationo. 1996. Inputs of mineral nutrients and crop residue mulch reduce wind erosion effects on millet in the Sahel. p. 145-160. *In* B. Buerkert et al. (ed.) Wind erosion in West Africa: The problem and its control. Proc. Int. Symp., Stuttgart, Germany. 5-7 Dec. 1994. Margraf Verlag, Weikersheim, Germany.

Chase, R., and E. Boudouresque. 1987. Methods to stimulate plant regrowth on bare Sahelian forest soils in the region of Niamey, Niger. Agric. Ecosyst. Environ. 18: 211-221.

Conway, G.R., and E.B. Barbier. 1990. After the green revolution; Sustainable agriculture for development. Earthscan Publications, London.

Gaouna, B.O. 1996. Wind erosion in Chad: The vastness of damages, the beginning of control and solutions in Bokoro region. p. 173-180. *In* B. Buerkert et al. (ed.) Wind erosion in West Africa: The problem and its control. Proc. Int. Symp., Stuttgart, Germany. 5-7 Dec. 1994. Margraf Verlag, Weikersheim, Germany. (in French).

Klaij, M.C., and W.B. Hoogmoed. 1989. Crop response to tillage practices in a Sahelian soil. p. 265-275. *In* Soil, crop, and water management in the Sudano-Sahelian zone. Proc. Int. Worksh., Niamey, Niger. 11-16 Jan. 1987. ICRISAT, Patancheru, India.

Klaij, M.C., and W.B. Hoogmoed. 1993. Soil management for crop production in the West African Sahel II. Emergence, establishment, and yield of pearl millet. Soil and Tillage Res. 25: 301-315.

Lamers, J.P.A., and P.R. Feil. 1995. Farmers' knowledge and management of spatial soil and crop growth variability. Netherlands J. Agric. Sci. 43: 375-389.

Mainguet, M., and M.C. Chemin. 1991. Wind degradation on the sandy soils of the Sahel of Mali and Niger and its part in desertification. Acta Mech. [Suppl] 2: 113-130.

Michels, K. 1994. Wind erosion in the southern Sahelian zone: Extent, control, and effects on millet production. Verlag Ulrich E. Grauer, Stuttgart, Germany.

Michels, K., M.V.K. Sivakumar, and B.E. Allison. 1995a. Wind erosion control using crop residue II. Effects on millet establishment and yields. Field Crops Res. 40: 111-118.

Michels, K., M.V.K. Sivakumar, and B.E. Allison. 1995b. Wind erosion control using crop residue I. Effects on soil flux and soil properties. Field Crops Res. 40: 101-110.

Mohammed, A.E., C.J. Stigter, and H.S. Adam. 1995. Moving sand and its consequences on and near a severely desertified environment and a protective shelterbelt. Arid Soil Res. and Rehabil. 9: 423-435.

Neef, A., J. Haigis, and F. Heidhues. 1996. Impact of institutional and legal pluralism on the introduction of erosion control measures - The case of Niger. p. 283-296. *In* B. Buerkert et al. (ed.) Wind erosion in West Africa: The problem and its control. Proc. Int. Symp., Stuttgart, Germany. 5-7 Dec. 1994. Margraf Verlag, Weikersheim, Germany. (in French).

Renard, C., and R.J. Vandenbelt. 1990. *Andropogon gayanus* Kunth borders as a means to control wind erosion in the Sahel. Agronomie Tropicale 45: 227-231. (in French).

Rinaudo, T. 1996. Tailoring wind erosion control methods to farmers' specific needs. p. 161-171. *In* B. Buerkert et al. (ed.) Wind erosion in West Africa: The problem and its control. Proc. Int. Symp., Stuttgart, Germany. 5-7 Dec. 1994. Margraf Verlag, Weikersheim, Germany.

Spencer, D.S.C., and M.V.K. Sivakumar. 1987. Pearl millet in African agriculture. p. 19-31. *In* Proceedings of the international pearl millet workshop. Patancheru, India. 7-11 April 1986. ICRISAT, Patancheru, India.

Sterk, G., L. Herrmann, and A. Bationo. 1996. Wind-blown nutrient transport and soil productivity changes in southwest Niger. Land Degradation Developm. 7: 325-335. (Chapter 5 in this volume).

Sterk, G., and W.P. Spaan. 1997. Wind erosion control with crop residues in the Sahel. Soil Sci. Soc. Am. J. (in press). (Chapter 6 in this volume).

Stigter, C.J., R.M.R. Kainkwa, A.E. Mohammed, and L.O.Z. Onyewotu. 1993. Essentials and cases of wind protection from scattered trees and shelterbelts. Paper presented at the ICRAF Int. Symp. on Farmed Parklands in the Semi-Arid Land of West Africa. Oct. 25-27. Ouagadougou, Burkina Faso.

Taylor-Powell, E. 1991. Integrated management of agricultural watersheds: Land tenure and indigenous knowledge of soil and crop management. TropSoils Bulletin 91-04. Texas A&M Univ., College Station, TX.

Chapter 8

Towards a Regional Mass Budget of Eolian Transported Material in a Sahelian Environment

L. Herrmann and G. Sterk

Published in revised form in: B. Buerkert et al. (ed.) 1996. Wind erosion in West Africa: The problem and its control. Proc. Int. Symp., Stuttgart, Germany. 5-7 Dec. 1994. Margraf Verlag, Weikersheim, Germany. p. 319-326.

Towards a Regional Mass Budget of Eolian Transported Material in a Sahelian Environment

ABSTRACT

Wind erosion research in the past has mainly concentrated on studying single transport processes rather than on total mass budgets. To understand the effects of wind erosion and deposition processes on cropping and ecosystems, it is needed to integrate different measurement techniques in the same area. A methodology is proposed for quantifying a mass budget of eolian transported material on a regional scale. The strategy is based on key units which are defined by different surface characteristics. The budget of each unit can be calculated on the basis of soil particle fluxes in saltation and suspension modes. To estimate the budget on a regional scale, it is necessary to combine ground based experiments, wind erosion modeling, remote sensing, and a geographical information system. The methodology is explained by taking southwest Niger as an example. The influence of the key units on the mass budget and measurement constraints are discussed.

Since the droughts of the 1970's and early 1980's wind erosion has been an important research topic in the Sahel. However, quantitative data on erosion and deposition processes in the Sahel are scarce. This is mainly due to the measurement problems related to the wind-driven transport mechanisms. Sediments can be carried over distances ranging from a few centimeters to thousands of kilometers, at a great range of heights, and in any direction (McTainsh et al., 1992).

Usually, measurements in the Sahel have concentrated on single transport modes, like saltation transport in agricultural fields (e.g., Michels et al., 1993; Sterk and Raats, 1996) or dust deposition on a regional scale (e.g., Drees et al., 1993; Herrmann et al., 1996). A total mass budget of eolian transported material, including creep, saltation, and suspension transport, would give important information about soil and nutrient losses or gains by wind action. To estimate such a budget, measurement techniques for the different transport modes need to be integrated in the same area. The objective of this paper is to describe the outline of a proposed method for quantifying mass budgets on a regional scale of approximately 100 km^2. The method is explained by using the circumstances in southwest Niger as a guide. The existing measurement constraints are discussed and it is shown how new techniques like remote sensing can be used for estimating eolian mass budgets.

METHOD

The proposed method for quantifying a storm based regional mass budget of eolian transported material consists of: (i) selection of key units; (ii) quantification of mass transport in each key unit; (iii) calculation of the total mass budget based on the contributions of separate key units.

ad (i). Key units are areas which are more or less equal in erodibility. Selection of key units is based on surface characteristics like soil type, soil surface roughness, and vegetation characteristics. Also, the presence of soil conservation measures should be taken into account.

ad (ii). Sediment transport can take place in either of the three transport modes: creep, saltation, and suspension. It is assumed that creep transport can be included in the saltation component (Fryrear and Saleh, 1993). This results in the following mass budget equation:

$$\Delta S = Sa\downarrow - Sa\uparrow + Su\downarrow - Su\uparrow \qquad [1]$$

where ΔS is the mass budget (kg m^{-2}), the subscripts a and u denote saltation and suspension, and the arrows ↓ and ↑ indicate input and output, respectively. For each key unit and storm, the four mass budget components need to be determined by experimentation at selected sites, resulting in a set of expressions for saltation and suspension transport.

ad (iii). A storm based mass budget for the defined region is calculated from the distribution of the key units within the region, the boundary conditions, the expressions for saltation and suspension transport, and the mean wind direction during the storm. The boundary conditions for input and output of particle mass transport are determined by the mean wind direction during the storm event.

These three steps are now further explained for an environment in southwest Niger.

REGIONAL MASS BUDGET ESTIMATION

Environment

The landscape of southwest Niger is dominated by broad, gently sloping laterite plateaus, with eroded, heavily crusted soils and sparse vegetation. Sometimes the crusted soil is covered by eolian deposits, which are often used for agriculture. In the valleys between the plateaus, broad plains of deep sandy soils are widespread (Wilding and Daniels, 1989). These sand plains form the main agricultural area in the Sahel, with pearl millet (*Pennisetum glaucum*) as the main crop. Traditionally, farmers leave parts of their land under bush fallow for restoring soil fertility. Due to population

pressure, the area under fallow has decreased dramatically during the past few decades (Klaij and Hoogmoed, 1989). This has led to severe soil degradation, resulting in areas with bare, crusted surfaces.

In general, two seasons can be distinguished in which eolian transport processes take place. In the dry season (October - April), the Harmattan wind transports dust in suspension from major Saharan sources in a southwesterly direction. Along the wind trajectory, deposition takes place mainly by gravitational settling during nighttime, when wind speeds are low. In addition, vegetation can act as a dust trap, due to an increase in surface roughness. Overall, the dry season is assumed to result in a net input of wind-blown particles on Sahelian soils.

During the first half of the rainy season (May - July), heavy thunderstorms, which travel in an east-west direction, occur frequently in the Sahel. These storms are usually preceded by short periods with high wind speeds, resulting in severe erosion of bare, unprotected soils. Very often, a rolling dust cloud in front of a thunderstorm is formed. During such an event, soil material is moved by creep, saltation, and suspension. The suspended material is partly deposited again with rainfall following the dust cloud, but dust may also be subject to long-range transport. Saltation and creep particles from erodible areas may be trapped by more vegetated areas downwind. Overall, the early rainy season causes a net output of eolian transported material.

Key Unit Scale

Based on the surface characteristics of soil and vegetation, three key units are distinguished in southwest Niger: bare surface, millet land, and fallow land. Possibly a fourth unit, i.e. plateau, could be added, but it is assumed that the three units are sufficient to describe also the conditions on the plateaus. Though realizing that subdividing an area of some 100 km^2 in only three different units is very rough, it is preferred for simplicity reasons. In a later stage, more key units can possibly be selected. Maps already existing, and aerial photographs or satellite images (remote sensing) can be used to determine the key unit distribution in a certain area.

Fallow land acts mainly as a deposition area for saltation and suspension material during the early rainy season, and as a dust deposition area during the Harmattan. Millet land and bare surfaces act as dust deposition areas during Harmattan events, and are the main erosion areas during the early rainy season. In Table 1, the importance of each key unit for the regional mass budget of eolian transported material is shown.

Table 1. The importance† of different key units for the mass budget‡ of eolian material in southwest Niger.

Key unit	Sa↓	Sa↑	Su↓	Su↑
Millet land	+	++	+	++
Fallow land	++	0	++	0
Bare surface	+	++	+	++

† ++ = important; + = relevant; 0 = of no relevance.
‡ Sa = saltation; Su = suspension; ↓ = input; ↑ = output.

For each key unit, a representative site for the field measurements is selected. At these sites, the four mass budget components are quantified. Saltation mass transport rates on millet land and bare surfaces depend on storm duration and wind speed. Saltation transport can be quantified with simple sediment catchers like the Modified Wilson and Cooke (MWAC) catchers (Sterk and Raats, 1996). During the 1993 rainy season, Sa↓ and Sa↑ were quantified during four storm events in a millet field at Sadoré, southwest Niger (Sterk and Stein, 1997). All four storms resulted in a net loss of saltation material (Table 2), and the total loss was equal to 4.6 kg m^{-2}, which is equivalent to a soil layer of ≈2.7 mm.

In fallow land, incoming saltation material is trapped due to the increase in surface roughness. This is virtually impossible to measure. However, under conditions of a sufficient dense fallow vegetation, it can be assumed that the saltation output (Sa↑) from millet fields or bare surfaces upwind from the fallow is equal to the saltation input (Sa↓) in the fallow, and is all trapped by the vegetation. The distance across which saltating particles penetrate into the fallow depends mainly on the vegetation density in the fallow site.

Table 2. Saltation mass budget† of four storms on a millet field in southwest Niger, 1993 rainy season.

Storm	Sa↓	Sa↑	ΔSa
	kg m^{-2}	kg m^{-2}	kg m^{-2}
1	4.7	5.9	-1.2
2	0.2	0.4	-0.2
3	1.4	1.9	-0.5
4	6.2	8.9	-2.7
Total	12.5	17.1	-4.6

† Sa = saltation; ↓ = input; ↑ = output; ΔSa = saltation mass budget.

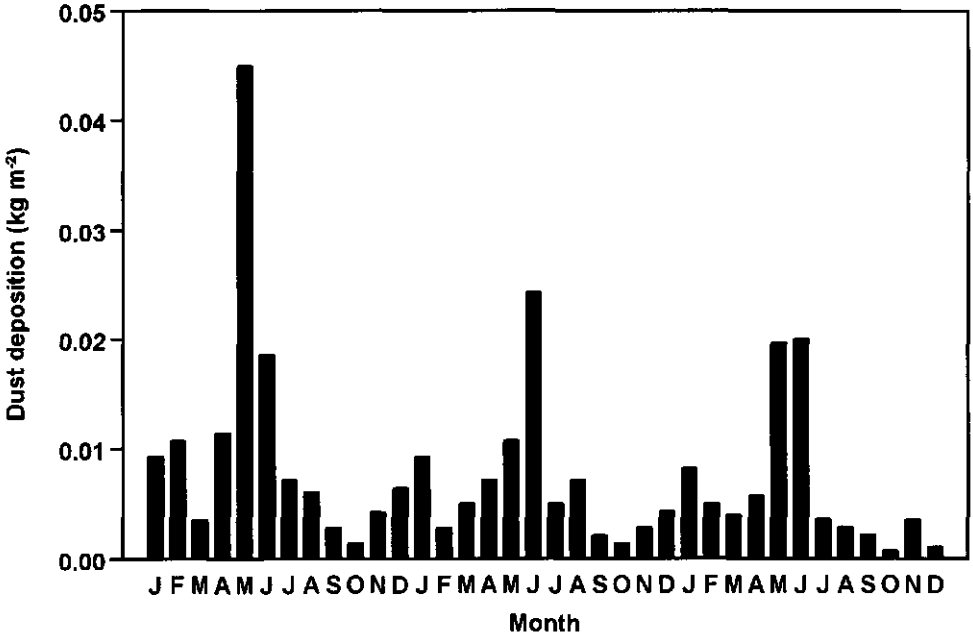

Figure 1. Vertical component of suspension input in a fallow site at Sadoré, 1992 - 1994.

Quantification of saltation transport with sediment catchers depends on the trapping efficiency of the sampler. Usually, the efficiency is determined in a wind tunnel where, compared with the field, the wind is rather homogeneous and the degree of turbulence low. This reduced turbulence may result in a trapping efficiency that is not correct for field conditions. So far, no techniques for determining the trapping efficiency of samplers under field conditions exist.

Input of suspension material can be divided into two parts: (i) vertical deposition by gravitational settling or rain wash-out; (ii) trapping of horizontal suspension transport mainly by vegetation. The vertical component can be measured with passive dust catchers (e.g., Drees et al., 1993; Herrmann et al., 1996). In Fig. 1, measured quantities of vertically deposited dust in a fallow area at Sadoré are shown. The deposition pattern is bimodal and season-dependent. The highest deposition rates, up to 45 g m^{-2} $month^{-1}$, were measured at the start of the rainy season with the occurrence of convective storms. During those events, the greatest share was deposited by rainfall directly following the dust storms (Herrmann et al., 1996).

Currently, there are no appropriate measurement techniques for quantifying the more dynamic horizontal dust deposition component, i.e. fall-out by collision or adhesion. A method to quantify the total suspension input at the soil surface is being developed (Herrmann, 1996). This method uses artificial soil surfaces consisting of washed quartz sand of the middle-size sand fraction (125 - 500 μm), which is the main grain size fraction in the predominant sandy soils of the region. The suspension input (Su↓) can be determined by wet sieving the dust deposit after exposing the artificial soil surface for a certain period of time.

Suspension output (Su↑) is difficult to measure. First estimates were made by using volume samplers to quantify vertical profiles of suspension transport (Nickling and Gillies, 1993; Rajot et al., 1996). Suspension losses can possibly be quantified with MWAC catchers as these samplers also trap suspension material. Although the maximum sampling height is only 1 m, the vertical profile through measured horizontal mass fluxes could be extrapolated to greater heights, and results of Nickling (1978) indicate that this is actually possible. However, prior to using this technique, a proper calibration of the catchers for the suspension component is needed, for instance by comparing the extrapolated mass flux profiles with suspension mass fluxes measured with volume samplers.

Solving the measurement constraints still requires further research. This research should focus on (i) improving techniques for the quantification of suspension transport and deposition, and (ii) development of methods for determining the trapping efficiency of erosion samplers under field circumstances.

Regional Scale

The field data obtained from the selected key unit sites can be used for calibration and validation of a storm based wind erosion model, e.g. the Wind Erosion Prediction System (Hagen, 1991). This dynamic model is process based and has a modular structure. It includes weather, soil, vegetation, hydrology, and tillage components. Wind-blown particle transport is modeled as the time dependent conservation of mass of two species, saltation and creep, with two sources, emission and abrasion, and two sinks, surface trapping and suspension. The soil flux is simulated at sub-hourly intervals when the friction velocity exceeds the threshold levels which were defined by field measurements. The soil surface conditions are updated periodically.

After validation of the wind erosion model, the regional mass budget is calculated using the scheme shown in Fig. 2. Remote sensing provides data on vegetation and soil surface characteristics.

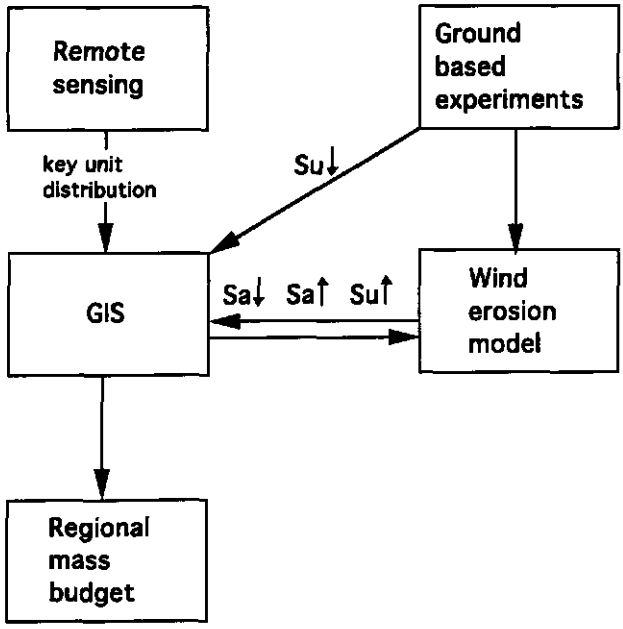

Figure 2. Integrated system for the estimation of a regional mass budget of eolian transported material.

Based on these data, the different key units are selected and the boundaries of the single key unit areas determined. The data are stored in a geographical information system (GIS). The ground based experiments include meteorological measurements for the wind erosion model, and dust deposition measurements since input of dust (Su↓) from remote areas cannot be calculated with the storm based wind erosion model. The model calculates the mass budget components Sa↓, Sa↑, and Su↑ on the basis of the meteorological data (wind speed, wind direction, rainfall, etc.) and geometry information of the single key unit areas. Based on the mass budgets for each separate key unit area, the total mass budget for the region is calculated by the GIS. In addition, the GIS provides the possibility to produce maps that show the spatial distribution of mass transport in the region.

CONCLUSIONS

The estimation of a regional mass budget of eolian transported material is difficult due to the complex nature of the different transport processes. Nevertheless, it is important to develop approaches in order to understand the effects of wind erosion and deposition on crop- and

ecosystems. Only a net budget of creep, saltation, and suspension material permits any reliable conclusions to be drawn about the regional effects of wind erosion.

The first constraints on the way towards a regional mass budget are the measurement techniques, especially of the suspension fluxes. There is a great need to develop methods for the quantification of suspension losses from agricultural fields. Furthermore, no reliable techniques exist that can quantify the trapping of suspended dust by vegetation canopies. As far as saltation transport is concerned, techniques to determine the trapping efficiency of sediment catchers in the field are needed.

To transfer the results of wind-blown mass transport measurements on the field scale to a regional mass budget, it is necessary to integrate tools that work at different scales. In our approach, these are the field measurements and the wind erosion model on the field scale, and remote sensing and GIS on the regional scale. The calibration of the wind erosion model by the field experiments and the inventory of the key units by remote sensing need intensive measurements with a high resolution and are therefore time consuming. However, in the long run the regional mass budget can be event based and the measurements can be reduced to the collection of meteorological and suspension input data.

The main difficulty in the Sahelian environment for this approach is the determination of the size and distribution of the key units. These units are dynamic due to the nature of the cropping system and population pressure. Therefore, the inventory of the key units may have to be repeated regularly.

REFERENCES

Drees, L.R., A. Manu, and L.P. Wilding. 1993. Characteristics of aeolian dusts in Niger, West Africa. Geoderma 59: 213-233.

Hagen, L.J. 1991. A wind erosion prediction system to meet user needs. J. Soil Water Conserv. 46: 106-111.

Fryrear, D.W., and A. Saleh. 1993. Field wind erosion: Vertical distribution. Soil Sci. 155: 294-300.

Herrmann, L. 1996. Dust deposition on soils of West Africa: Properties and source regions for dust and influence on soil and site properties. Hohenheimer Bodenkundlich Hefte 36. Univ. of Hohenheim, Stuttgart, Germany. (in German).

Herrmann, L., K. Stahr, and M.V.K. Sivakumar. 1996. Dust deposition on soils of southwest Niger. p. 35-47. *In* B. Buerkert et al. (ed.) Wind erosion in West Africa: The problem and its control. Proc. Int. Symp., Stuttgart, Germany. 5-7 Dec. 1994. Margraf Verlag, Weikersheim, Germany.

Klaij, M.C., and W.B. Hoogmoed. 1989. Crop response to tillage practices in a Sahelian soil. p. 265-275. *In* Soil, crop, and water management in the Sudano-Sahelian zone. Proc. Int. Worksh., Niamey, Niger. 11-16 Jan. 1987. ICRISAT, Patancheru, India.

McTainsh, G.H., C.W. Rose, G.E. Okwach, and R.G. Palis. 1992. Water and wind erosion: Similarities and differences. p. 107-119. *In* H. Hurni, and K. Tato (ed.) Erosion, conservation, and small scale farming. Walsworth Publ. Co., Marceline, MS.

Michels, K., M.V.K. Sivakumar, and B.E. Allison. 1993. Wind erosion in the southern Sahelian zone and induced damage to pearl millet. Agric. For. Meteorol. 67: 65-77.

Nickling, W.G. 1978. Eolian sediment transport during dust storms: Slims River Valley, Yukon Territory. Can. J. Earth Sci. 15: 1069-1084.

Nickling, W.G, and J.A. Gillies. 1993. Dust emission and transport in Mali, West Africa. Sedimentology 40: 859-868.

Rajot, J.L., M. Sabre, and L. Gomes. 1996. Measurement of vertical fluxes of soil-derived dust during wind erosion events in a Sahelian region (Niger). p. 49-56. *In* B.Buerkert et al. (ed.) Wind erosion in West Africa: The problem and its control. Proc. Int. Symp., Stuttgart, Germany. 5-7 Dec. 1994. Margraf Verlag, Weikersheim, Germany.

Sterk, G., and P.A.C. Raats. 1996. Comparison of models describing the vertical distribution of wind-eroded sediment. Soil Sci. Soc. Am. J. 60: 1914-1919. (Chapter 3 in this volume).

Sterk, G., and A. Stein. 1997. Mapping wind-blown mass transport by modeling variability in space and time. Soil Sci. Soc. Am. J. (in press). (Chapter 4 in this volume).

Wilding, L.P., and R. Daniels. 1989. Soil-geomorphic relationships in the vicinity of Niamey, Niger. TropSoils Bulletin no. 89-01. North Carolina State Univ., Raleigh, NC.

Chapter 9

Summary and Conclusions

Summary and Conclusions

Rainfed agriculture in the Sahelian zone of Niger is characterized by physically and chemically impoverished sandy soils, and harsh climatic conditions. Crops can only be grown during the short rainy season, from the end of May until the end of September. Wind erosion occurs during two distinct seasons. During the dry season (October - April), the strong Harmattan wind blows and may cause moderate erosion. In the second half of the dry season it often carries dust from remote Saharan sources and some of this is deposited in the Sahel. The second and most important wind erosion season is the early rainy season (May - July). Then, thunderstorms develop throughout the Sahel and bring the first rains of the new season. The rain events are usually preceded by short (typically 10 - 30 min) wind storms that severely erode unprotected soils.

During a storm, soil particles are moved by saltation, creep, and suspension. Saltating sand grains jump and bounce over the surface, reaching maximum heights of ≈ 1 m. When saltating particles fall to the soil surface they not only eject other saltating particles but also induce creep, the rolling and sliding of larger particles, and suspension, the raising of fine particles. The three transport modes result in different travel distances of the particles. Creep moves particles across distances from a few centimeters up to several meters. The saltation range is from a few meters up to a few hundred meters, and suspended dust may travel up to thousands of kilometers.

The winds during early rainy season storms are characterized by a high degree of turbulence. Instantaneous measurements of wind speed and saltation flux carried out in this study showed that saltation transport is highly correlated with fluctuations in horizontal wind speed. Fluctuations in vertical wind speed did not influence saltation flux, indicating that the horizontal drag force is more important for saltation transport than the turbulent shear stress generated. Therefore, instead of using the shear stress, as many current models of wind erosion do, the horizontal wind speed and its fluctuations should be used as the driving variable in wind erosion models.

Data on wind-blown mass transport were collected using Modified Wilson and Cooke (MWAC) sediment catchers. The catcher has seven traps attached to a central pole at heights between 0.05 and 1.00 m. Each trap consists of a plastic bottle with an inlet and an outlet entering the bottle through the cap. The inlet and outlet are glass tubes with an opening of 50.3 mm^2, and are both bent 90° in opposite directions on the outside. The materials trapped at seven heights during an erosion event were used to calculate seven horizontal mass fluxes. Through the observations, a model was fitted

to describe the vertical profile of horizontal mass fluxes. Two existing models were tested and it was shown that a two-term, combined saltation-suspension model gave the best results. In general, the profiles showed a maximum mass flux at the soil surface which decreased rapidly with height. By integrating the profile over height, and correcting for the trapping efficiency of the catcher (0.49), a total mass transport rate at the point of sampling was obtained. This value represented the total mass of material passing a strip 1 m wide per unit of time.

In the literature, it has been mentioned that the separate terms of the combined saltation-suspension model describe saltation and suspension mass fluxes, respectively. However, sieving trapped materials from two catchers revealed that the model should not be used for this purpose. It may only be used to determine total mass fluxes of a mixture of saltation and suspension material.

Field measurements of wind-blown mass transport are often characterized by a considerable spatial variation, which makes quantitative modeling of wind erosion difficult. Here, geostatistics were applied to model the spatial variation of total mass transport observations, quantified with 21 MWAC sediment catchers in a plot of 40 by 60 m during four storms. To have sufficient data for the analysis, the variance of the four storms was pooled by creating one large data set from the four separate data sets. Storm based maps of total mass transport were created by kriging, a spatial interpolation technique, and stochastic simulation with simulated annealing.

The simulated maps clearly showed the spatial distribution of mass transport from which sink and source areas for erosion material could be distinguished. Combining these maps with other maps of soil characteristics, surface roughness, topography, etc. may elucidate wind erosion processes in the field.

The maps produced by kriging were used to calculate a mass budget, so that storm based soil losses could be estimated. In total, 45.9 Mg ha^{-1} was lost from the experimental plot during the four sampled storms. This is equivalent to a soil layer ≈2.7 mm thick. As the sandy Sahelian soils are very deep (>3 m), soil losses of a few millimeters per year are not the biggest concern for farmers. The loss of plant nutrients with the wind-blown material is more important.

During the first and the fourth storm of the 1993 season, materials trapped at three heights (0.05, 0.26, and 0.50 m) were collected, and total element (TE) contents of potassium (K), carbon (C), nitrogen (N), and phosphorus (P) were determined. In general, the particles trapped at the lowest level were as rich in nutrients as the topsoil. At the 0.50 m level, the material was about three times richer in nutrients than the topsoil. The increase in nutrient content with height was explained by

an increase in the proportion of silt and clay particles that contain larger amounts of nutrients compared with the coarser sand that is transported just above the soil surface. Combining the vertical mass flux profile with the vertical profiles of TE contents resulted in mass flux profiles of the four elements, K, C, N, and P. These profiles showed a maximum value in the saltation layer just above the soil surface, and decreased sharply with height. The TE mass fluxes transported by saltation were an order of magnitude higher than the suspended TE mass fluxes. By integrating the TE mass flux profiles over height and calculating a mass budget, the losses of the four elements from the experimental plot during the two storms were estimated. They were found to be ≈3% of the TE masses present in the top 0.10 m of the soil.

As saltation is a short-range transport process it merely results in a regional redistribution of soil particles and nutrients. Material may be transported from unprotected fields towards protected areas, such as mulched fields or vegetated areas. Within-field transport of soil particles and nutrients may also occur, since many fields have obstacles like trees and shrubs that trap saltation material. Although the absolute fluxes are much smaller than the saltation fluxes, suspended material can be transported over long distances, resulting in regional losses of soil particles and nutrients. It should therefore be considered as a serious soil degradation process as well.

To determine the effects of wind erosion on a scale larger than the scale of individual fields, it is necessary to integrate different measurement techniques in the same area. A proposed method to estimate total mass budgets of eolian material at scales of ≈ 100 km^2 combines remote sensing with a wind erosion prediction model and field measurements. The area is divided into different key units, based on surface characteristics. The wind erosion model is calibrated for each key unit, using field data from selected sites. A geographical information system is used to combine all information and to calculate the mass budget for the whole area. Several measurement constraints, mainly concerning quantification of suspension transport need to be solved before such a method can be implemented.

Soil and nutrient losses by wind erosion can be prevented by leaving crop residues in the field as a mulch. In the Sahelian farming systems, mulching is limited by low biomass production and multiple uses of the stalks. In a previous study it was shown that 2000 kg ha^{-1} of millet residues gives sufficient protection, whereas a mulch cover of 500 kg ha^{-1} does not reduce sediment transport. In this study, two low mulch cover rates of 1000 and 1500 kg ha^{-1} were tested for their efficacy in soil protection during two wind erosion seasons. The 1500 kg ha^{-1} cover rate gave good protection

during all sampled storms. However, the lower rate protected the soil adequately during weak storms with wind speeds below 10 m s^{-1} only. It did not result in sufficient reduction during strong storms. During one storm with a wind speed of 11.3 m s^{-1} the sediment transport in the protected plot was even greater than in the control plot. This increase in erosion is attributable to enhanced turbulence around the millet stalks. It is therefore recommended to use at least 1500 kg ha^{-1} of millet stalks for wind erosion protection in the Sahel.

To complement the on-station research, an on-farm survey was conducted in seven villages in southern Niger. A total of 138 farmers was interviewed to ascertain their knowledge and perceptions of wind erosion processes. Most farmers (63%) consider wind-blown soil transport as damaging to their crops. In their view, plants are damaged by abrasion, or are lost due to burial in sand. Nearly all farmers have a clear perception of soil productivity changes caused by wind erosion. Fields or isolated spots that gain material by deposition were said to have a better soil fertility than eroded areas. Most farmers (92%) apply one or more wind erosion control techniques in the field. The indigenous measures are mulching with crop residues or tree branches, and application of manure. New techniques have been introduced by an agricultural development project. These techniques are farmer-managed regeneration of woody vegetation, tree planting, and application of *zai*, a method of soil preparation from Burkina Faso, using pits filled with compost for planting crops. Regeneration of woody species was reported to be very effective in reducing wind erosion, and is the most promising control method available, given the limited availability of mulch material and manure under current farming practices.

Samenvatting en Conclusies

Regenafhankelijke landbouw in de Sahel-zone van Niger wordt gekenmerkt door fysisch en chemisch arme zandgronden en een extreem klimaat. Gewassen kunnen alleen worden verbouwd tijdens het korte regenseizoen dat van eind mei tot eind september duurt. Winderosie treedt op tijdens twee seizoenen. In het droge seizoen (oktober - april) waait de harde Harmattan wind die matige erosie in de Sahel kan veroorzaken. Tijdens de tweede helft van het droge seizoen voert de Harmattan veel stof aan dat afkomstig is uit de Sahara. Een deel van dit stof wordt afgezet in de Sahel. Het tweede en meest belangrijke erosieseizoen is het begin van de regentijd (mei - juli). In die periode ontwikkelen zich in de Sahel zware onweersbuien die de eerste regens van het nieuwe seizoen brengen. Voorafgaand aan de regen treden vaak hoge windsnelheden op gedurende korte periodes (10 - 30 min.), waardoor veel erosie wordt veroorzaakt.

Tijdens een dergelijke storm worden bodemdeeltjes getransporteerd door drie verschillende processen: saltatie, kruip en suspensie. Salterende zandkorrels springen over het oppervlak waarbij maximale hoogtes van ca. 1 m worden bereikt. Als een salterend deeltje botst met het oppervlak worden niet alleen andere zandkorrels in een salterende beweging gebracht, maar worden tevens grotere korrels vooruit gerold of geschoven (kruip) en fijn bodemmateriaal in suspensie gebracht. De drie processen transporteren het bodemmateriaal over verschillende afstanden. Kruipend materiaal legt afstanden af van een paar centimeters tot enkele meters. Door saltatie beweegt materiaal over afstanden variërend van een meter tot enkele honderden meters, terwijl het fijne stof getransporteerd kan worden over afstanden tot enige duizenden kilometers.

De wind tijdens stormen in het vroege regenseizoen is in hoge mate turbulent. Continue metingen van saltatiefluxen vertoonden een sterke fluctuatie die goed gecorreleerd was met de fluctuaties in de horizontale windcomponent. Fluctuaties in de verticale windcomponent vertoonden geen correlatie met de saltatieflux. Hieruit kan worden geconcludeerd dat de sleepkracht van groter belang is dan de schuifspanning. Modellen van saltatietransport zouden daarom gebruik moeten maken van de windsnelheid en niet van de schuifspanning zoals de meeste huidige modellen doen.

Voor het bepalen van het massatransport tijdens een storm werd gebruik gemaakt van sedimentvangers van het type Modified Wilson and Cooke (MWAC). Dit instrument heeft zeven vangeenheden die over een hoogte van 0,05 tot 1,00 m aan een mast bevestigd zijn. Elke vangeenheid

bestaat uit een plastic flesje dat afgesloten is door een schroefdop. In de dop zijn een inlaat en een uitlaat bevestigd. Dit zijn ronde, glazen buisjes met een opening van 50,3 mm^2. Beide buisjes zijn aan de buitenkant 90° in tegengestelde richting gebogen. Het tijdens een storm ingevangen materiaal werd verzameld en gebruikt om per vanger en per storm zeven horizontale massafluxen te berekenen. Door de zeven waarnemingen werd een model gepast om het verticale profiel van horizontale massafluxen te beschrijven. Twee bestaande modellen werden hiervoor getest en het bleek dat een gecombineerd saltatie-suspensie model de beste resultaten geeft. De verticale massafluxprofielen vertoonden een maximum aan het oppervlak en namen sterk af met de hoogte. Door het profiel te integreren over de hoogte en vervolgens te corrigeren voor de efficiency van de sedimentvangers (0,49) werd een totaal massatransport op het punt van observatie verkregen. Deze waarde is gelijk aan de totale massa aan bodemmateriaal die een strook van 1 m per tijdseenheid is gepasseerd.

In de winderosie-literatuur is gemeld dat de afzonderlijke termen van het gecombineerde saltatie-suspensie model respectievelijk saltatie- en suspensie-massafluxen beschrijven. Echter, door ingevangen materiaal te zeven en te wegen bleek dat het model hiervoor niet gebruikt mag worden. Het kan slechts worden toegepast om totale massafluxen, bestaande uit zowel saltatie- als suspensiemateriaal te bepalen.

Veldmetingen van massatransport worden vaak gekenmerkt door een grote ruimtelijke variabiliteit, waardoor kwantitatieve modellering van winderosie bemoeilijkt wordt. In dit onderzoek werd geostatistiek toegepast om de ruimtelijke variabiliteit in waarnemingen van massatransport te modelleren. Met behulp van 21 MWAC sedimentvangers werden metingen gedaan in een proefveld van 40 bij 60 m tijdens vier stormen in het regenseizoen van 1993. Om voldoende waarnemingen te hebben voor de analyse werden de vier stormen samengevoegd tot één gegevensset. Voor elk van de vier stormen werden kaarten gemaakt van het totale massatransport met kriging (een ruimtelijke interpolatietechniek) en simulated annealing (een stochastische simulatietechniek).

De gesimuleerde kaarten toonden duidelijk de ruimtelijke verdeling van het massatransport. De kaarten zijn geschikt om erosie- en depositieplekken in het veld te onderscheiden. Combineren van de kaarten met kaarten van bodemkarakteristieken, oppervlakteruwheid, topografie enz. kan een beter inzicht verschaffen in winderosieprocessen.

De geïnterpoleerde kaarten werden gebruikt om massabalansen te berekenen, waardoor bodemverliezen per storm konden worden bepaald. In totaal ging 45,9 Mg ha^{-1} verloren van het proefveld gedurende de vier stormen. Dit verlies komt overeen met een bodemlaag van ca.

2,7 mm dikte. Uit het feit dat de zandgronden in Niger diep zijn (>3 m) blijkt dat bodemverliezen van enkele millimeters per jaar niet het grootste probleem zijn voor de Nigerijnse boeren. Van groter belang is het verlies aan nutriënten dat tijdens de stormen optreedt.

Tijdens twee van de vier stormen in 1993 werd ingevangen sediment op drie hoogtes (0,05; 0,26 en 0,50 m) verzameld. Van dit materiaal werden de gehaltes aan totale elementen (TE) van kalium (K), koolstof (C), stikstof (N) en fosfor (P) bepaald. Over het algemeen bevatte het materiaal op 0,05 m evenveel nutriënten als de bovengrond. Op 0,50 m was het sediment ca. drie keer rijker in nutriënten dan de bovengrond. Deze toename in nutriëntengehaltes met de hoogte kan worden verklaard uit de toename van de gehaltes aan klei- en siltdeeltjes in het sediment. Dit fijne bodemmateriaal bevat meer nutriënten dan het grovere zand dat net boven het bodemoppervlak wordt getransporteerd.

Het combineren van het verticale profiel van de massaflux met de verticale TE-profielen resulteerde in TE-massafluxprofielen voor de vier elementen K, C, N en P. Deze profielen vertoonden een maximum in de saltatiezone net boven het oppervlak en namen sterk af met de hoogte. Door de TE-massafluxprofielen te integreren over de hoogte en massabalansen te berekenen werden de verliezen aan K, C, N en P van het proefveld geschat. Deze verliezen bedroegen ca. 3% van de totale massa die aanwezig was in de eerste 0,10 m van de bovengrond.

Saltatie transporteert materiaal over geringe afstanden en daardoor resulteert het voornamelijk in een regionale herverdeling van bodemdeeltjes en nutriënten. Het materiaal wordt getransporteerd van onbeschermde akkers naar gebieden die beschermd zijn door vegetatie of bodemconserverings-maatregelen. Ook kan herverdeling optreden binnen hetzelfde veld. Vaak zijn er in de akkers bomen en struiken aanwezig die salterend materiaal uit de omgeving invangen. De suspensiefluxen zijn veel geringer dan de saltatiefluxen, maar het materiaal in suspensie wordt over veel grotere afstanden getransporteerd. Suspensietransport kan daardoor tot een regionaal verlies aan nutriënten leiden en moet dus ook als een belangrijk bodemdegradatieproces worden beschouwd.

Voor het bepalen van de effecten van winderosie op een schaal groter dan de veldschaal is het nodig dat verschillende meettechnieken worden geïntegreerd in hetzelfde gebied. Een voorgestelde methode voor het schatten van een totale massabalans van eolisch materiaal in een gebied van ca. 100 km^2 combineert remote sensing met een winderosiemodel en veldmetingen. Het gebied wordt daarbij onderverdeeld in uniforme eenheden die geselecteerd worden op basis van oppervlakte-kenmerken. Het winderosiemodel wordt geijkt voor iedere uniforme eenheid door middel van de

veldgegevens. Een geografisch informatie systeem wordt gebruikt voor het combineren van alle informatie en het berekenen van de totale massabalans van eolisch materiaal voor het hele gebied. Alvorens deze methode toegepast kan worden is het noodzakelijk dat een aantal meetproblemen, voornamelijk betrekking hebbende op de suspensiecomponent, wordt opgelost.

Bodem- en nutriëntenverliezen kunnen worden tegengegaan door gewasresten in het veld te laten als mulch. Een probleem is dat onvoldoende materiaal beschikbaar is voor een goede bodembescherming. In de Sahel is de biomassa-produktie laag en worden gewasresten ook voor andere doeleinden gebruikt. In een eerdere studie werd aangetoond dat bedekking van de bodem met 2000 kg ha^{-1} gierststengels een goede bescherming tegen winderosie geeft, terwijl 500 kg ha^{-1} geen effect had. In dit onderzoek werd de reductie in winderosie door twee hoeveelheden gierststengels (1000 en 1500 kg ha^{-1}) getest gedurende twee seizoenen (1994 en 1995). Bedekking van de bodem met 1500 kg ha^{-1} gaf een goede bescherming tijdens alle gemeten stormen. Echter, de bedekking met 1000 kg ha^{-1} gaf slechts voldoende bescherming tijdens zwakke stormen met windsnelheden onder de 10 m s^{-1}. Tijdens één storm met een windsnelheid van 11,3 m s^{-1} trad zelfs meer sediment-transport op als gevolg van de gierststengels. Deze toename in erosie kan worden verklaard door een versterkte turbulentie rond de gierststengels. Daarom wordt geadviseerd om tenminste een hoeveelheid van 1500 kg ha^{-1} gierststengels te gebruiken voor bodembescheming in de Sahel.

Naast de veldexperimenten werden 138 boeren uit zeven dorpen geïnterviewd naar hun kennis van winderosieprocessen en bodemconserveringstechnieken. De meeste boeren (63%) beschouwden winderosie als schadelijk voor hun gewassen. Planten worden beschadigd door de schurende werking van zand (abrasie), of ze gaan verloren doordat ze worden bedekt met zand. Bijna alle boeren toonden een goed begrip van de invloed van winderosie op de bodemvruchtbaarheid. Naar hun mening worden velden of plekken waar eolisch materiaal wordt afgezet verrijkt, terwijl erosie een verlies aan bodemvruchtbaarheid veroorzaakt. De meeste boeren (92%) gebruikten één of meerdere bodem-conserveringstechnieken in het veld. De traditionele maatregelen zijn bedekking van de grond met mulch en bemesting met organische mest. Nieuwe technieken zijn geïntroduceerd door landbouw-projecten. Deze technieken zijn regeneratie van natuurlijke vegetatie, aanplant van bomen en het gebruik van *zai*. Deze laatste is een techniek afkomstig uit Burkina Faso waarbij gezaaid wordt in met compost gevulde gaten. Regeneratie van natuurlijke vegetatie werd door de boeren die deze techniek toepassen als succesvol omschreven en lijkt de meest geschikte bodemconserveringsmethode, omdat de hoeveelheden mulchmateriaal en mest beperkt zijn binnen de huidige landbouwsystemen.

Résumé et Conclusions

L'agriculture pluviale dans la zone Sahélienne du Niger est caractérisée par des sols sablonneux pauvres en matières physique et chimique combinée à un climat extrême. L'agriculture n'est pratiquée que pendant la courte saison des pluies qui va de fin mai à fin septembre. Il y a deux saisons pendant lesquelles il est question d'érosion éolienne. La saison sèche apporte le vent fort, nommé Harmattan, qui provoque une érosion modérée dans le Sahel. Au cours de la dernière partie de cette saison beaucoup de poussière en provenance du Sahara est apportée par l'Harmattan. Cette poussière retombe partiellement dans le Sahel. Le début de la saison des pluies (mai - juillet) est la période d'érosion la plus importante. Pendant ce temps-là de très forts orages se développent dans le Sahel apportant les premières pluies de la nouvelle saison. Ces orages sont souvent précédés de courtes périodes (de 10 à 30 minutes) de vent soufflant à grande vitesse ce qui cause beaucoup d'érosion.

Pendant une telle tempête des particules de sol sont soulevées et transportées au moyen de trois processus différents: saltation, reptation et suspension. On parle de saltation lorsque les grains de sable se déplacent sur la surface par bonds successifs atteignant des hauteurs maximales d'à peu près 1 m. Au moment où un tel grain de sable retombe sur le sol non seulement d'autres grains de sable sont heurtés et commencent à bondir (saltation), mais également des grains plus gros sont poussés en avant (reptation) et des matières plus fines sont mises en suspension. Par les trois processus nommés ci-dessus des particules de sol sont déplacées sur des distances différentes. Du matériel en reptation se déplace de quelques centimètres à quelques mètres. La saltation cause un déplacement de matériel qui varie d'un mètre à quelques centaines de mètres, tandis que le transport des matières plus fines en suspension peut atteindre une distance de quelques milliers de kilomètres.

Le vent qui souffle pendant les tempêtes du début de la saison des pluies est extrêmement turbulent. Le mesurage continu des flux de saltation montrait une forte fluctuation qui était en corrélation avec les fluctuations de la composante horizontale de la vitesse du vent. Les fluctuations de la composante verticale de la vitesse du vent ne montraient pas de corrélation avec le flux de saltation. Ceci justifie la conclusion que la force de frottement est de plus haute importance que la contrainte de cisaillement. C'est pourquoi des modèles de transport par saltation devraient plutôt se servir de la vitesse du vent que de la contrainte de cisaillement, comme il en est question actuellement dans la plupart des modèles.

Pour déterminer le transport de masse pendant une tempête on utilise des capteurs de sédiment, du type "Modified Wilson and Cooke" (MWAC). Cet instrument est composé de sept unités de captage qui sont fixées sur un mât à des hauteurs variant de 0,05 à 1,00 m. Chaque unité de captage est constituée d'une petite bouteille de plastic fermée par un bouchon vissant. Dans ce bouchon une admission et un échappement sont fixés. Ce sont des tubes de verre ronds avec un trou de 50,3 mm^2. A l'extérieur, les deux tubes sont courbés à 90 degrés en direction inverse. Le matériel ainsi obtenu au cours d'une tempête est attrapé et utilisé pour calculer, par capteur et par tempête, sept flux de masse horizontaux. Au moyen des sept observations un modèle est ajusté pour décrire le profil vertical des flux de masse horizontaux. Dans ce but deux modèles courants ont été testés et il se trouve qu'un modèle alliant saltation et suspension donne les meilleurs résultats. Les profils de flux de masse verticaux montrent un maximum à la surface du sol qui diminuent fortement selon les hauteurs. En intégrant le profil en hauteur et après correction de l'efficacité d'attraper des capteurs de sédiment (0,49), un transport de masse total fut obtenu à l'endroit d'observation. Cette valeur est conforme à la masse totale du matériel de sol qui a passé une bande d'un mètre par unité de temps.

La littérature au sujet de l'érosion éolienne signale que les termes séparés du modèle combinant saltation et suspension décrivent respectivement les flux de masse de saltation et de suspension. Après tamisage et pesage du matériel attrapé il s'est cependant avéré que ce modèle ne peut pas être utilisé à cet effet. Ce modèle ne peut être appliqué que pour la détermination des flux de masse totaux qui sont composés de matériel aussi bien de saltation que de suspension.

Les mesurages de terrain du transport de masse sont souvent caractérisés par une grande variabilité spatiale, ce qui rend difficile d'évaluer quantitativement l'érosion éolienne. Pour cet examen, l'analyse géostatistique est appliquée pour modeler la variabilité spatiale dans les observations de transport de masse. A l'aide de 21 capteurs de sédiment MWAC des mesurages de terrain furent faits sur un champ d'expérimentation large de 40 à 60 mètres pendant quatre tempêtes de la saison des pluies de 1993. Afin d'avoir suffisamment d'observations pour réaliser l'analyse, on a joint celles des quatre tempêtes. Pour chaque tempête des cartes furent faites du total de transport de masse avec "kriging" (une technique d'interpolation spatiale) et "simulated annealing" (une technique de simulation stochastique).

Les cartes simulées montrèrent clairement la division spatiale du transport de masse. Ces cartes sont utilisées pour distinguer les endroits d'érosion et de déposition sur le champ. Si l'on combine

les cartes avec celles des propriétés du sol, de la rugosité du sol et de la topographie, etc., on peut arriver à mieux comprendre les processus d'érosion éolienne.

Les cartes interpolées furent employées pour calculer les bilans de masse, ce qui permit de déterminer les pertes du sol par tempête. La perte totale du champ d'expérimentation fut de 45,9 Mg ha^{-1} pendant les quatre tempêtes. Cette perte correspond à une couche de sol d'environ 2,7 mm en épaisseur. Du fait que les terrains sablonneux au Niger sont profonds (plus de 3 m de profondeur) on peut conclure que la perte du sol de quelques millimètres par an n'est pas le problème majeur des agriculteurs Nigériens. La perte des nutriments causée par les tempêtes est de plus grande importance.

Pendant deux des quatre tempêtes en 1993, du sédiment fut attrapé à trois hauteurs (0,05; 0,26 et 0,50 m). Le matériel obtenu ainsi que la quantité d'éléments totaux (ET) en potassium (K), en carbone (C), en azote (N) et en phosphore (P), fut déterminée. En général, le matériel obtenu à une hauteur de 0,05 m contenait autant de nutriments que le sol en surface. A 0,50 m le sédiment était à peu près trois fois plus riche en nutriment que le sol en surface. Cette augmentation en valeurs de nutriments selon les différentes hauteurs peut être expliquée par l'augmentation des valeurs de particules d'argiles et de limon du sédiment. Ce matériel fin du sol contient plus de nutriments que le sable à plus gros grains qui est transporté juste au-dessus de la surface du sol.

En combinant le profil vertical du flux de masse avec les profils ET verticaux on obtint les profils ET de flux de masse des quatre éléments K, C, N et P. Ces profils montrent un maximum dans la zone de saltation juste au-dessus de la surface et diminuent fortement selon les hauteurs. En intégrant les profils ET de flux de masse selon la hauteur et en calculant les bilans de masse on arrivait à estimer les pertes en K, C, N et P sur le champ d'expérimentation. Ces pertes s'élevaient à 3% environ de la masse totale présente dans les premiers 10 centimètres du sol de la surface.

Par saltation, du matériel est transporté sur de minimes distances, ce qui donne pour résultat qu'il n'est question que de redistribution régionale de particules de sol et de nutriments. Le matériel est transporté de sols non-protégés vers des endroits protégés par la végétation ou par mesures de conservation du sol. On voit également la redistribution du sol à l'intérieur des bords d'un terrain. Ce sont souvent les arbres et les buissons sur les champs qui attrapent le matériel en saltation des environs. Bien que les flux de suspension soient beaucoup moins grands que les flux de saltation, le matériel en suspension est transporté sur des distances beaucoup plus grandes. De cette manière,

le transport en suspension peut mener à une perte régionale des nutriments et ainsi il doit être considéré comme un processus important de dégradation du sol.

Pour la détermination des effets d'érosion éolienne sur une échelle plus grande que l'échelle de terrain, il est nécessaire que les différentes techniques de mesure soient intégrées dans la même région. Une méthode proposée pour estimer le bilan de masse total de matériel éolien dans un endroit d'environ 100 km^2 combine la télédétection avec un modèle d'érosion éolienne et des mesurages de terrain. Pour cela, l'endroit est divisé en unités uniformes sélectionnées sur la base de caractéristiques de surface. Pour chaque unité uniforme, le modèle d'érosion éolienne est vérifié au moyen des données de terrain. Un système d'information géographique est employé pour combiner toute information recueillie et pour calculer le bilan de masse total de matériel éolien pour tout le terrain. Avant de pouvoir appliquer cette méthode il est nécessaire qu'un nombre de problèmes de mesurage, se rapportant principalement à la composante de suspension, soit résolu.

Les pertes du sol et des nutriments peuvent être réduites en utilisant les résidus de récolte comme paillage. Cependant il y a le problème d'un manque de matériel nécessaire pour une bonne protection du sol. Dans le Sahel la production de biomasse est peu élevée. De plus, les résidus de récolte sont utilisés pour d'autres buts. Une étude faite antérieurement a prouvé que le recouvrement du sol avec 2000 kg ha^{-1} de tiges de mil assure une bonne protection contre l'érosion éolienne; une quantité de 500 kg ha^{-1} ne donna aucun résultat. Lors de cet examen on a testé la réduction d'érosion éolienne à l'aide de deux quantités de tiges de mil (1000 et 1500 kg ha^{-1}) pendant deux saisons (en 1994 et en 1995). Le recouvrement du sol avec 1500 kg ha^{-1} donna une bonne protection pendant toutes les tempêtes mesurées. Cependant, quand il s'agissait de recouvrement du sol avec 1000 kg ha^{-1}, la protection était insuffisante pendant des tempêtes faibles (développant des vitesses du vent sous 10 m s^{-1}). Pendant une tempête avec une vitesse du vent de 11,3 m s^{-1} on a même mesuré qu'il y avait plus de transport de sédiment à cause des tiges de mil. Cette augmentation d'érosion était causée par une turbulence plus forte autour des tiges de mil. C'est la raison pour laquelle on a recommandé d'utiliser au moins 1500 kg ha^{-1} de tiges de mil pour la protection du sol dans le Sahel.

En plus des expérimentations sur le terrain, on a interviewé 138 agriculteurs en provenance de sept villages afin de vérifier leur connaissance des processus d'érosion éolienne et des techniques de conservation du sol. La plupart des agriculteurs (63%) considéraient l'érosion éolienne comme une cause importante des pertes de leur récoltes. Des plantes sont abîmées par abrasion du sable ou sont perdues parce qu'elles sont couvertes de sable. Il s'est avéré que la majorité des agriculteurs

a une bonne notion des influences d'érosion éolienne sur la fertilité du sol. D'après eux les terrains, où le matériel éolien retombe, sont rendus plus fertiles, tandis que l'érosion cause une dégradation de la fertilité du sol. 92% des agriculteurs utilisaient une ou plusieurs techniques de conservation du sol. Les mesures traditionnelles sont: l'application de paille avec des résidus de récolte ou des branches, ainsi que l'amendement de fumier. Des nouvelles techniques sont introduites par le moyen de projets agricoles. Ces techniques sont: la régénération de végétation naturelle, le plantation d'arbres et l'usage de *zai*, une technique provenant du Burkina Faso où l'on sème les graines ou plantes dans des trous remplis de compost. Les agriculteurs appliquant la régénération de végétation naturelle la considéraient comme une technique qui donne de bons résultats, et elle a l'air d'être la technique la plus utile pour la conservation du sol, parce que les quantités de matériel de paille et de fumier sont limitées en vue des systèmes agricoles actuels.

Curriculum vitae

Geert Sterk was born at Ee in the northern part of The Netherlands on 23 November 1966. After finishing secondary school, he started studying at Wageningen Agricultural University in 1985. In 1991 he graduated in Soil and Water Management. During his studies, he went two times to South-East Asia. In 1988, he stayed seven months in Indonesia, where he worked on a hydrological description of a watershed in the southern limestone area of east Java. In 1991 he stayed three months in the Mekong delta of southern Vietnam, and studied leaching processes in acid sulphate soils. After graduating, he started working at the Department of Irrigation and Soil & Water Conservation. First as a research assistant, and in 1992 he continued with working on the wind erosion research project in Niger. Currently he is working on the EU-project WELSONS: Wind Erosion and Loss of SOil Nutrients in semi-arid Spain.